

*Mytilus edulis* haemocytes variability:  
technique, individual and environment

Submitted by

**Lionel Jouvét**

For the Degree of Doctor of Philosophy

Supervisors: Dr Liz Dyrinda, Dr Valerie Smith, Dr Derek Jamieson

School of Life Sciences

Heriot Watt University

Edinburgh

July 2010

*The copyright in this thesis is owned by the author. Any quotation from the thesis or use of any of the information contained in it must acknowledge this thesis as the source of the quotation or information*

## Abstract

The widely distributed marine bivalve *Mytilus edulis* is used as a sentinel organism for ecological and toxicological assessments. As a filter feeder, it has the potential to bioaccumulate pollutants. It has been assumed that the cell concentration and cell type ratio of its circulating immune cells, haemocytes, could become complementary sub-lethal indicators of toxicology. These two parameters are respectively referred to as total haemocyte count (THC) and differential cell count (DCC). This study examines these commonly used methods, quantifies their limitations, and develops alternative techniques. The circulating immune cells are investigated to assess their fluctuations. Finally, impacts of environmental challenges on the circulating haemocytes are examined.

Despite its importance in the field of *Mytilus edulis* immunology, THC evaluation is present in only 20% of publications in this field, and DCC in 10%. Ultimately, only 9% of papers consider both THC and DCC before further analyses. The remaining studies disregard THC and DCC, or regard these parameters as being constant and homogenous in *M. edulis* populations.

This study initially quantifies the systematic error induced by sampling, and suggests improvements. For example, a systematic error of 26% is attributed to the use of low precision syringes, and can be reduced with use of higher precision sampling equipment. While the systematic errors in visual count and image analysis of THC and DCC evaluations are equivalent, the computerised methods allow the throughput of larger data sets, reduce workload, and avoid tedious eye counts. Flow cytometry was found to be the most accurate method in THC and DCC evaluation. Furthermore, repeated bleedings influence DCC, triggering the decrease of circulating eosinophils (up to 20%) and the increase of hyaline cells (up to 30%). To mitigate this reaction to sampling, a maximum volume of 50µl using a permanent cannulation is recommended.

However, even with improved methods reducing systematic error by half, this study still reports variations as high as 20-fold in the haemocyte concentration in populations of healthy individuals. In addition, over a 2-hour period in a single cannulated individual, fluctuation of the DCC is observed to be as high as 30% for eosinophils, 10% for hyaline cells, and 20% for basophils. These measured variations are explained by haemocyte reservoirs in the tissues. Eosinophils are found in large numbers in epithelial

association in the gills, guts and in the mantle, where their numbers have been evaluated at  $3 \times 10^7$  cells.

As a case study, *Mytilus edulis* challenged with barium sulphate smothering, used by the oil industry in drilling muds, shows gill damage and their subsequent infiltration by eosinophils. In bacterial outbreak, basophilic cells are observed to infiltrate the tissue surrounding the stomach and eosinophils are depleted from the epithelium of the digestive tissues. THC is 10-fold lower than in healthy organisms and eosinophils are depleted from the haemolymph.

In conclusion, the THC and DDC methods are shown to be unreliable despite the use of more accurate methods. In addition, *Mytilus edulis* circulating haemocytes present large variations and the assumption of their homogeneity in terms of time, individuals or methods used cannot be made. These results challenge the conclusions of many past publications regarding causalities established between potential stresses and measured effects. Further research is necessary to understand the mechanisms regulating the circulating haemocytes, the inter-individual variability and to improve investigation methods.

## **Acknowledgements:**

I will like to thank Dr Liz Dyrinda for help and advices in this work and its write-up, to Dr Peter Morris for his comments, to Dr Derek Jamieson, and Dr Valerie Smith for their numerous opportunities given.

I will like to thanks Sean Mc Menamy for his generosity. Thanks also to my collaborators Maia Strachan and Maiwenn Kersaudy-Kerhoas, which were able to deal with my ridiculous accent that tortured the language of Hume and Shakespeare for many years, and to Dr Philippe Roch, having similar accent, for his challenging and sharp investigative mind.

My deepest regards for Margaret Strobie and Douglas Paton for their unforgettable support, advices and teachings.

Finally, to all the people that support, argued, constructed me through this work: Maria, Sarah, Calum, Vickie, Paul, Luxy, Melodie, Louis, Sophie, Jean-François, Marie-Therese, Guillaume, Lucie, Aimee, Sarah, Lenka, Olga, Stephane, Coba, Martin, Michel, Magali, Chantal, Thomas, François et Stephanie, Mathieu et Sylvain, Debora, Md et Ms Mouligneau, all my family, and so many more, that could not fit on this page.

ACADEMIC REGISTRY  
**Research Thesis Submission**



Name:			
School/PGI:			
Version: <i>(i.e. First, Resubmission, Final)</i>	Degree Sought (Award <b>and</b> Subject area)		

**Declaration**

In accordance with the appropriate regulations I hereby submit my thesis and I declare that:

- 1) the thesis embodies the results of my own work and has been composed by myself
- 2) where appropriate, I have made acknowledgement of the work of others and have made reference to work carried out in collaboration with other persons
- 3) the thesis is the correct version of the thesis for submission and is the same version as any electronic versions submitted\*
- 4) my thesis for the award referred to, deposited in the Heriot-Watt University Library, should be made available for loan or photocopying and be available via the Institutional Repository, subject to such conditions as the Librarian may require
- 5) I understand that as a student of the University I am required to abide by the Regulations of the University and to conform to its discipline.

\* Please note that it is the responsibility of the candidate to ensure that the correct version of the thesis is submitted.

Signature of Candidate:		Date:	
-------------------------	--	-------	--

**Submission**

Submitted By <i>(name in capitals)</i> :	
Signature of Individual Submitting:	
Date Submitted:	

**For Completion in Academic Registry**

Received in the Academic Registry by <i>(name in capitals)</i> :			
<i>Method of Submission</i> <i>(Handed in to Academic Registry; posted through internal/external mail):</i>			
<b>E-thesis Submitted (mandatory from November 2008)</b>			
Signature:		Date:	

# Contents

1 Introduction .....	2
1.1 Biology of <i>Mytilus edulis</i> .....	2
1.1.1 Morphology .....	2
1.1.2 Distribution and reproduction .....	3
1.2 <i>Mytilus edulis</i> Immune system .....	4
1.2.1 Description of <i>M. edulis</i> circulating immune system .....	4
1.2.2 <i>Mytilus</i> haemocytes investigation techniques .....	7
1.3 Individuality .....	10
1.3.1 Individuality and species .....	10
1.3.2 Unclear nomenclature of agents of the self .....	11
1.4 Environment and externalities .....	11
1.4.1 Externalities and internalisation .....	11
1.4.2 Stratification of an individual's environment .....	12
1.5 Structure of the study .....	12
2 Materials and methods .....	14
2.1 Animal collection and maintenance .....	14
2.1.1 Environmental data collection .....	14
2.2 Chemicals, Reagents, Animals, and Other Materials .....	15
2.2.1 Solutions and buffers .....	15
2.2.2 TBS, 3xTBS and 3.8% formaldehyde in 3xTBS .....	16
2.2.3 Marine agar .....	16
2.3 Histological investigations .....	16
2.4 Animal experimentation .....	17
2.4.1 Conventional sampling of haemolymph .....	17
2.4.2 Cannula construction .....	18
2.4.3 Surgical window and gill activity .....	21
2.4.4 <i>Mytilus edulis</i> euthanasia .....	23
2.5 Cell investigation .....	24
2.5.1 Cell separation on discontinuous Percoll gradients .....	24
2.5.2 Ocular investigation .....	26
2.5.3 Image analysis investigation .....	27
2.5.4 Flow cytometry .....	37
2.6 Microfluidics experimental setup .....	39
2.7 Impact of barium .....	40

3 Investigation of circulating haemocytes of <i>Mytilus edulis</i> .....	43
3.1 Introduction.....	43
3.2 Visual cell count using bright field microscopy and Wright's stain.....	45
3.2.1 Uncertainty level of THC.....	45
3.2.2 Investigation of results of THC.....	46
3.2.3 Ambiguity of cytospin technique.....	47
3.2.4 Investigation of results of differential count.....	48
3.3 Evaluation of image analysis.....	49
3.3.1 Evaluation of THC macro.....	49
3.3.2 Investigation of THC results by image analysis.....	50
3.3.3 Comparison of visual against the image analysis differential count.....	51
3.4 Identification of cell population in flow cytometry.....	52
3.4.1 Indirect identification.....	52
3.4.2 Direct identification.....	57
3.5 Behaviour of haemocytes in microfluidics system.....	59
3.6 Discussion.....	62
3.6.1 Visual cell count using bright field microscopy and Wright's stain.....	62
3.6.2 Evaluation of image analysis.....	63
3.6.3 Identification of cell populations in flow cytometry.....	64
3.6.4 Discussion of behaviour of haemocytes in the microfluidics system.....	65
4 Variability in circulating haemocytes of <i>Mytilus edulis</i> .....	67
4.1 Introduction.....	67
4.2 Variations in the cell population level.....	68
4.2.1 Cell types in <i>Mytilus edulis</i> .....	68
4.2.2 Variation of THC and haemocyte types.....	71
4.3 Inter-individual variability in circulating haemocytes of <i>Mytilus edulis</i> .....	72
4.3.1 Results from environmental sampling.....	72
4.3.2 Results from laboratory sampling.....	77
4.4 Individual variability in of <i>Mytilus edulis</i> circulating haemocytes.....	78
4.4.1 Position of the adductor muscle with regards to the mussel size.....	78
4.4.2 Individual variation of haemocyte populations.....	79
4.5 Investigation of a potential haemocyte reservoir in <i>Mytilus edulis</i> .....	82
4.5.1 Observation of the <i>Mytilus edulis</i> mantle.....	82
4.5.2 Observation of the visceral mass of <i>Mytilus edulis</i> .....	86
4.5.3 Observation of the gills tissue of <i>Mytilus edulis</i> .....	88
4.6 Discussion.....	89
4.6.1 Variations in the cell population level.....	89
4.6.2 Inter-individual variability in circulating haemocytes of <i>Mytilus edulis</i> .....	90
4.6.3 Individual variability of <i>Mytilus edulis</i> circulating haemocytes.....	91
4.6.4 Investigation of a potential haemocyte reservoir in <i>Mytilus edulis</i> .....	91

5 Induced variability in the <i>Mytilus edulis</i> immune system.....	93
5.1 Introduction.....	93
5.2 Impact of physical stress: .....	94
5.2.1 Impact of wave exposure on circulating haemocyte ratio.....	94
5.2.2 Impact of air exposure on circulating haemocyte ratio.....	95
5.2.3 Impact of iron oxide coverage on circulating haemocyte ratio.....	96
5.2.4 Barium sulphate .....	98
5.3 Impact of biological stress: .....	108
5.3.1 Biofouling of the shell.....	108
5.3.2 Bacterial exposure.....	109
5.4 Discussion .....	117
5.4.1 Impact of physical stress .....	117
5.4.2 Impact of biological stress .....	118
6 Conclusion .....	121
References .....	130



# List of figures

## Chapter 1

Figure 1.1: Brightfield light microscopy photography of haemocytes called hyaline cells stained with Wright's stain.	5
Figure 1.2: Bright-field light microscopy photography of haemocytes.	5
Figure 1.3: Technique of <i>Mytilus sp</i> haemocytes investigation in the literature (1980-2008).	7
Figure 1.4: Principle of flow cytometer used in the study.	10

## Chapter 2

Figure 2.1: Map of the main sampling site for <i>Mytilus edulis</i> .	14
Figure 2.2: Presentation of the site data compilation using Google Earth.	15
Figure 2.3: Standard sampling procedure of <i>Mytilus edulis</i> haemolymph.	17
Figure 2.4 : 1.5ml centrifuge tube and Screw-cap preparation preparation.	18
Figure 2.5 : Cannula body preparation.	19
Figure 2.6 : Fixation of the cannula.	20
Figure 2.7: <i>Mytilus edulis</i> (I) and <i>Modiolus modiolus</i> (II) with surgical window showing an overview on the gills.	21
Figure 2.8: Scheme of the major steps of the surgical window protocol.	22
Figure 2.9: Description of <i>Mytilus edulis</i> euthanasia.	23
Figure 2.10 : Scheme of preparation horizontal flow pipette tip used for the set-up of discontinuous Percoll gradient.	24
Figure 2.11 : Scheme of the discontinuous gradient.	25
Figure 2.12: Original picture of the Neubauer observation field.	29
Figure 2.13: First analysis step to change the coloured raster into a gray scale raster.	29
Figure 2.14: Process of 'find the edges' and threshold.	30
Figure 2.15: Artefact removal and particle counting.	30
Figure 2.16: Translation of 32-bit coloured picture into 8-bit greyscale image.	33
Figure 2.17: Image processing to establish the number of cells.	33
Figure 2.18: Image processing sequence for differential cell count.	35
Figure 2.19: Scheme of a microfluidics chip used as a cell concentrator.	39
Figure 2.20: Experimental setup to study the impact of barium on bivalves.	41

## Chapter 3

Figure 3.1 : Distribution of THC using the conventional Neubauer cell count.	46
Figure 3.2: Pictures of cell agglomeration found at the edge of cytopsin preparations.	47
Figure 3.3: Circulating cell populations investigated under bright field microscopy.	48
Figure 3.4 : Distribution of THC using the cell concentration image analysis macro.	50
Figure 3.5 : Comparison of visual against image analysis differential cell count.	51
Figure 3.6: Flow cytometric data of basophilic and eosinophilic dominance samples.	52
Figure 3.7: Flow cytometric data of cells collected at interfaces of the Percoll gradient.	53
Figure 3.8 : Overlays of flowcytometric charts of cell populations separated on Percoll gradient.	54
Figure 3.9 : Flow cytometry results of the DiOC <sub>6</sub> staining.	55
Figure 3.10 : A Flow cytometry result of the Wright's staining.	56
Figure 3.11 : Flow cytometry chart of the sample used for the cell sorting.	57
Figure 3.12 : Three charts of the control of the cell sorting effectiveness.	57
Figure 3.13: Picture of the three cell types sorted by flow cytometry.	58
Figure 3.14: Turbidity of concentrated cell sample against the serum sample.	59
Figure 3.15 : Microscopy observation of the concentrated cells against serum sample.	60
Figure 3.16: Overlay of relative size spectra of the haemolymph sample injected at 10ml/hr.	60
Figure 3.17: Overlay of relative size spectra of the haemolymph sample injected at 1ml/hr.	61

## Chapter 4

Figure 4.1 : Graphic representation of the cell group variability of the mussel.	69
Figure 4.2 : Unusual spectrum cell type of the mussel immune system, spectrum type V.	70
Figure 4.3 : Cell count against the cell type by flow cytometry.	71
Figure 4.4 : Sampling sites on Harris, Lewis and the Uists.	72
Figure 4.5: Recorded pictures of the sample mussels and their scale.	74
Figure 4.6 : Variation in circulating haemocyte types observed in Harris.	75
Figure 4.7: Variation in circulating haemocyte types observed in Lewis and Uists.	75
Figure 4.8: Circulating haemocytes population variation observed in Argyll.	76
Figure 4.9: Sampling sites in Argyll (Scotland, UK).	76
Figure 4.10: Population of haemocytes observed in aquarium-kept organisms.	77
Figure 4.11 : Relative position of the adductor muscle.	78
Figure 4.12 : Drilling positioning tool.	78
Figure 4.13: Measured variation of haemocyte populations over 13 days.	79
Figure 4.14: Measured variation of haemocyte populations over 5 days.	80
Figure 4.15: Measured variation of haemocyte populations over 12 hours.	81
Figure 4.16: <i>Mytilus edulis</i> ' mantle from 23 fields of view under bright field microscopy.	82
Figure 4.17: <i>Mytilus edulis</i> ' mantle from 11 fields of view under bright field microscopy.	83
Figure 4.18: <i>Mytilus edulis</i> ' mantle from 11 fields of view under bright field microscopy.	84
Figure 4.19: <i>Mytilus edulis</i> ' mantle from 5 fields of view under bright field microscopy.	85
Figure 4.20: <i>Mytilus edulis</i> ' visceral mass from 20 fields of view under bright field microscopy.	86
Figure 4.21: <i>Mytilus edulis</i> ' visceral mass from 30 fields of view under bright field microscopy.	87
Figure 4.22: <i>Mytilus edulis</i> ' gills from 8 fields of view under bright field microscopy.	88

## Chapter 5

Figure 5.1: Percentage of haemocytes in exposed and sheltered mussels.	94
Figure 5.2: Percentage of haemocytes in mussels immersed in seawater over five days.	95
Figure 5.3: Percentage of haemocytes in non-immersed mussels over five days.	95
Figure 5.4: Sampling sites in Blackhall (UK).	96
Figure 5.5: Haemocyte percentages on the 17/09/06.	97
Figure 5.6: Haemocyte percentages on the 20/09/08.	97
Figure 5.7: Macro picture of a fully re-grown shell.	98
Figure 5.8: Pictures of impact of barium sulphate on gills of <i>Mytilus edulis</i> .	99
Figure 5.9: Pictures of impact of barium sulphate on gills of <i>Modiolus modiolus</i> .	100
Figure 5.10: Transverse section of <i>Mytilus edulis</i> ' gills under bright field microscopy.	101
Figure 5.11: Section of the visceral mass of <i>Mytilus edulis</i> .	102
Figure 5.12: Percentages of circulating haemocytes in control and barium sulphate treated cannulated mussels.	103
Figure 5.13: Change in circulating haemocyte populations of Cramond mussels over five days.	104
Figure 5.14: Change in circulating haemocyte populations of farmed mussels over five days.	105
Figure 5.15: Change in circulating haemocyte populations of horse mussels over five days.	106
Figure 5.16: Haemocytes percentage of clean and biofouling mussels.	108
Figure 5.17: Upper part of visceral mass of a bacterially challenged <i>Mytilus edulis</i> .	112
Figure 5.18: Lower part of visceral mass of a bacterially challenged <i>Mytilus edulis</i> .	113
Figure 5.19: <i>Mytilus edulis</i> stomach from 29 fields of view under bright field microscopy.	114
Figure 5.20: Circulating haemocytes in shore, control and bacterially challenged <i>Mytilus edulis</i> .	116

## List of tables

### Chapter 1

Table 1.1: <i>Mytilus</i> spp. reproduction and spreading potential.....	3
Table 1.2: List of examples of cellular and sub-cellular techniques and mechanisms investigated in the literature. ....	8

### Chapter 2

Table 2.1: Description of the script of cell concentration macro. ....	28
Table 2.2: Macro script for cell count .....	32
Table 2.3: Macro script for red cell count .....	36

### Chapter 3

Table 3.1: Typical image analysis results for cell concentration evaluation. ....	49
Table 3.2: Automatic calculation of required sample dilution for cytopspin procedure. ....	49

### Chapter 4

Table 4.1: Environmental observations of each sampling site. ....	73
---	----

### Chapter 5

Table 5.1: Variation encountered in haemocyte populations during the 5-day experiment. ....	107
Table 5.2: Characteristics of isolated strains of bacteria collected from the aquarium environment .....	109
Table 5.3: Characteristics of isolated strains of bacteria collected from the aquarium environment. ....	110
Table 5.4: Compilation of the bacterial strains found in the control and outbreak tanks. ....	111

# Chapter 1

## Introduction



Title: Why? (trapped in the question)

Photo taken on the union canal linking Edinburgh to Glasgow (Scotland, UK). The shot is trapping the blurred reflection of the author in the distorted image of the pontoon forming a Y shape.

The letter Y is homophonic to the questioning word 'why?'. This image introduces the introduction chapter by setting the limits of the actual knowledge that are supporting our understanding.

## 1 Introduction

Marine organisms were historically at the corner stone of the study of the immune system. In 1882, studying comparative embryology, Ilya Ilyich Mechnikov was working on starfish larvae. Stabbing them with rose thorns, he observed cells trying to digest the inserted thorn. He named this mechanism phagocytosis. He received the Nobel Prize in 1908 for this work. The research on marine faunal immunity continues.

Such work has chosen the model *Mytilus edulis* for its ease of sampling, its resilience and its ubiquity. Toxicologists and ecologists found, in the biology of this organism, a potential to use it as a sentinel organism. This chapter will present why *Mytilus edulis* received such attention, and the biology, ecology and immunity of the animal will be introduced. The central question posed at the outset of this work is: will the mussel immune system reveal itself as promising to constitute a biomarker?

### 1.1 Biology of *Mytilus edulis*

#### 1.1.1 Morphology

The blue mussel shell has an uneven oval shape, allowing the organism to sustain the mechanical stress of the tidal and sub-tidal environment. Its colouration varies from light brown to dark blue due to melanin trapped in the calcareous matrix of the shell. For experimental purposes, this structure is of a particular interest as the shell can be drilled, and a cannula, needed for the sampling of the immune system, inserted, or cut and replaced by a glass slide to allow an in-vivo observation of the feeding behaviour.

The shell is produced by the underlying mantle, which also has reproductive and storage functions. The adult form is semi-sessile and epibenthic. Mussels fix themselves to the substratum via byssus threads secreted by a gland located at the base of the muscular foot, overlying the visceral mass. They mainly live in batches on rocks, fixed sediments or artificial substratum. Their physical characteristics allow them to colonise one of the toughest environments: the intertidal shores. Their resilience allows them to withstand high variation in salinity, temperature, humidity, pollution, and radiation.

### 1.1.2 Distribution and reproduction

Their distribution pattern is locally linked to substratum availability, physical (temperature, turbidity), chemical (salinity, pH) and biological factors such as predation, micro-flora, or parasites (Bayne, 1976). On a global scale, *Mytilus edulis* has colonised the Arctic, North Pacific and North Atlantic (FAO.©, 2003-2009). This wide distribution can be understood by its method of sexual reproduction. *Mytilus edulis* releases its gametes in the water column, and has a pelagic larval phase before settling on an intertidal benthic environment for its adult phase. The number of annual reproductive cycles is dependent on the latitude, water temperature, food availability and the organisms' energy reserves. In adult form, a sexual bimorphism is observed: the mantle of the male has a pale cream colour, the female orange due to the vitellium.

This reproductive strategy leads to a greater gene mixing potential and therefore a greater heterogeneity of individuals in a species. Table 1.1 describes the reproductive strategy of *Mytilus* species: *M. edulis* (Linnaeus, 1758), *M. galloprovincialis* (Lamarck, 1819), or *M. trossulus* (Gould, 1850). It is difficult to discriminate *Mytilus* species, and it is suggested that all of the smooth-shelled mussels belong to the same species (Seed, 1991). Therefore, it is expected to see strong individual character variations and their distribution to be geographically widespread unless linked to local adaptation.

Table 1.1: *Mytilus* spp. reproduction and spreading potential.  
Sources : Biological Traits Information Catalogue (BIOTIC)  
Ref: <http://www.marlin.ac.uk/biotic/browse.php?sp=4250>

<b>Adults</b>	
Reproductive type	Gonochoristic
Developmental mechanism	Planktotrophic
Reproductive Season	April to September
Reproductive Location	Water column
Reproductive frequency	Annual protracted
Age at reproductive maturity	1-2 years
Generation time	1-2 years
Fecundity	Up to 40,000,000 eggs for large females
Egg/propagule size	Fertilized eggs 60-90 µm
Fertilization type	External , pelagic
<b>Larvae/Juveniles</b>	
Larval/Juvenile dispersal potential	>10km
Duration of larval stage	1-6 months

### 1.1.2.1 *General ecology*

The blue mussel is a suspension feeder: through its gills, the water column is filtered to capture organic particles, phytoplankton and bacteria. Trapped in the gill mucus, the food is actively transported towards the stomach. The reserves are stored as glycogen in the mantle.

In processing an average of 7 litres of seawater per hour through its gills, *Mytilus edulis* has a potentially high challenge from micro-organisms living in the water column. The immune system is the diffuse tissue that regulates the micro-flora and its potentially deleterious impact. The following pages will present its effectors and mechanisms.

## 1.2 *Mytilus edulis* Immune system

### 1.2.1 Description of *M. edulis* circulating immune system

*M. edulis*' immune system is innate; it does not possess acquired immunity, the mechanisms of memory and specificity found in vertebrates. The blue mussel has a circulatory lymphatic system containing haemolymph, which carries through the organism open circulatory system cells named haemocytes. Components of the haemolymph include phagocytosis factor enhancers, opsonins, such as glycoprotein binding lectins and agglutinins. Being an open circulatory system with the haemolymph bathing the cell's tissue, it is common to find in it spermatozoa when the organism is spawning.

#### 1.2.1.1 *Circulating haemocytes*

This system in *Mytilus* is traditionally described in the literature as three different groups of circulating immune cells (Bayne et al., 1979; Pipe, 1990), often discriminated using Wright's stain method and bright field microscopy observations (Figures 1.1 and 1.2).

The agranular cells, that show no intracellular granular bodies, are also called hyaline cells (3-4 $\mu$ m in diameter). Smallest of the three groups, the hyaline cells stain in blue by the Wright's stain and have a high nucleus/cytoplasm ratio. Their role and activity is still unclear.

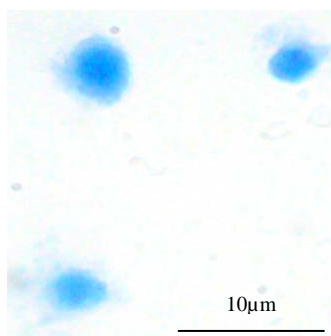


Figure 1.1: Brightfield light microscopy photography of haemocytes called hyaline cells stained with Wright's stain.

The granular cells are commonly divided in two groups regarding their histochemistry.

Basophils (7-8 $\mu$ m in diameter):

In the literature, they are also called basophilic granular haemocytes. Their known action is cytotoxic activity through the production of oxygen radical, antibacterial peptides, and phagocytosis.

Eosinophils (10-12  $\mu$ m in diameter):

Also known as eosinophilic granular haemocytes, they are coloured in pink with a blue nucleus by Wright's stain. Their main known activity is the phagocytosis. The digestion of the encapsulated body is processed by enzymes (lysozyme) and oxygen metabolites.

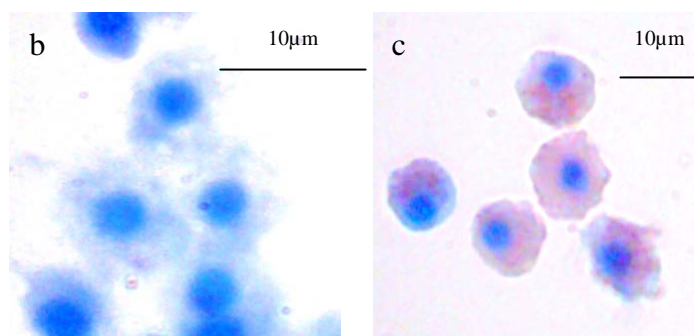


Figure 1.2: Bright-field light microscopy photography of haemocytes. basophils (b) and eosinophils (c) stained with Wright's stain.



### 1.2.1.2 *Haemocyte regulation*

Very few investigations exist on the subject in bivalves. From insect biology and toxicological studies, a few indications have arisen regarding the mechanisms behind hemopoiesis and immune cell population regulation. Strong correlations with reproductive status have been established with the dominance of eosinophil cells (Bayne, 1976) both in the circulating system and in the tissues (mantle principally). Hormonal control has to be suspected: a rapid modulation of the function of mussel haemocytes is reported through the activation of a transduction pathway involving different kinase mediated cascades (Canesi et al., 2006). Hormones also influence gene expression subject to modulation by kinase and phosphatase. Yet, most molecular research has been established using as normalisation the total haemocyte count (THC). This measure does not take into account the variation of the different cell populations. Knowing the difference of activity of each type (hyaline, basophilic, and eosinophilic cells), the appreciation of these different cell types should be necessary to discuss results of high specificity such as genic or proteomic technologies.

## 1.2.2 *Mytilus* haemocytes investigation techniques

### 1.2.2.1 Investigation techniques and literature

The literature illustrates a large variety of technical approaches to investigate bivalve immunity. Figure 1.3 presents the number of publications related to a particular technical approach, and is intended to underline the assumptions taken by the investigators in the literature in the research on *M. edulis* immune system. Only 9% of the published papers investigated in Figure 1.3 assess the number (THC) and type (differential count) of the circulating haemocytes. The other publication assumed that *Mytilus* immune system is homogenous from one individual to another. In the investigation presented in this thesis, it will be demonstrated that this assumption can dramatically influence the results. The techniques introduced in the figure are presented in detail in the following sub-chapters.

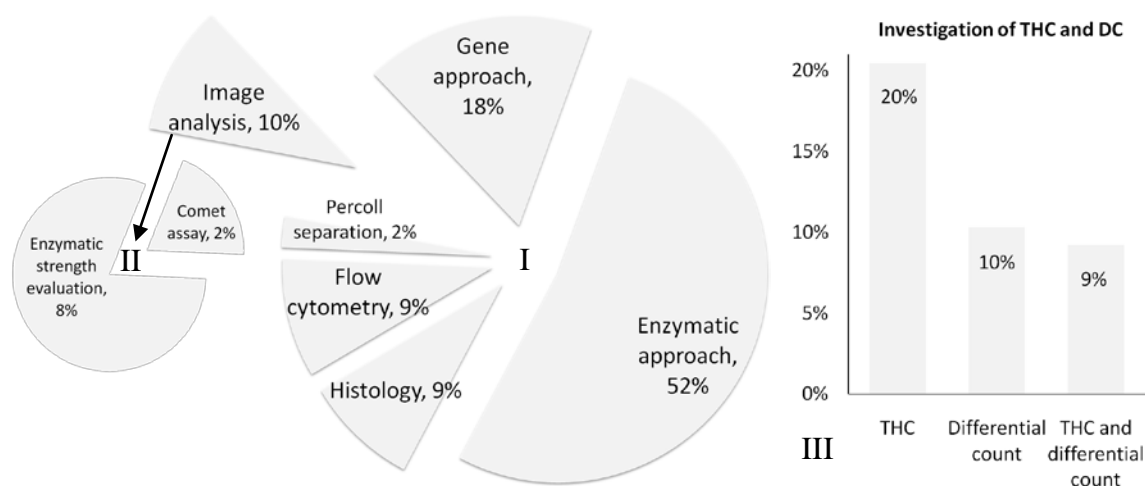


Figure 1.3: Technique of *Mytilus sp* haemocytes investigation in the literature (1980-2008).

I: Pie chart of the techniques used to investigate haemocytes.

II: Detail pie chart of the image analysis used.

III: Graphic representation of the place of THC and differential cell count (DCC) in literature.

### 1.2.2.2 Histology

Haemocytes of *Mytilus edulis* were investigated by light microscopy histology for diagnostic purposes in neoplasia (Moore et al., 1991), impact of toxics (Sunila, 1988), or in differential cell count technique. They also were investigated using transmission electron microscopy to investigate their internal morphology or the distribution of peptides in the haemocyte' granules (Pipe et al., 1993).

### 1.2.2.3 *THC*

The circulating haemocyte concentration is established visually by microscopy using a Neubauer chamber or by flow cytometry. In this last technique, two techniques are dominant: the addition into the measured sample of a known concentration of fluorescent beads that will allow a relative evaluation (Beckman Coulter flow cytometers, US) or by absolute concentration determination (Partec®, Germany).

### 1.2.2.4 *Differential count: Cytospin and Wright's stain technique*

Briefly, haemocytes are attached on a microscope slide, and the highly saline serum removed by centrifugation. The fixed cells are stained using Wright's stain. The cell populations analysed are the ones that attach to the slide. Hence, the assumption undertaken is that all cell types adhere in even proportion and all the cell types stick to the slide.

### 1.2.2.5 *Density gradient centrifugation on Percoll gradient*

The technique allows the segregation of the different cell types using their relative density in a discontinuous Percoll gradient (Friebel and Renwranz, 1995). This technique allows a good separation of the eosinophilic cells but does not achieve discrimination between hyaline and basophilic cells.

### 1.2.2.6 *Molecular, sub-cellular, and cellular investigations*

Cellular and sub-cellular investigation techniques are presented in Table 1.2, showing examples of previous studies and some of the mechanisms targeted. Most of these studies take no account either of the THC or differential count of both, with some recent exceptions (Parisi et al., 2008).

Table 1.2: List of examples of cellular and sub-cellular techniques and mechanisms investigated in the literature.

Lysosomal enzyme activity	(Viarengo et al., 1995), (Canesi et al., 2008; Canesi et al., 2007; Ciacci et al., 2009; Li et al., 2008a)
phagocytic activity	(Akaishi et al., 2007; Auffret et al., 2002; Canesi et al., 2007; García-García et al., 2008; Hagger et al., 2005; Sauvé et al., 2002; Winston et al., 1996)
respiratory burst	(Bussell et al., 2008; Costa et al., March 2009 ; García-García et al., 2008)
gene expression (Hsp70, cell signalling)	(Canesi et al., 2008; Costa et al., 2009; Costa et al., March 2009 ; Li et al., 2008a; Mitta et al., 2000)

### 1.2.2.7 *Image analysis*

Computerised image analysis was used in the literature mainly as a measurement of staining strength, to allow numerical quantification of enzymatic reaction.

In most other studies, it was used in conjunction with the comet assay. This technique allows the evaluation of the nuclear DNA integrity. Tested haemocytes are fixed, their membrane disrupted, inserted in an agar gel containing the fluorescent stain ethidium bromide and submitted to an electric field. The DNA migrates in relation to its size in the electric field. The gel is photographed under UV. Then, the DNA migration is evaluated by the measurement of the fluorescent tail by image analysis. The genotoxicity is evaluated by the increasing length of the tail due to the fragmentation of the nuclear DNA.

Nevertheless, no literature mentions the use of image analysis for THC or for differential count.

### 1.2.2.8 *Flow cytometry*

The flow cytometry technology arose in the 1960's with the development of lasers and earlier studies of laminar flow (Reynolds, 1883). The first apparatus was developed in 1968 by Wolfgang Göhde from the University of Münster (Germany) and commercialized in 1968/69 by German developer and manufacturer Partec. Its principle is presented in Figure 1.4. In brief, the cells from a sample are forced into a laminar flow that separates and focuses them at the centre of the sheath. The cells, then, are individually presented through a laser beam, the induced forward light scattering (FSC) being proportional to the cell size and the perpendicular scattering proportional to the cell internal complexity (SSC). The emitted light intensity of different fluorescence wavelengths can also be measured for each passing cell. For each cell analysed, a set of parameters are recorded by a computer: size, internal complexity, and fluorescence.

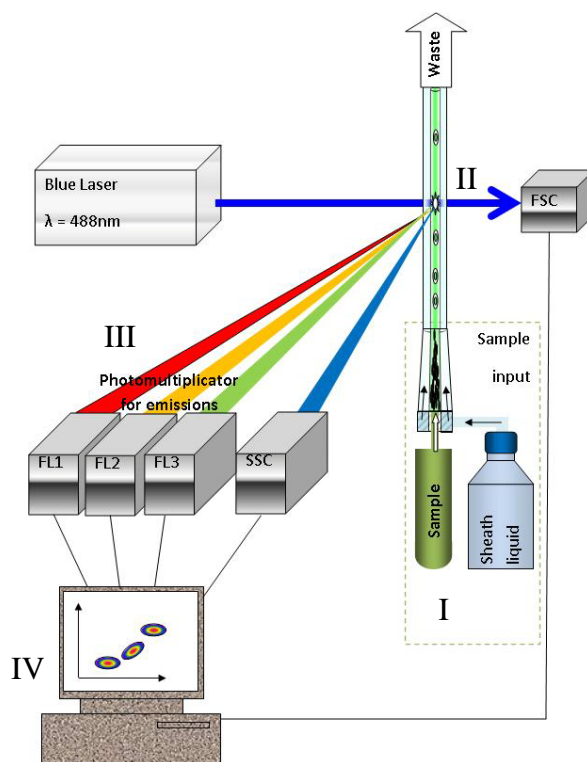


Figure 1.4: Principle of flow cytometer used in the study.

I: Cells from the sample are forced into a laminar flow that separates and focuses them at the centre of the sheath.

II: Cells are individually presented through a laser beam; the induced forward light scattering (FSC) is proportional to the cell size.

III: Perpendicular scattering proportional to the cell internal complexity (SSC). Emitted light intensity, from fluorescence, is perpendicularly measured for each passing cell at different wavelengths (FL1: 520nm, FL2:590nm and FL3: over 620nm).

IV: Data are collected by a computer for analysis.

These techniques have been used in this investigation, and their susceptibility to the inter-individual variability of the immune parameters was measured.

### 1.3 Individuality

#### 1.3.1 Individuality and species

The notion of individuality is unclear. First, the individual can be defined in association with the species to which it belongs. The 'level' of individuality in a species will be defined genetically to discriminate one individual from another one. In this case, the level of individuality is strongly impacted by the type of reproduction and ability of the member of a species to transmit and acquire new characters or genes. For example, asexual reproduction leads to a great homogeneity of the individuals of a species: bacteria (binary fission), hydra (budding), clonal colony plants (vegetative

reproduction), and also figures in the bivalve genus *Lasaea* (Foighil and Thiriott-Quievreux, 1991).

### 1.3.2 Unclear nomenclature of agents of the self

Individuality is based on the genotype; it is also sustained, in the organism's life, by the immune system that will regulate the integrity of the self. In *Mytilus* spp., the agents of self-sustainability are the cells of the immune system. By electron microscopy, they are presented as agranular or granular leukocytes (Rasmussen et al., 1985). When investigated by Wright's stain and bright field microscopy, they are presented as a set of three circulating haemocyte types, namely hyaline cells, basophils and eosinophils (Coles and Pipe, 1994). Using flow cytometry, these haemocytes are respectively given the names agranular, semi-granular, and granular cells (García-García et al., 2008). Other publications use both terminologies (Bussell et al., 2008). This illustrates the observed variability in terminology used in the literature as well as in the investigated cells. Nevertheless, in the present study, the cell types will be presented using the hyaline, basophilic, and eosinophilic cells nomenclature as the terminology regarding their granularity is often synonymous to insect and crustacean haemocytes.

## 1.4 Environment and externalities

### 1.4.1 Externalities and internalisation

It appears important to take into account in the notion of self (intern) the immediate surrounding (external) of the individual. The limits of the self are not as well marked as commonly thought: we have to internalise (take as self) some externalities (commensal flora). It was reported by collaborators (pers. com., P. Roch, Montpellier II University), that bacteria were present in the haemolymph. Further, in the Metchnikoff's legacy conference organised by the Institut Pasteur in Paris (2008), Prof. Lynn Margulis discussed the chimerical status of so called individuals; she also reported that the commensal flora of *Mytilus edulis* could be constituted by five species of bacteria, in opposition to more than 2500 bacterial species in *Homo sapiens sapiens*. She saw, in this magnitude of order, the difference between innate and acquired immune system: the evolution of self-agents' tools to deal with different complexities of a closed ecosystem (or self complexity).

### 1.4.2 Stratification of an individual's environment

As the project started, most of the circulating immune cell protocols were explored to investigate the potential impact of the environment on the system meant to regulate it. Like in most practical sciences (applied mathematics, physics and applied physics), when it is applicable, the establishment of a closed system is required.

Modelisation language UML (United Modalisation Language) was approached. This graphic language has been developed to explain technical knowledge to non-competent personnel (management, direction, finances). Recruited to use in environmental science, this particular tool reveals itself to be very relevant. As developed in 'The Extended Phenotype (Dawkins, 1999): The long reach of the gene', the point of view and the assumptions taken at the beginning of an investigation will condition its understanding. The notion of a discrete organism can be contemplated as a local ecosystem (1.4.1 ). This local ecosystem is regulated by immune cells and is composed by viruses, bacteria, algae, specialised cells, physical and chemical environment. The key was to develop a simplification of a living entity in its own complexity and with the direct environment it encounters. Like in physics, where the system studied is defined and formalised, the model presented in Appendix I has for our purpose to define the information routes and therefore the unknown or the variability factors of the system.

### 1.5 Structure of the study

After a description of the materials and methods, the available technologies are examined to evaluate their qualities, uncertainty levels, and relevance. The level of individuality and inter-individual variations are then considered. Finally, relationships linking environment and *Mytilus edulis* immune system are explored to examine the relevance of establishing the cell type ratio and concentration of circulating haemocytes as a biomarker.

# Chapter 2

## Materials

## and

## Methods



Title: Investigation (tools and techniques of the aftermath)

Photo of the first testing of the cannula technique: the adductor muscle of *Mytilus edulis* cannulated through its shell. Metaphor of a crime scene, the victim lays on its side, stabbed, an ugly wound on its back, where a syringe of formidable proportions enters its once shielded body.

The colours and image quality are set to give the impression of a criminal investigation scene set in a dark side street on a rainy night. The dominance of basic colours (yellow, red, grey and black) is giving a feeling of discomfort, and of a sharply contrasted image. The latent anxiety is exacerbated by the pixellated quality of the photo, and by the shift from sharp to blurry. It mirrors a criminal enquiry, the sharpness of the facts, and the blur of the driving forces.

The detective, like a researcher, faces the facts; the sequence of agents and actions has to be discovered, understood, and formalised using a set of investigation tools and methods.



## 2 Materials and methods

### 2.1 Animal collection and maintenance

Live animals were mainly collected on the cross way to Cramond Island (North-West Edinburgh, UK) at low tide. They were brought back to the aquarium within 2 hours of sampling, and transferred into 50-litre plastic tanks of aerated, filtered seawater. The location of the sampling site is showed in the Figure 2.1.

#### 2.1.1 Environmental data collection

The largest spectrum of sites has been targeted, sampling throughout Scotland, from pristine to heavily impacted shores as the opportunities arose. Google Earth has been used for the compilation of the sampling sites as presented in Figure 2.2. Each site contains a quick summary of the suspected stresses observed at the sampling time. The subjective stress encountered was then colour coded: light green for pristine sites, yellow for detectable signs of stress (water outfall, large human population concentration, industrial activity), and dark red for obvious adverse effects (abiotic zone, abnormal animal/vegetal population, oil leaks).

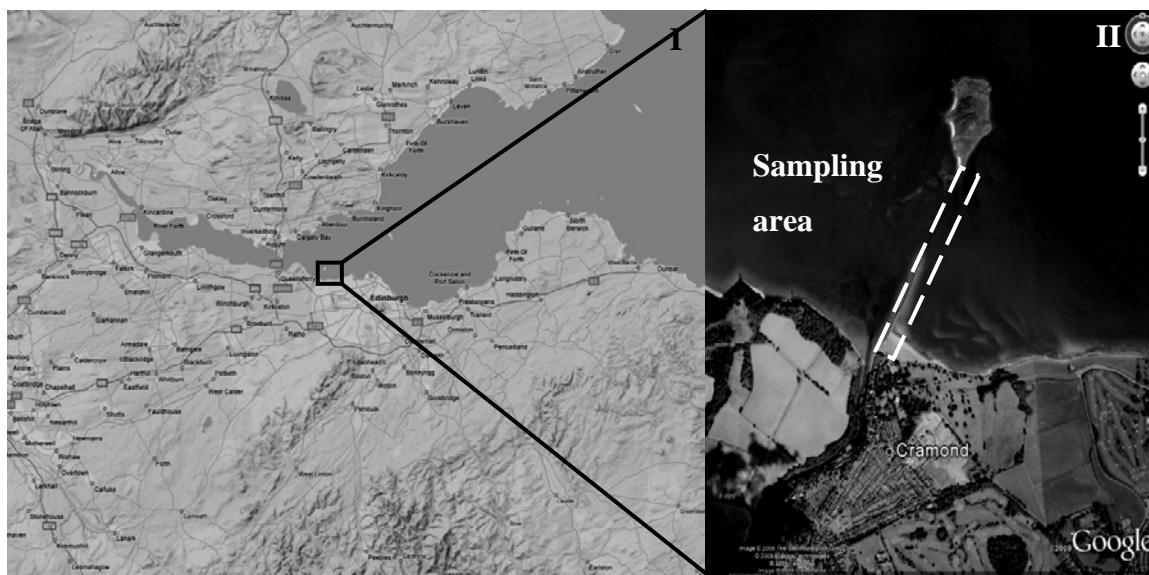


Figure 2.1: Map of the main sampling site for *Mytilus edulis*.

(sources: Google Map (I), Google Earth© 5.0 (II))

*Mytilus edulis* was growing in this area as large mats fixing underlying sandy mud substratum. The individuals were selected by their size (>4cm) on the east side of the footpath.

Maps scale:      I: 1cm = 10km  
                          II: 1cm = 0.3km

These comments were added to the map as ‘place-marks’ where the latitude and longitude were recorded. It was also possible to save these place-marks as a separate file, so the data could be exchanged with other people. Sites from the Outer Hebrides (Scotland) have been recorded photographically using a Konica Minolta Z6™.



Figure 2.2: Presentation of the site data compilation using Google Earth.  
(source: Google Earth© 5.0)

This map represents an example of the type of information stored in a place-mark. The user has only to click on the icon to access the site ecological description and the precise location.

## 2.2 Chemicals, Reagents, Animals, and Other Materials

Chemicals and reagents used in this work were obtained from the following suppliers, Fisher Scientific, Sigma Chemical Co, and VWR-international, unless stated otherwise in the appropriate section.

### 2.2.1 Solutions and buffers

Chemical solutions used for haemolymph sampling were prepared with distilled water. The solutions used for live cells were sterilized by filtration through a 0.2µm cellulose nitrate membrane (Whatman).

Solutions and their compositions used in this project are listed in their relevant sections. Solutions were stored at room temperature unless stated otherwise.

### 2.2.2 TBS, 3xTBS and 3.8% formaldehyde in 3xTBS

One litre of TBS was prepared with distilled H<sub>2</sub>O. The solution contained 8g of NaCl, 0.2 g of KCl and 3 g of Tris base. For 3xTBS, the quantities of NaCl, KCl and Tris base were tripled. Concentrated HCl was used to adjust the solution at pH 7.4.

The haemolymph fixative was prepared by a 1:10 dilution of 38% formaldehyde in 3xTBS.

### 2.2.3 Marine agar

Fifty two grams of Difco™ Marine Agar 2216 were dissolved in 850 ml of distilled water. Fifteen grams of agar were then added, the pH adjusted to 7.8 and the volume brought to one liter. The medium was autoclaved for 15 minutes at 121°C and was poured in sterile Petri dishes held near a Bunsen flame.

## 2.3 Histological investigations

Mussels were fixed in formaldehyde 10% in one strength TBS. Individuals were dissected into the following tissue groups: adductor muscle, visceral mass, mantle, gills, and foot. The samples were dehydrated in successive baths of 70% ethanol, 90% ethanol, absolute ethanol, Histo-clear® (xylene subs., National Diagnostics, Manville, NJ) and then in paraffin wax at 60°C. They were embedded in wax, and cut at 7 µm thickness. The preparations were dewaxed in two baths of Histo-clear for 5 minutes. They were rehydrated in successive baths of ethanol 90%, ethanol 70% and in acidified tap water. Finally, they were stained in Wright stain for 90 seconds, washed in tap water, and air-dried. The slides were mounted in DepeX mounting solution (BDH Laboratory, Poole, Dorset, UK).

Microscopic photography was undertaken on a Zeiss Microscope (Zeiss, Germany) equipped with an AxioCam MR™ and recorded with the software AxioVision™ 4.7. The photos were assembled as a map on MS PowerPoint (slide size: 140cm x 140cm).

## 2.4 Animal experimentation

### 2.4.1 Conventional sampling of haemolymph

*M. edulis* were sampled on site. The valves were forced open using dissection scissors. Haemolymph samples were collected from the adductor muscle using a 23G needle on a 2.5ml syringe filled with a solution of 3.8% formaldehyde (Sigma) in 3xTBS as shown in Figure2.3. The cells were then left for 1hour for the fixative to take effect.

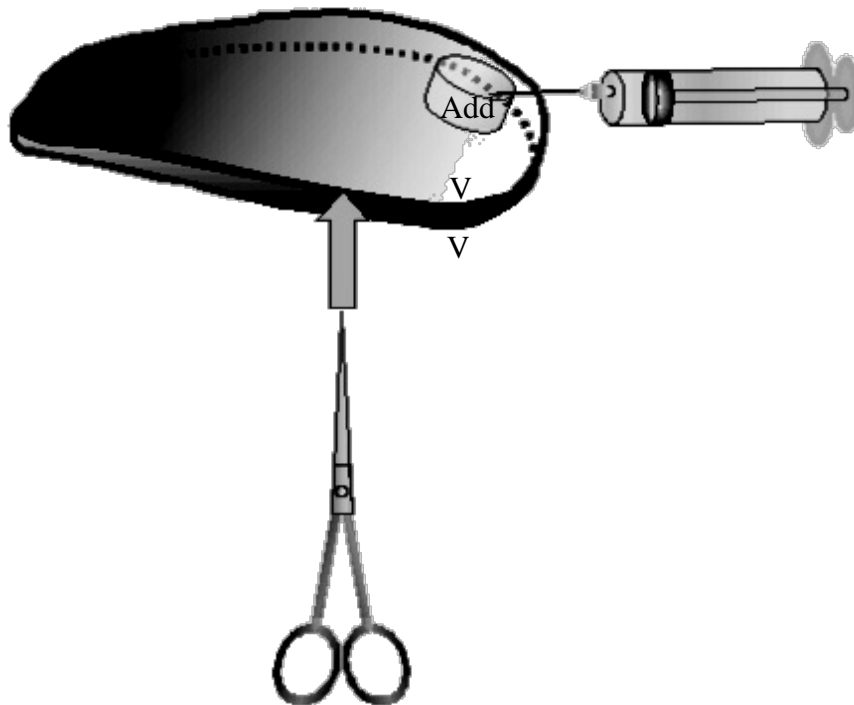


Figure2.3: Standard sampling procedure of *Mytilus edulis* haemolymph.

The valves (V) were forced open using dissection scissors inserted in the top 1/3 length of the shell. Haemolymph samples were collected from the adductor muscle (Add), visible as a white tissue surrounded by the brown mantle edge and the orange/yellow mantle. The needle was puncturing the peri-muscular membrane to reach the haemolymphatic sinus at the adductor muscle centre.

### 2.4.2 Cannula construction

In an attempt to overcome the inter-individual variability, a cannula system was developed that was an improved version of the technique developed by Staff and Widdows (personal communication) from Plymouth Marine Laboratory (Appendix II). To increase the protection of the cannula, an Eppendorf with screw cap was used. The top 1cm was cut using the disk cutter tool of the Dremel power tool (Wisconsin, USA). The centre of the screw cap was filled with silicon (Henkel (Unibond® Super All Purpose Silicone Sealant), Winsford, UK) using a silicon gun and left to set for at least 24h.

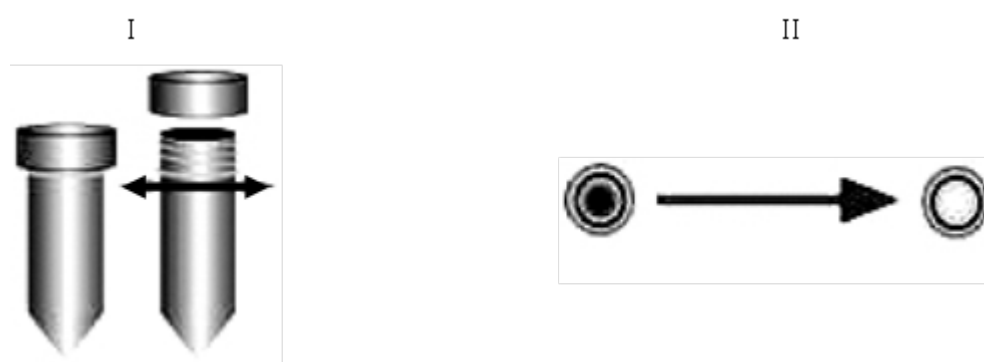


Figure 2.4 : 1.5ml centrifuge tube and Screw-cap preparation preparation.

I: The tube should be cut 1mm below the lower ring as it gives a better adhesion property to the mussel shell.

II: The inner sides of the cap should be slightly altered using the rotary ball tool to allow a better attachment of the silicon. When injected, the nose of the silicon gun should touch the top of the cap, and then should retract as the silicon is filling the cap. As the internal cavity is full, an extra amount of silicon should be added to allow a good sealing of the cannula when it is assembled.

The cannula itself was cut out of a gas chromatographic column (GCC, Chromopack, wcot fused silica, 50 m x 0.32 mm, coating CP-SIL 8 CB low bleed/MS, DF=0.25) cut into 2.5 cm sections. A polyester block was covered with aluminium foil. The GCC section was inserted 1cm vertically into the polyester. The cut base of the Eppendorf was then positioned, with the cannula in its centre, onto the aluminium using super glue. Using a 1ml plastic syringe, 3 to 4 mm of epoxy was injected into the setup to hold the cannula into the cut Eppendorf (Figure 2.5). The system was left to set for at least 24 hours.

Both set-ups were left at least 24 hours under UV for sterilisation. The Eppendorf complex was dissociated from the aluminium easily as the gluing strength was higher on the plastic than the aluminium. The excess of GCC sections were cut short at the top (as the siliconed screw cap closed it) and at 2 mm at the bottom to compensate for the shell thickness and the epoxy layer required to fix the cannulation setup onto the organism.

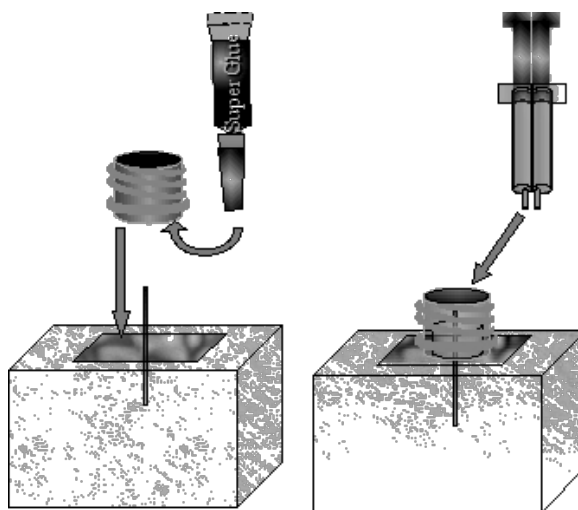


Figure 2.5 : Cannula body preparation.

The bottom part of the centrifuge tube was applied with superglue, it was pressed gently for 10 seconds to allow a good contact with the underlying aluminium foil. When the epoxy was injected, the syringe made gentle circles around the cannula to avoid trapping air bubbles. No epoxy dribble should be left on the side of the inner tube, as it would have prevented the cap to fit.

Mussels were prepared by first roughening the area of the shell corresponding to the adductor muscle with sand paper. The shell was then cleaned up with 70% ethanol (to clean, disinfect and dry). A hole was drilled (0.5-1.0 mm diameter) vertically above the adductor mussel with a Dremel. The cannulation setup was set in place with epoxy resin. The animals were placed back into the tank to recover for a minimum of 1 week.

Haemolymph samples were collected from the cannula using a 30G needle on a 1ml syringe, and filled with a solution of 3.8% formaldehyde (Sigma) in 3xTBS. The sample was analysed by flow cytometry as presented in Chapter 2.5.4.1 .

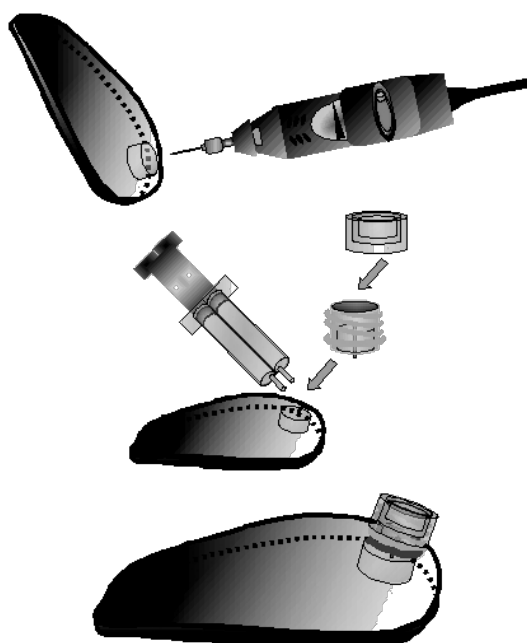


Figure 2.6 : Fixation of the cannula.

A metal mesh was used at high speed to drill through the shell. Fast setting epoxy was applied at the bottom of the cannulation. When the shell had dried from the ethanol, the cannulation was set in place. The recovering animal was then laid so that the cannulation was horizontal until the setting of the epoxy.

### 2.4.3 Surgical window and gill activity

A setup has been adapted to observe the gills directly (Foster-Smith, 1975). A 4 cm<sup>2</sup> hole was cut in the shell using the disk tool of the Dremel. The underlying mantle has been excised and a standard cover slit was glued with epoxy to allow the direct observation of the gills.

To investigate the gills activity, in a joint project with Maia Strachan (PhD student, School of Life Sciences, Heriot Watt University), *Mytilus edulis*, *Dosinia lupines* (Linnaeus, 1758), *Modiolus modiolus* (Linnaeus, 1758), and *Venerupis senegalensis* (Gmelin, 1791) had their shells cut to set-up a surgical window allowing an in-vivo observation of the gills. The organisms were kept in 50 l plastic tanks in aerated filtrated seawater and fed once a day with *Tetraselmis ohui* cultured in F/2 media (Stein, 1973).

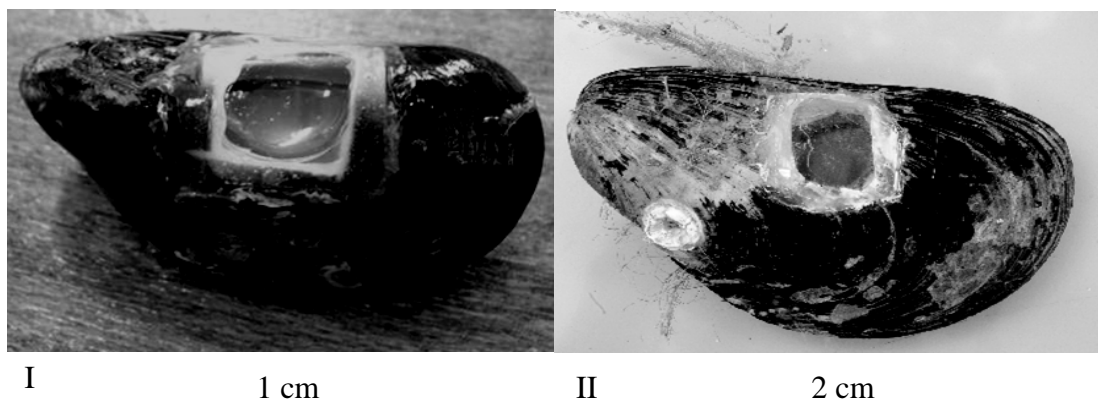


Figure 2.7: *Mytilus edulis* (I) and *Modiolus modiolus* (II) with surgical window showing an overview on the gills.



Using dissection tweezers, glass cover slips were heated over a Bunsen burner until the softening point (to gain a good plasticity). Then different curves were given, and the glass was air cooled for 30 seconds. They were brought back to the flame once again to reduce the internal tensions as much as possible (process known as ‘annealing’). The annealed glass slip was then let to air cool slowly to avoid thermal shock that could lead to its breakage<sup>1</sup>. The best fitting cover slip was selected for a specific individual by trial and error.

The shell of the individual was cleaned of any epizoic organisms and the targeted area disinfected with a cloth impregnated with ethanol 70%. Once the area was dried, a disk fixed on a Dremel was used to cut the desired area. The protection of goggles and mask was necessary as the work can be generating large amounts of dust. The cut area was cleaned up using a cotton bud and 70% ethanol.

Once the shell had dried, epoxy glue was set on the edges and the glass applied. The quick setting epoxy was left to polymerise for 2 hours before the organisms were transferred to the aquarium. A very low mortality was observed after 1 week (<5-10%) in *Mytilus edulis* and *Modiolus modiolus*. On the other hand, *Dosinia lupines* and *Venerupis senegalensis* showed higher mortality rates (up to 50% after a week).



Figure 2.8: Scheme of the major steps of the surgical window protocol.

The process requires the simultaneous work of two persons, one person carrying out the surgical intervention, the other one gluing the cover slip onto the shell. This allows a good quality of work and a good survival rate.

<sup>1</sup> <http://www.ecu.edu/glassblowing/gb.htm>

#### 2.4.4 *Mytilus edulis* euthanasia

To minimise the stress of euthanasia, several leads were followed. The first protocol investigated was the frozen death, but some survivals have been reported in the literature where *Mytilus* tolerated temperatures as low as  $-20^{\circ}\text{C}$  (Loomis et al., 1988); (Vallière et al., 1990). For that reason, a second method was introduced. The nervous system of the animal was mechanically disrupted as presented in Figure 2.9.



Figure 2.9: Description of *Mytilus edulis* euthanasia.

A mechanical disruption of the nervous system was therefore necessary to permit an ethical euthanasia. The bivalve was slightly opened (1), the adductor muscle was sectioned (2) allowing a comfortable access to the soft tissues, then the visceral mass and the underlying nervous system was sectioned (3).

## 2.5 Cell investigation

### 2.5.1 Cell separation on discontinuous Percoll gradients

To separate *Mytilus edulis* cell populations, based on their relative density heterogeneity, a discontinuous Percoll gradient was used.

Friebel and Renwartz (1995) have demonstrated the relevance of the discontinuous Percoll gradient (Pharmacia, Uppsala, Sweden) to segregate fixed *M. edulis* haemocytes. The density separation allows a high purity of eosinophils (up to 95%), but does not segregate properly the basophils from hyaline cells.

The Percoll was diluted in saline solution in 100 ml aliquots. The layers consisted of 1.5 ml of the desired Percoll dilution successively added in a 15 ml centrifuge tube. The sample (1.5 ml) was added at the surface of the discontinuous gradient and was centrifuged at 120g for 15 minutes.

To improve the speed and ease of the discontinuous gradient layering, 1000  $\mu$ l pipette tips were transformed to change their vertical flow into horizontal flow as follows:

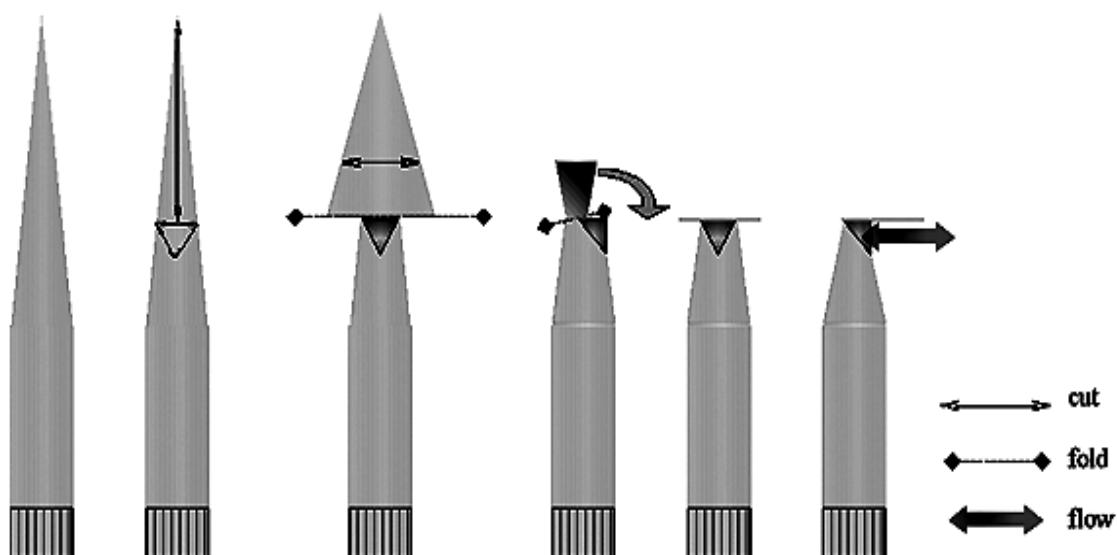


Figure 2.10 : Scheme of preparation horizontal flow pipette tip used for the set-up of discontinuous Percoll gradient.

This technique allowed a quick setup of the discontinuous gradient and was cheap and quick to prepare.

The five layers from the discontinuous gradient were ranging from 90%, 43%, 38%, 33%, and 14% in saline solution. The technique was visually improved by the addition of five microlitres of eosin in the 43% Percoll aliquot and five microlitres of malachite green in the 33% aliquot as shown in Figure 2.11

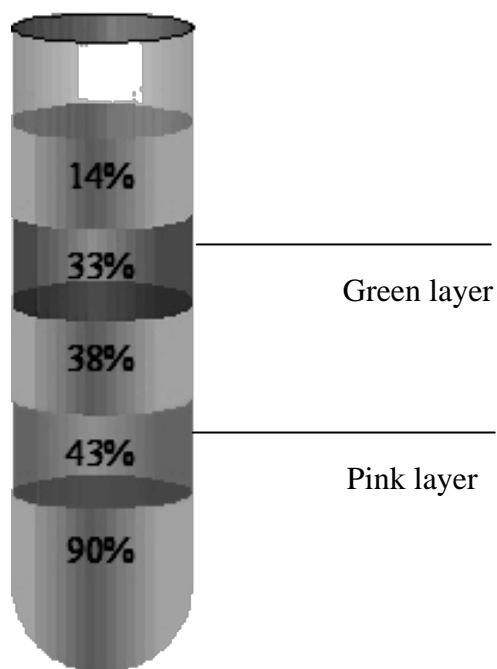


Figure 2.11 : Scheme of the discontinuous gradient.

These stain additions allowed a visual control of the good discontinuous gradient conservation as well as a partial staining of the cells passing through the coloured layer.

## 2.5.2 Ocular investigation

### 2.5.2.1 *Ocular cell concentration measurement under light microscopy*

Haemolymph cell counts were made using an enhanced Neubauer chamber under bright field microscopy. Seven microlitres of the fixed cell suspension were injected into the chamber. Cells were counted with the help of a hand counter and the total concentration per millilitre was established using the formula:  $c = n * 10^4$  (where:  $c$  = cell concentration in cells/ml,  $n$  = number of cells/mm<sup>2</sup> area, and  $v$  = volume counted =  $1 \times 10^{-4}$ ml).

### 2.5.2.2 *Wright's stain colouration*

The Wright's staining technique allows the discrimination of cell populations of haemocytes. Haemolymph samples from *Mytilus edulis* were collected from the adductor muscle using a 23G needle (BD Microlance™ 3, Fraga, Spain) on a 2.5ml syringe (Terumo®, Leuven, Belgium) filled with a solution of 3.8% formaldehyde (Sigma, UK) in 3xTBS. The cells were then left for one hour for the fixative to take effect. The total cell count was determined as previously described (Total cell count per field of view). Slides for making differential cell counts were prepared using a Shandon Elliott cytopsin. One hundred microlitres of the fixed cell suspension (approximately  $10^5$  cells) were placed in a cytopsin funnel and centrifuged for 10 minutes at 1000 rpm. The slides were then removed and air dried for 10 minutes (Auffret and Oubella, 1997) before staining in order to distinguish the different cell subpopulations.

To permeabilise the cells, each slide was covered with methanol for 30 seconds, with the excess poured off. A drop of concentrated Wright's staining solution (Gurr™) was added to the slide for 90 seconds. Finally, the slide was washed with tap water and air-dried. Slides were mounted in DePex mounting medium (Sigma, UK) and the cells counted under bright field, at 400x magnification, counting at least 200 cells over at least four fields of view.

With early results, the need to increase the number of cells counted per individual from 200 to more than 1000 appeared necessary. As the methods previously used were time consuming and labour intensive, a more efficient method had to be developed. Image analysis tools were then developed and engineered. This method improved significantly the speed of THC and differential cell count.

### **2.5.3 Image analysis investigation**

#### *2.5.3.1 Cell concentration measurement under light microscopy using image analysis*

The cells were processed as described above and image analysis methods were used to make the counts from the Neubauer chamber as described in 0 .

Images from the Neubauer chamber and microscope slides were captured via a USB video camera (Meaden™, Holland) and were analysed using the freeware program ImageJ (Abramoff et al., 2004), which allowed convenient storage automatization of captured images. Macros were constructed using the record function of the software in a similar manner to MS Excel. This widespread software allows the creation of customised macros. The computer records the macro while the user performs the sequence of functions desired to make them automatic. The recorded sequence is translated into a computing language, which can later be edited as text and rewritten if necessary.

The Neubauer chamber filled with a haemolymph sample was examined under the microscope at 200x magnification. The image was sent to the computer using the TWAIN protocol. The aim of the following macro was to retain relevant information from the image and remove the irrelevant ones. To present the analysis of the cell concentration, we will follow the procedure step by step:

A Neubauer haemocytometer was filled with 10 µl of haemolymph fixed in 3.8 % formaldehyde TBS solution. Five fields of view were photographed using a USB camera under 100x magnifications in bright field. The software used for the data acquisition was Ulead photo explorer SE®.

The original pictures (640x480 pixels) were stored as jpeg files, designated by the sample name and its sampling date. These files were imported into ImageJ as coloured

raster (Pixelised image, as opposed to vector image). The sentences of the following pages are the code lines of the macro. They are described sequentially for a better understanding. Each step of the following macro description will be illustrated as a corresponding sequence of treated images (Figure 2.12 to Figure 2.15). The sequence of image analysis is presented as a sequence of instruction coded in macro language, and each instruction are commented in Table 2.1.

Table 2.1: Description of the script of cell concentration macro.

A: The imported coloured 32-bit images were translated into 8-bit grey scale to allow the image compatibility with further treatments.

B: The function “find the edges” isolates areas with a sharp change in shade (i.e. contrasted forms in comparison with the background). With these fixed haemocytes, the rapid intensity change was due to the haemocyte membrane, bubbles or unwanted artefacts in comparison with the homogeneous background.

C: A threshold was set-up on the treated image, using the value “0” as the background and “1” as a region of high intensity change, such as cells, dust, or small particles.

D: Following the application of the threshold to the image, in order to remove small artefacts (e.g., precipitates, small particles), the image was eroded and dilated. **Erode** removes pixels from the edges of black objects and **Dilate** adds pixels to the edges of black objects. Smaller surfaces were thus removed, the larger ones (i.e. haemocytes) were conserved and the form rounded by the dilatation.

E: The ImageJ function “analyse particles” is counting the number of remaining areas. It is scanning the image until it finds the edge of an object. It then outlines the object, and measures it, and then resumes scanning until it reaches the end of the image. A comprehensive result was displayed automatically in a table giving both the number of areas and a value for each area in pixels. This table can either be recorded on its own or copied to an Excel sheet for later analysis. Further filtration criteria (e.g. area) were applied in Excel to remove artefacts such as small areas (those not removed by the erode/dilate function), and large areas (e.g. air bubbles, mussel tissue, hairs).

<code>run ("8-bit");</code>	A
<code>run ("Find Edges");</code>	B
<code>setAutoThreshold ();</code>	C
<code>//run ("Threshold...");</code>	
<code>setThreshold ( 36, 234 );</code>	
<code>run ("Threshold", "thresholded remaining black");</code>	
<code>run ("Erode");</code>	D
<code>run ("Dilate");</code>	
<code>run ("Dilate");</code>	
<code>run ("Analyze Particles...", "size=12-Infinity circularity=0.00-1.00 show=Nothing display exclude");</code>	E
<code>saveAs ("Measurements", "C:\\Data\\Results.xls");</code>	

MS Excel macros were set-up to calculate the final concentration of the haemocytes from the data table generated in ImageJ. The concentrations of cells were calculated from the number of particles (N), the surface observed ( $S=0.081\text{mm}^2$ (using the graduation visible on the Neubauer chamber)) and the depth of the Neubauer chamber ( $D=0.1\text{mm}$ ), using the formula:

$$C = \frac{N}{S \times D}$$

The result was expressed as cells per microlitre.

The illustrations Figure 2.12 until Figure 2.15 present how to access specific information out of a complex image. In this case, the information is the number of cells, not their shape, not their size or complexity.

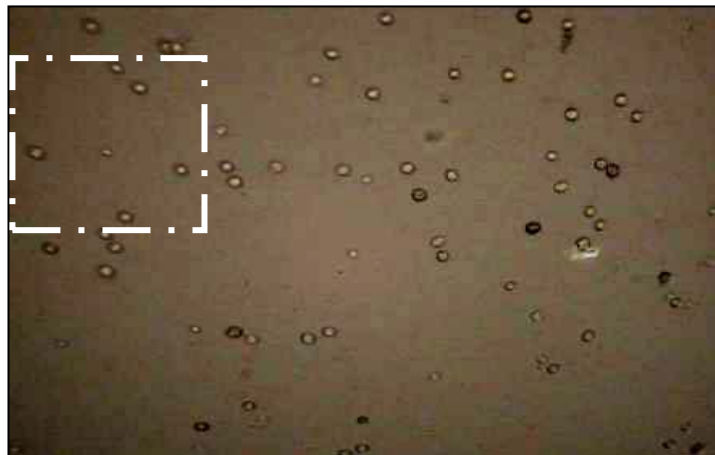


Figure 2.12: Original picture of the Neubauer observation field.

The visual sequence of the analysis will be presented showing only the boxed area of the picture for better visual understanding of the data retrieval procedure.

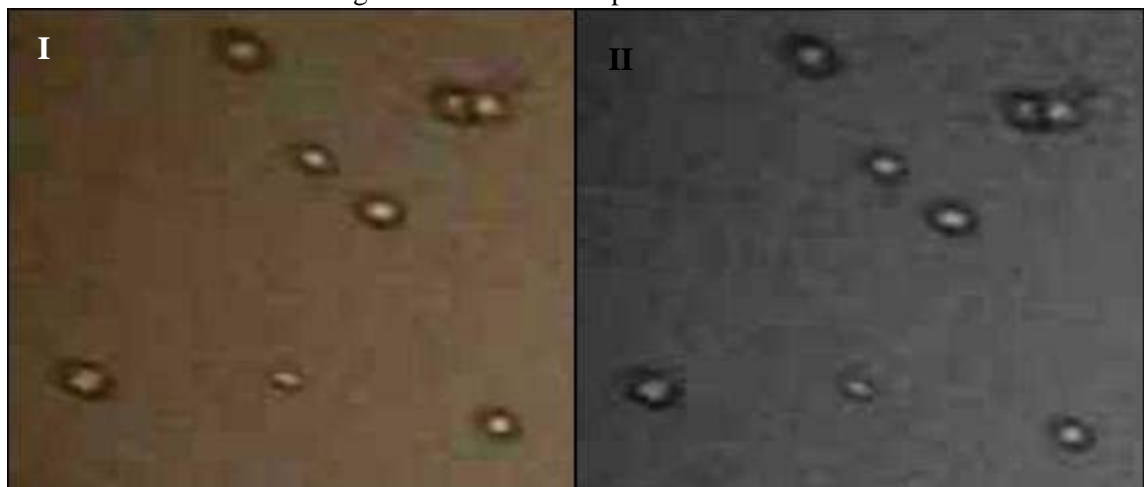


Figure 2.13: First analysis step to change the coloured raster into a gray scale raster. The picture is translated in greyscale; particles in a grey background are the cells.



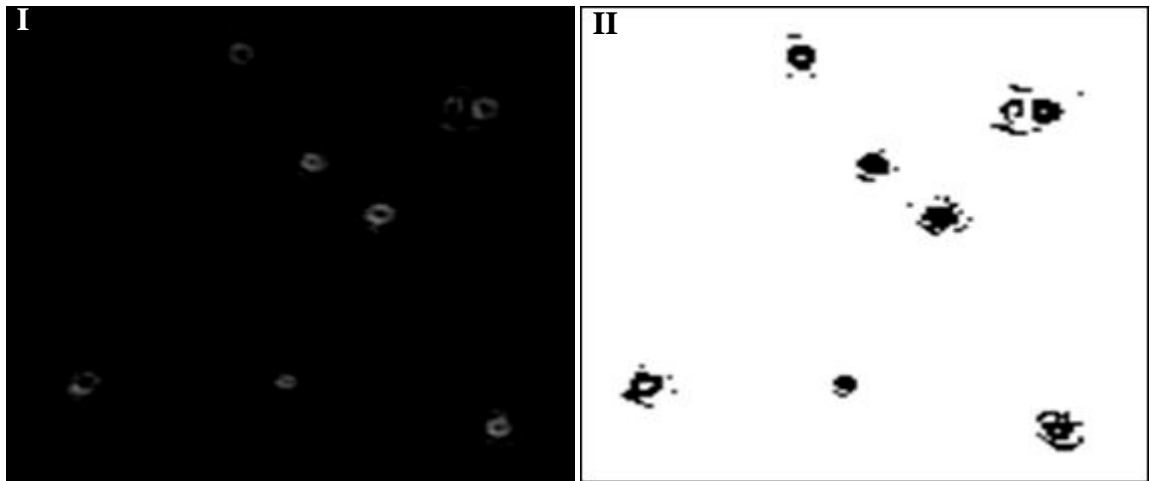


Figure 2.14: Process of 'find the edges' and threshold.

**I:** The function “find the edges” allowed to isolate highest contrasted forms in comparison with the background. In this case, the rapid intensity changes due to the haemocytes membrane in comparison with the homogeneous background.

**II:** A threshold is set-up to transform the previous image into a binary image; the value “0” is the background (white), “1” a region of high intensity change (red): cell, dust, small particles.

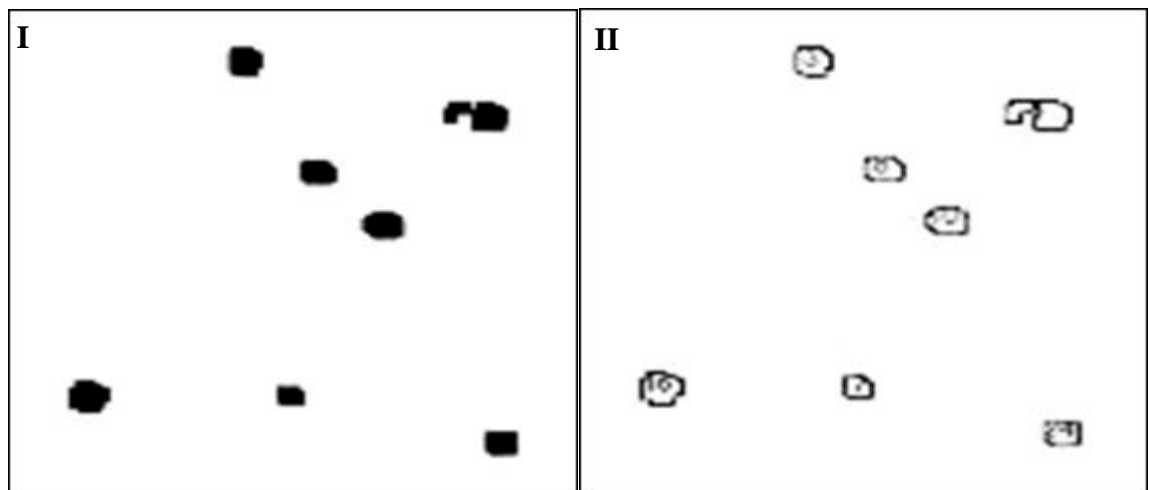


Figure 2.15: Artefact removal and particle counting.

**I:** To remove small artefacts (dust, small particles), the resulting image from the threshold is eroded and dilated. Therefore, smaller surfaces are removed, and bigger surfaces (haemocytes) are conserved and the form is rounded up by the dilatation.

**II:** ImageJ' function “analyse particles” allows us to assess the number of remaining areas and gives a comprehensive result in form of an MS Excel table giving the number of areas and the area in pixels. Further filters (area criteria) could be applied to remove artefact such as large areas (air bubble, mussel tissue, hairs).

### 2.5.3.2 *Using light microscopy and image analysis to determine Cell population count*

This technique was very similar to that described previously (2.5.3 ), with the main difference coming from the setup of a coefficient of confidence to indicate the quality of the analysis achieved by the computer. The previous analysis was aiming to provide a cell concentration. For this analysis, accurate counting was necessary to facilitate the differential cell count of the different haemocyte types. The total number of cells was subtracted from the total number of red cells (0) to obtain the relative percentage of the two populations.

#### **Total cell count per field of view**

The method used to determine the accuracy of the cell count was to detect artefacts of the reworked image. The cleaning up of the artefacts was relatively simple because of their relative small area in comparison with the cells. A lower area limit has to be set-up, allowing us to avoid them in our result.

To discriminate when the computer was analysing as one cell what were in fact two adjacent cells, two functions of the freeware were used: a circularity coefficient (CC) and a ratio perimeter/area (Fe).

A single cell is round, and has a CC close to one (circle); a coefficient close to zero has an irregular shape. From this coefficient, we can establish the confidence of the analysis. By setting up a ranking system (0-0.7=1(irregular shape); 0.71-1=0(circular shape)) and by adding the rank at the end of the analysis, an arbitrary confidence index has been created. A high value of this index suggests that a visual check of the data was necessary and a change of the analysis parameters was advisable. This index was used to reduce the impact of the staining variability.

The ratio perimeter/area (Fe), also called the Feret coefficient, allows the CC to be double-checked. Nevertheless, to avoid the problem of adjacent cells, the microscope magnification was increased to x400 and the post-analysis process improved (using CC and Fe).

The Table 2.2 formalizes the image analyses process in the macro language.

Table 2.2: Macro script for cell count

The script of the macro has been generated directly with the macro generative tool of ImageJ freeware. The script has been later reedited as a text file to fine tune the values of the threshold, or the lower particles size. **A** is the transformation of a coloured picture into a grey scaled picture. **B** is the setup of a threshold converting the grey scale into a binary image based on the value of grey. Finally, **C** is the analysis that will allow the count of the number of cells, and the establishment of confidence for the quality of the analysis.

```

run("Subtract Background...", "rolling=50 white");
run("8-bit");                                     A
setAutoThreshold();
//run("Threshold...");
setThreshold(30, 195);                             B
run("Threshold", "thresholded remaining black");
setAutoThreshold();
run("Analyze Particles...", "minimum=100 maximum=999999
bins=10 show=Outlines display flood record size"); C

```

Subsequent to the image analyses, the numerical data are transferred to MS Excel sheet for further analysis. Each image analysis generates a table with n lines for n cells. The result from the next image of the same slide will be added at the tail of the previous table. The output table of a succession of images allows the possibility of larger samples than could be obtained by eye count, as well as keeping a trace of the original data. The data is used to determine the relative percentage of blue cells against red cells.

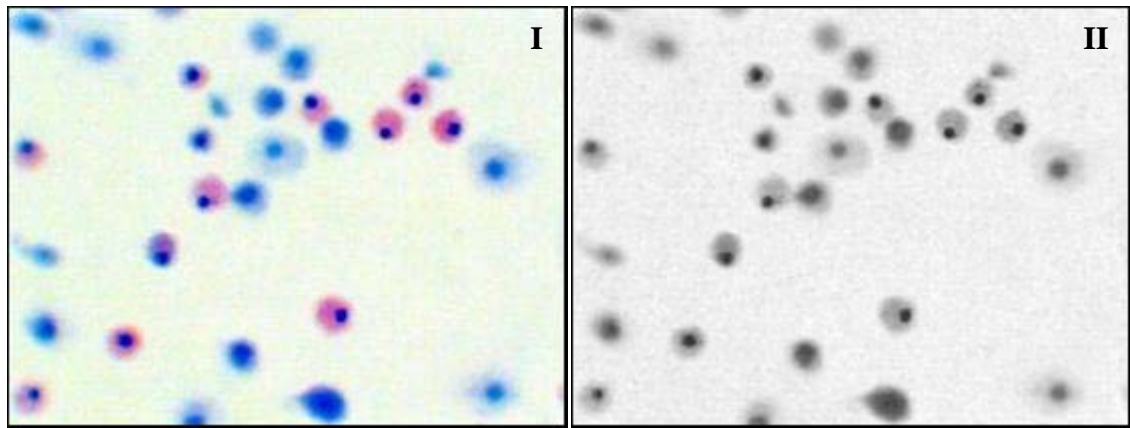


Figure 2.16: Translation of 32-bit coloured picture into 8-bit greyscale image.

In the two pictures, the sequence of information extraction is presented. I is the 32-bit picture. II is the transformation of a coloured picture into a grey-scaled picture.

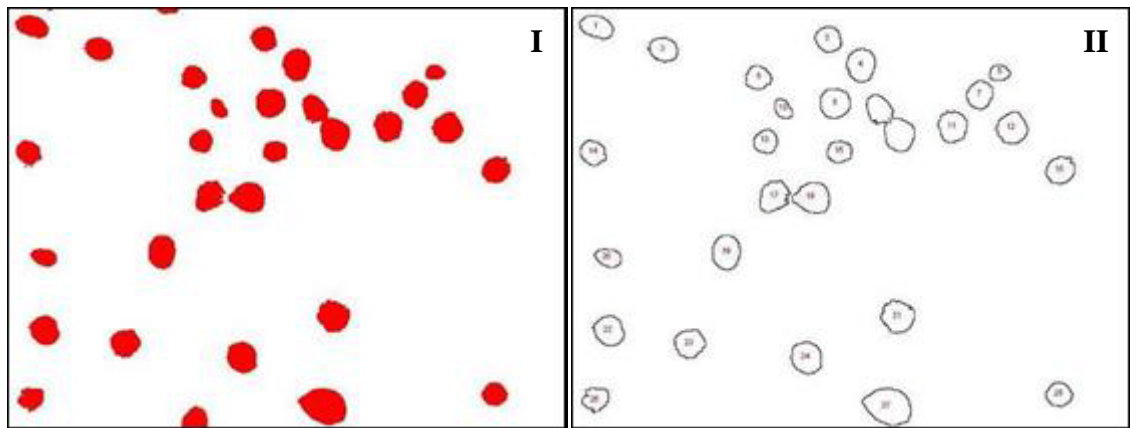


Figure 2.17: Image processing to establish the number of cells.

In the two pictures, the sequence of information extraction is presented: I is the setup of a threshold converting the grey scale into a binary image based on the value of grey. II is the analysis that will allow the count of the number of cells, and the establishment of confidence for the quality of the analysis.

### **Determination of differential cell count**

Several methods exist to identify cells of a particular colour, but all have limits. Some methods require the computer to learn the variation of colours. The learning method was investigated with the software Visiopales® developed by the French company Opales© for quality control by image analysis in industry, but due to the levels of staining variability, the developer of the software advised us to follow another approach.

The ImageJ program allowed reworking and compiling an image based on each of its fundamental colours, splitting it into its red, blue and green components. The green component of the picture was of a bad quality; caused by the characteristics of the CMOS sensor of the video camera used. The red and blue, components were of higher quality, and were subtracted. The resulting picture showed the red cells without the background.

This allowed accessing the targeted information: the red stained cells. This method was less prone to staining variability when this variation came from its strength, but in some cases, an uneven staining and non-specific staining could not be analysed. Other ways was investigated, without satisfactory result (use of the green component, other logic operations on the image, independent rework of each component, etc.).

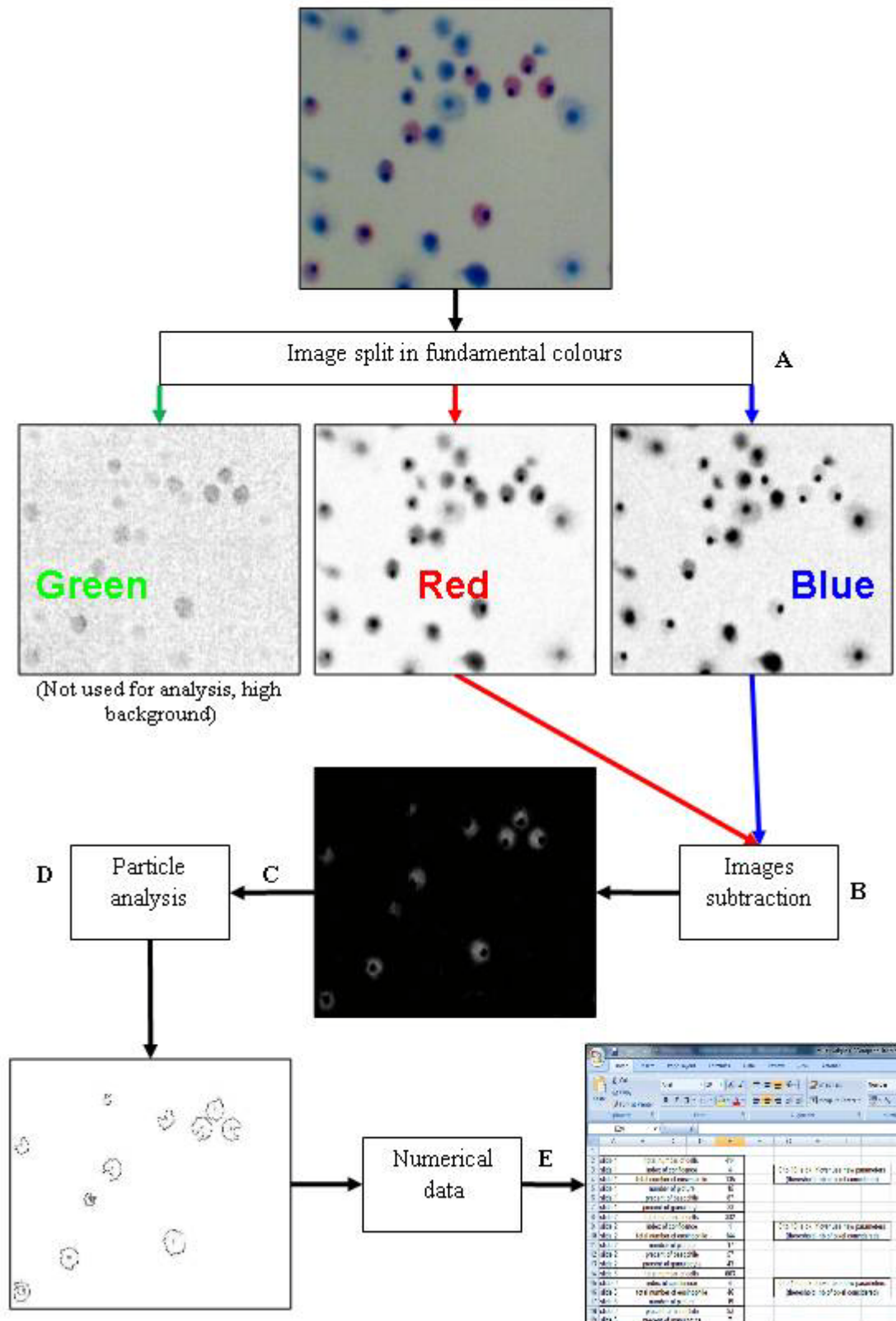


Figure 2.18: Image processing sequence for differential cell count.  
(see Table 2.3 for A-E)

Table 2.3 shows the image analyses process in the macro language.

Table 2.3: Macro script for red cell count

The previous page and this table are presenting the sequence of information extraction out of the coloured image. **A** is the split of the original picture (OP) into its three fundamental colours. **B** is the subtraction of the red from the blue component of the OP; this allows the specific extraction of the regions of OP with high levels of red. **C** is the setup of a threshold to select specifically the region of high red dominance. **D** is the count of the resulting particles. Finally, **E** is the exportation of the numerical data to Excel.

<code>run ("RGB Split");</code>	<b>A</b>
<code>run ("Image Calculator...");</code>	<b>B</b>
<code>setAutoThreshold ( );</code>	
<code>//run ("Threshold...");</code>	
<code>setThreshold ( 24, 52 );</code>	<b>C</b>
<code>run ("Threshold", "thresholded remaining black");</code>	
<code>setAutoThreshold ( );</code>	
<code>run ("Analyze Particles...", "minimum=35 maximum=999999 bins=20 show=Outlines display flood record size");</code>	<b>D</b>
<code>copy/paste data to Excel</code>	<b>E</b>

Subsequent to the image analyses, the numerical data are transferred to an Excel sheet for further analysis. Each image analysis generates a table with n lines for n cells. The resulting next image of the same slide was added at the tail of the previous table. The output table of a succession of images allows to have larger samples than the equivalent obtained by eye count, as well as to keep a trace of the original data.

## 2.5.4 Flow cytometry

The opportunity to use this technique arose after the development of the image analysis tool. Due to its ease and speed of use, accuracy and precision achieved through flow cytometry were greater than in previously described methods (see 0), so that it became the main technique used for the acquisition of haemocyte data.

### 2.5.4.1 Normal sample analysis

A flow cytometer (Partec SL) used for the measurements was equipped with a true volumetric absolute counting device allowing the measurement of the sample cell concentration (see introduction). The illumination source was a 488nm solid-state laser, and the parameters used were forward and side scatter as they allowed a good discrimination of the three cell types. In addition, the fluorescence at 520nm (green, FL1) was also used for data 'clean-up' as the cells have a measurable auto fluorescence. The data were acquired using the FlowMax© software (Partec, Germany), recorded in a 2.0 FCS format and later analysed with the freeware WinMDI (**Windows Multiple Document Interface for Flow Cytometry**, <http://facs.scripps.edu/software.html>).

For a normal data acquisition, the cells were not stained: 200µl of haemolymph were diluted in 800µl of 3xTBS in the sample tube. The recorded parameters were FSC (forward scatter), SSC (side scatter), FL1 (fluorescence at 520nm), FL2 (fluorescence at 590nm) and FL3 (fluorescence at over 620nm).

### 2.5.4.2 DiOC<sub>6</sub> staining

DiOC<sub>6</sub> (3, 3'-dihexyloxacarbocyanine iodide), a fluorescent dye, specifically stains the cells' endoplasmic reticulum, vesicle membranes and mitochondria. Binding to these structures occurs via the dye's hydrophilic groups. The DiOC<sub>6</sub> has its maximum absorbance at 484nm and emits at 501 nm. The 488nm blue laser was therefore able to excite it and the 520nm filter permitted the measurement of its emission. To stain cells, five microlitres of DiOC<sub>6</sub> (50 nM, dissolved in DMSO) were added to the sample five minutes before analysis.



#### 2.5.4.3 *Wright staining*

The use of the same stain in flow cytometry, than in microscopic observation, allowed a more reliable comparison of previous data. Wright's stain is composed of methylene blue (not fluorescing), methanol, and eosin (maximum excitation at 490nm and emission at 530nm). Five microlitres of Wright were mixed with 100µl of fixed haemolymph diluted in 895µl of 3xTBS. After 10 minutes of reaction, the sample was analysed as a normal run.

#### 2.5.4.4 *Other flow cytometers used*

Later in the project, two opportunities arose. The use of a BD FACS™ flow cytometer allowed us to double check our local instrument data in S<sup>t</sup> Andrews University. This tool was also used in the analysis of cells separated on discontinuous Percoll gradient (2.5.1).

The direct evidence by cell sorting on the BD FACSCalibur™ in the Queen's Medical Research Centre (University of Edinburgh) confirmed the different cell populations.

## 2.6 Microfluidics experimental setup

Microtechnologies allowed novel activities to be performed on cells. In collaboration with Maïwenn Kersaudy-Kerhoas (PhD student, School of Engineering and Physical Sciences, MISEC), we investigated a microfluidics system that allowed a segregation of the plasma from the cells (detailed outline of the system available in the publication in Appendix VIII). The chips were manufactured by Epigem Ltd (Redcar, UK) using a standard lithography process (further information on the fabrication process in the publication in Appendix VIII).

The primary function of the setup was a system that could separate cells from their medium. The equivalent technique used in a laboratory on the macro scale was centrifugation. This method was more stressful for the cells: an increase of the cell debris was observed by flow cytometry, as well as an increased cell aggregation. The microchip technique represents a gentle way to separate cells from their medium.

Briefly, a sample of cells was injected into the microchip at known flow-rate. The cell concentrations were later determined in the outputs of the chip using relative turbidity by eye, light microscopy and flow cytometry. The system was tested at different flow rates and with different lengths of collector tubes. For the details on the precise procedures and mechanisms, see the publication in the Appendix VIII.

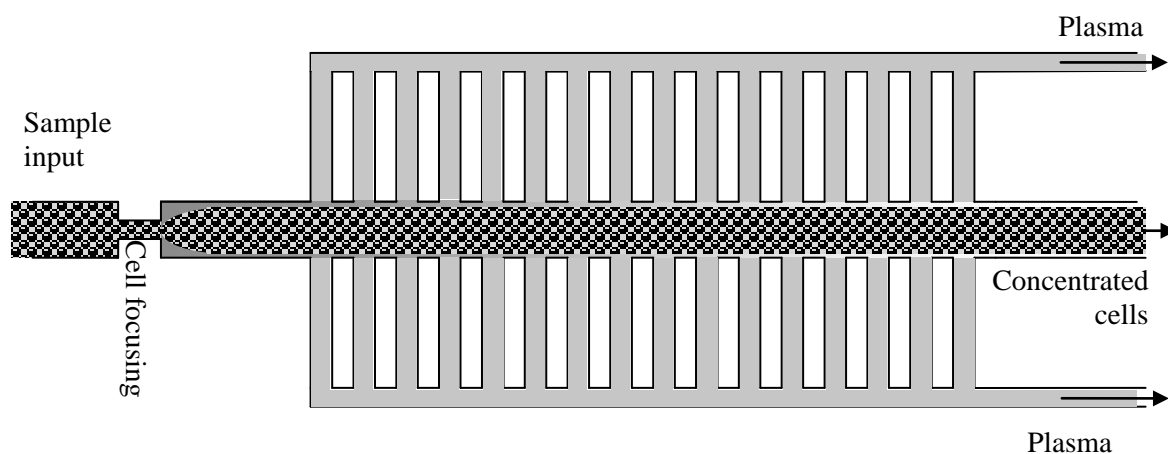


Figure 2.19: Scheme of a microfluidics chip used as a cell concentrator.

This drawing presents the principle of the microchips' effects on haemolymph studied in the joint project

## 2.7 Impact of barium

To investigate the impact (feeding patterns, survival, immune patterns) of suspended solids on *Mytilus*, the following process was adopted.

Briefly, three species were exposed to a homogeneous amount of barium over a period of five days using an experimental setup of Maia Strachan (Figure 2.20). Barium is a compound used by offshore oil platforms in the drilling processes. This compound is known to be chemically none reactive.

The organisms were fed every morning with an algal suspension. The mussels used for the experiments came from Cramond Island for cannulated and not cannulated *Mytilus edulis*, from Loch Creran for the horse mussel and from Oban for the farmed mussel, purchased at Eddie's Seafood Market (7 Roseneath Street, Edinburgh EH9 1JH).

For animals with a surgical window, photography work was done using a Leica® camera mounted on a Leica® M50 and acquired on the Adobe® software PaintShopPro™.

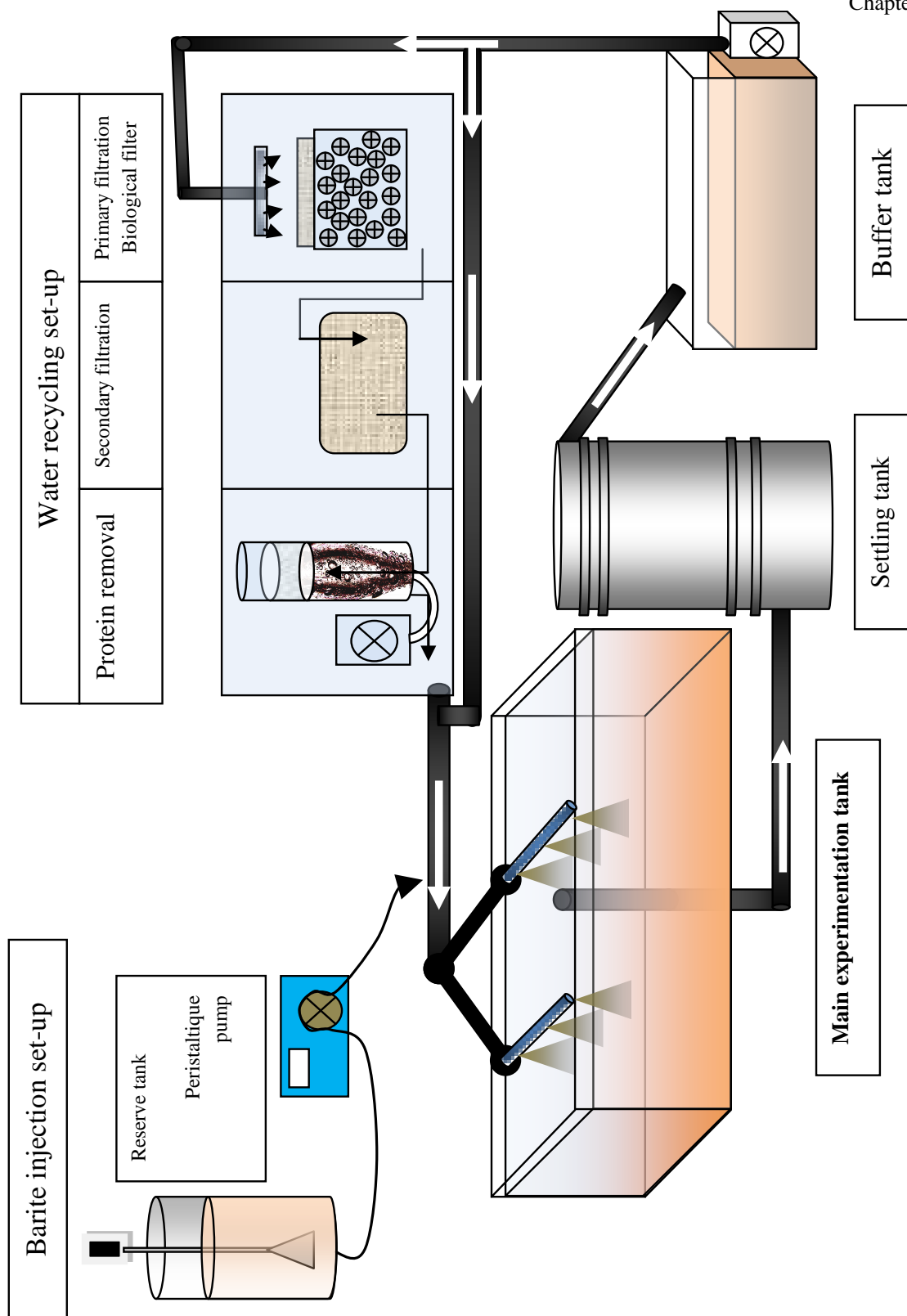


Figure 2.20: Experimental setup to study the impact of barium on bivalves. The water is first mixed with the barium, homogeneously added in the main experimental tank. The excess water is collected at the centre of the tank, is let to settle in the stelling tank then sent to the buffer tank. A pump re-injects the water back in the system and in the treatment system to remove the excess nutrient through a biological filter, and to remove the protein using an air trap.

# Chapter 3

## Investigation of circulating haemocytes of *Mytilus edulis*



Title: Reflexions  
(the point of view twists the reality)

Photo of the Union canal between Edinburgh and Glasgow (Scotland).

This photo has not been altered, only set upside down. The resulting effect leaves the observer with the impression of indefinable abnormality.

This metaphoric image infers the misleading understanding of experimental results when the undertaken assumptions are unfortunate.

### **3 Investigation of circulating haemocytes of *Mytilus edulis***

#### **3.1 Introduction**

As presented in Chapter 1, the investigation of circulating haemocytes was originally carried out by bright field microscopy, and then the investigation evolved with the tools available. In a similar manner, this project has been following a temporal dynamic of investigation technologies. They evolved from opportunities arising by new contacts and new equipments, the curiosity in new technology development and the questioning of the previously used technique.

As the project was developing, large variability was observed in the published and generated data sets. Questions were, at first, directed on the tools used during experiments. Uncertainty analysis was established to evaluate the possible variation arising from the laboratory equipment. The accuracy of the result is the sum of the accuracies of every tool used in an experiment.

In the conventional study of circulating haemocytes, data obtained are (1) their concentration (C) obtained by the Neubauer chamber count and data obtained by differential count of the cell populations as the percentage of the three differentiable cell types (2, 3, 4), by bright field microscopy count of Wright' stained haemocytes preparation. Therefore, the data collected are four sets of information, namely: cell concentration and percentage of hyaline cells, basophils and eosinophils.

The experimental section 3.2 investigates the accuracy of the conventional procedures. As the methodologies were judged inaccurate, alternative methods were investigated. The use of image analysis allows the elimination of the observer bias and increases the sampled size from 200 counted cells to up to 1000 counted cells. However, it reduces the information collected, as the technique could not discriminate hyaline cells from basophilic cells. The data collected was a set of three information, namely: cell concentrations and percentages of blue cells (hyaline and basophils) and red cells (eosinophils). It was hoped that the enhancement of sample size would mitigate the effects of variability. The image analysis method increased the number of measurement, (number of analysed haemocytes), but the resulting biological variability from organism to organism was not decreased as showed in the section 3.3. In addition, both methods (conventional and image analysis) are relying on the assumption that all haemocytes are equally adhesive to the microscope slide during the cytospin preparation. If not, the percentage of the haemocytes population calculated could be subject to a bias due to a differential adhesiveness of the different cell types due to their shapes and sizes, presented in 3.2.3. It was concluded that the sample size had to be increased and a technology not depending on cell adhesion used.

Flow cytometry avoided the problem of the cell adhesion question as the cells are in suspension in a liquid during the measurement, but it required first to compare it with previous methods to validate its use. This comparison is presented in 3.4. It allows an increase of analysed cells (up to  $10^5$  haemocytes). A similar technology is investigated in a lab-on-chip project (3.5). The lab-on-chip project allows a first approach of the cell behaviour in a moving liquid. The flow cytometry allows the analysis of a large number of cells and gives more information than the previously described methods. The data collected are six sets of information, namely: cell concentration, cell size, cell complexity, and cell fluorescence on three wavelengths, at a lower uncertainty level.

The results presented in the following paragraphs present the uncertainty levels within the technique calculated for each method in relation to the observed variability, the validation test of the methods and the data obtained in the microfluidics project.

## 3.2 Visual cell count using bright field microscopy and Wright's stain

### 3.2.1 Uncertainty level of THC

The measurement of the uncertainty of the observer was established by repeating the conventional method of eye count against the rigorous method of photo spotting. In this method, the field of view counted by eye is photographed. The image is then counted by marking systematically each cell observed by a coloured on the computer screen where the picture is displayed. The method is time consuming but leaves no room for miscounting. The comparison of the eye count and the spotting count give the uncertainty of the variability induced by the observer. On a set of 20 haemolymph samples, each sample was represented by at least 10 pictures. The count was done under the microscope and then using screen counting. The average uncertainty was evaluated at +/-5%.

After evaluating the observer bias, the uncertainty was evaluated for the experimental procedure of the Neubauer chamber count. The error levels from the syringe were estimated, and for the pipette are taken as levels given by the manufacturer. The following equation represents the uncertainty level of the typical Neubauer count result:

From the procedure:  $\Delta_{total} = \Delta_{syringe} * 2 + \Delta_{micropipette} + \Delta_{observer}$

Where:

From the sampling:

$\Delta_{syringe} = +/-100\mu\text{l}$  of  $750\mu\text{l}$  (or 13% for a measurement of  $750\mu\text{l}$ )

as it is used to measure successively the fixative volume and then the haemolymph volume, the uncertainty is doubled, therefore  $\Delta_{syringe} = +/- 26\%$

From the Neubauer chamber count:

$\Delta_{micropipette} = +/-2\%$  of volume

$\Delta_{observer} = +/-5\%$  typical uncertainty (3.2.1)

Therefore, the experimental procedure generates a potential maximum uncertainty of 33%.



### 3.2.2 Investigation of results of THC

The conventional method of investigating the concentration of the circulating immune system of *M. edulis* was investigated with 20 individuals collected in Cramond and acclimatised in the aquarium for at least three days. We observe a variation of up to a factor 10 in the cell concentration through the different individuals.

A high variability is observed when using eye THC determination, and the data variation can be explained in the third of their proportion by the experimental procedure. The distribution of the THC does not appear to be normally distributed.

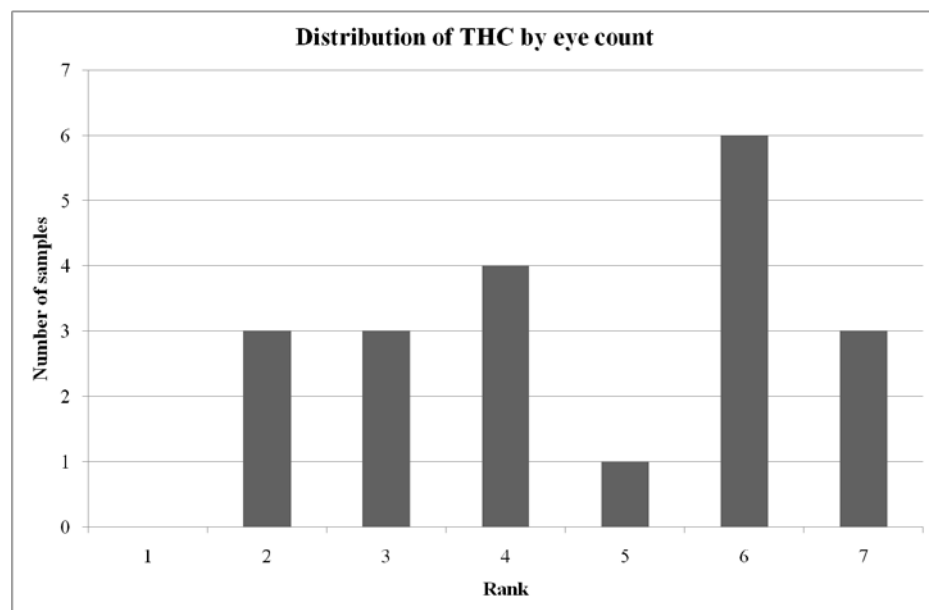


Figure 3.1 : Distribution of THC using the conventional Neubauer cell count.

### 3.2.3 Ambiguity of cytopsin technique

To assess the question of the differential attachment of the different cell types, it must be considered that the haemocytetes are fixed in formaldehyde. The mechanical properties of cells are altered and present an increased rigidity (Vassar et al., 1972). As the rigidity is increased, we can assume that the smaller cells have a smaller attachment surface in comparison with bigger cells. This assumption then allows us to question the homogeneity of cell attachment of the different cell types.

This hypothesis was assessed qualitatively by the observation of the surface edges of cytopsin preparations. A boundary of agglomerated cells is systematically observed (Figure 3.2). This artefact is a consequence of the sample migration from the microscope slide surface to the absorbant paper surrounding the preparation area during the attachment phase of the centrifugation. The observed cells are generally big and have strongly stained (dark blue or very red) eosine.

The total uncertainty of the technique cannot be established as the output of the experiment as a percentage and the reproducibility of cytopsin preparation has not been established, in the point of view that no study has been established to prove the equal attachment of each cell type to the slide. But, as presented later in Figure 3.17, hyaline cells show a different behaviour in microfluidic systems compared with the two other groups.

Figure 3.2 shows the aggregated cells at the fringe of the cytopsin preparation stained with Wright's stain.

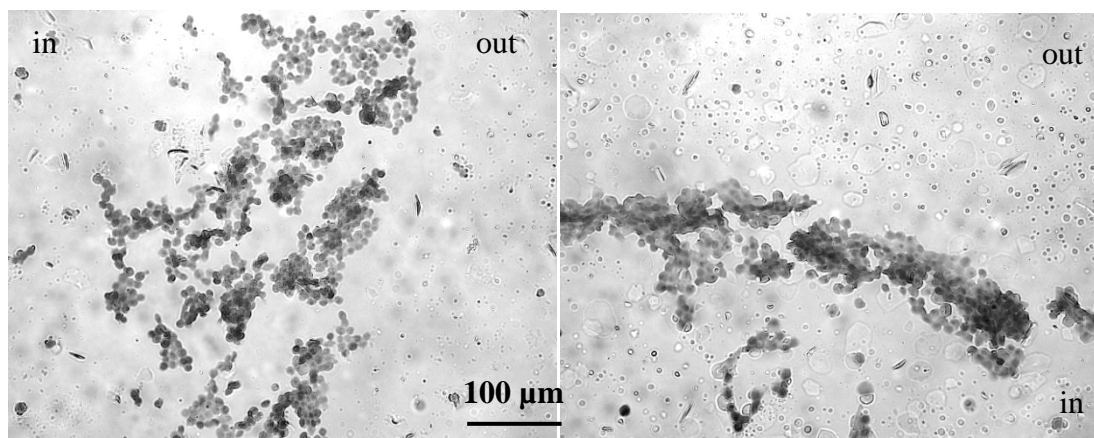


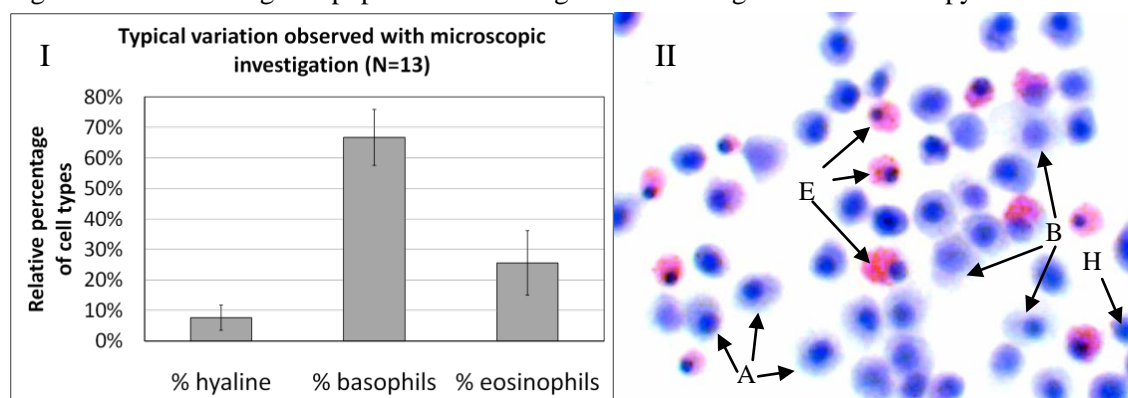
Figure 3.2: Pictures of cell agglomeration found at the edge of cytopsin preparations. It has been assumed that all fixed cells had the same adhesive capacities to physically attach to the glass slide, but all the cells vary in size, complexity and membrane properties.

### 3.2.4 Investigation of results of differential count

The circulating immune cell types of *M. edulis* were investigated using the conventional Wright's stain procedure. Mussels were collected in Cramond and acclimatised in the aquarium for at least three days. The organisms' batch was homogenous in size and collected in the same location. The haemolymph were conventionally collected as described in the chapter 2.4.1.

The Figure 3.3.I presents the percentage of circulating haemocytes measured by differential count. In practice, limitations arise. As the cells are attached to the glass slide, their relative size and shape are highly variable. The identification of cell characteristics relies entirely on the judgement of the investigator. As presented in the picture 3.3.II, numbers of cells (A) have transitory characteristics of basophils (B) to eosinophils (E); the cells have the general characteristics of basophils but also contain eosinophilic granules. We also observe an under-representation of hyaline cells and an over-representation of basophilic cells.

Figure 3.3: Circulating cell populations investigated under bright field microscopy.



I: relative percentage of the three cell types (+/-standard deviation)

II: photography of Wright' stain cell preparation under bright field microscopy (1000x magnification under oil immersion)

-H: hyaline cells

-B: basophils

-E: eosinophils

-A: ambiguous or cells having intermediary characters.

### 3.3 Evaluation of image analysis

#### 3.3.1 Evaluation of THC macro

Table 3.1 and

Table 3.2 illustrate the output of the macro used to evaluate the cell concentration from the sample. It allows the evaluation of the dilution required for the deposit on the cytopsin to obtain correct cell coverage density for the staining and later for the differential image analysis. The technique requires the cells not to touch each other and that enough cells appear in the field of view.

The confidence index is a tool to evaluate the quality of the analysis. It is based on the Feret index, which reflects the ratio of the circumference of the particle against the surface. A high ratio will indicate a complex form (overlapping cells, artefacts, or muscle fibres). The multiplication of a high number of such events will be given by a high value of the confidence index. When this value is higher than 10, the data set is not taken into account.

Table 3.1: Typical image analysis results for cell concentration evaluation.

The table is presenting the name of the sample and the data extracted from the image: the confidence of the analysis (0-10: reliable analysis, >10: poor analysis), the number of cells, and their calculated concentration.

Confidence of image analysis		0
Slide 9	number of cells	510
	volume ( $\mu\text{l}$ )	1.95
	concentration of cell/ml	$2.6 \times 10^5$

Table 3.2: Automatic calculation of required sample dilution for cytopsin procedure.

The table presents in bold letters the appropriate dilution required for the following step: the cytopsin

Dilution required for optimal staining conditions		
Sample	Buffer	concentration final of cells
100	900	29
250	750	87
500	500	<b>262</b>
750	250	785
1000	0	261538
required bracket of 200-300 cells		

### 3.3.2 Investigation of THC results by image analysis

The average uncertainty has been evaluated at 10% using the technique described in 3.1. The uncertainty of the experimental procedure generates a total uncertainty of 38%.

Therefore, a high variability is observed when using image analysis for the THC determination, and one third of the data variation can be explained by the experimental procedure similar to the eye count. Figure 3.4 shows the distribution of the THC normally distributed. In addition, the procedure presents the advantages of high through put, a normalised quality control of the data sets, of an excellent ratio cost/performance and allows to store the raw data (cells photos, quality control data).

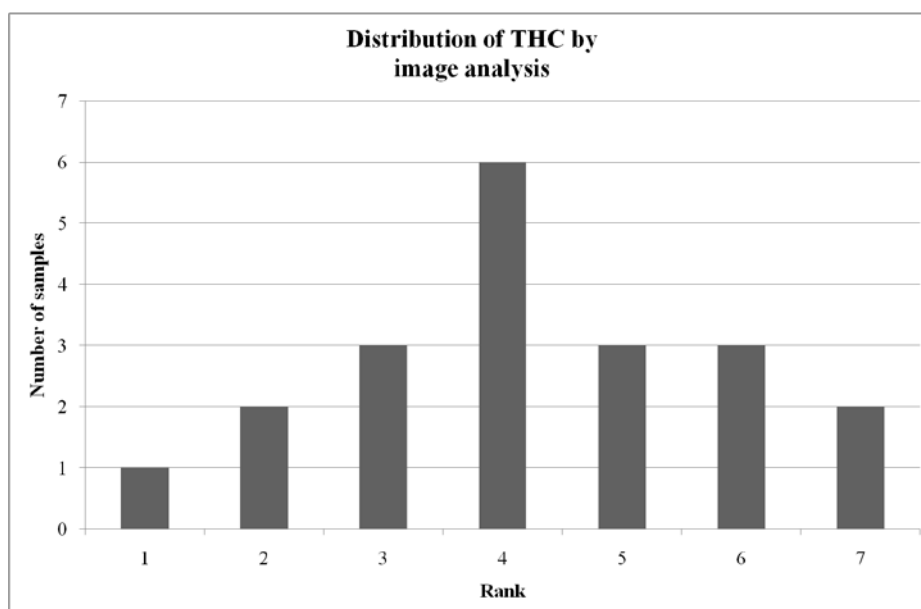


Figure 3.4 : Distribution of THC using the cell concentration image analysis macro.

### 3.3.3 Comparison of visual against the image analysis differential count

Figure 3.5 represents the analysis of the same 17 slides analysed in two different ways:

- by eye, in a conventional bright illumination microscopy
- by the numeric photography of 10 fields of view per slide, and their treatment using image analysis macro explained in the materials and methods.

The photographic output results are different from the eye counts, as the computer cannot discriminate between hyaline cells and basophils. In an eye count, hyaline counts are often dependent on the discrimination of the observer. Nevertheless, we can observe that the results of the two techniques are close. The discrimination between the different cell types is highly personal as the limits for a specific group are indistinct. The computer offers a more objective output as the criteria do not depend on a subjective evaluation. When comparing the two sets of data using a chi square test, we reject the hypothesis of difference of the sets of data (Chi square value of 0.8 with 16d.f.). However, as opposed to the eye investigation, the image analysis yields objective data. Furthermore, the variability of the data is in part related to the experimental procedure but is not fully explained by it.

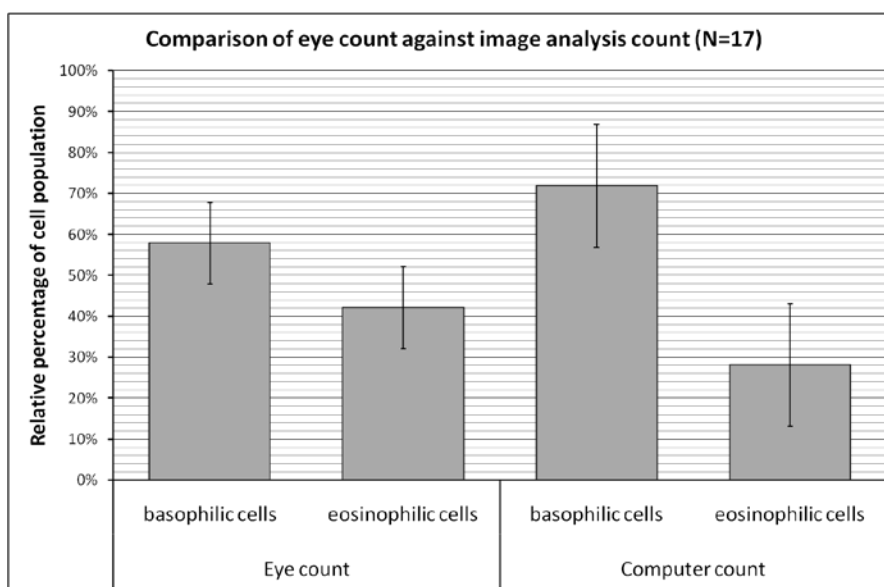


Figure 3.5 : Comparison of visual against image analysis differential cell count. The mean results of the analysis are presented with the uncertainties of the methods, in addition the standard deviation of the eye count was  $\pm 23\%$  and for the image analysis  $\pm 18\%$  ( $\pm$  uncertainty).

### 3.4 Identification of cell population in flow cytometry

#### 3.4.1 Indirect identification

As the opportunity arose, and due to limitations of the previously described techniques, flow cytometry was chosen allowing the acquisition of larger data sets with higher experimental accuracy. For the validation of this technique and for the compatibility with the previously obtained data, it was necessary to compare flow cytometric data with well-established techniques. The validation of flow cytometric analysis of circulating haemocytes was done initially by indirect evidence such as comparison with microscopic investigation, staining techniques or density segregation on Percoll discontinuous gradient.

##### 3.4.1.1 Comparison with light microscopy

Relationships between microscopic observation and flow cytometric data had to be established; therefore, the first approach was to find samples that had a strong dominance of one cell type relative to the others. From visual observation under bright field microscopy, two samples were identified that demonstrated eosinophilic cell dominance (E) and basophilic dominance (B). The hyaline cells are harder to identify in comparison with basophils, and no samples were identified as hyaline-dominant. From the literature, we know that eosinophils are slightly larger and contain more and larger granules than basophils (Coles and Pipe, 1994). From the two samples with strong dominant cell types (basophil or eosinophil), two peaks can be observed per graph, the higher X/Y from B coincide with the lower of E. The higher X/Y peak of graph E is correlated with the eosinophilic population: high granularity and big size. The coinciding peaks are the basophilic cells. Finally, the lower X/Y peak of graph B is the hyaline cells; they are agranular and smaller in size than the two previous categories (Coles and Pipe, 1994; Dyrzynda et al., 1997).

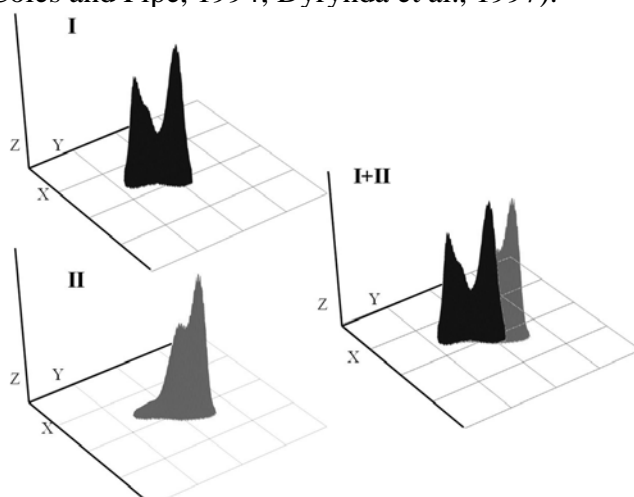


Figure 3.6: Flow cytometric data of basophilic and eosinophilic dominance samples.

I: flow cytometric chart of the basophil-dominant sample (B)

II: flow cytometric chart of eosinophil-dominant sample (E)

I+II: the overlay of the charts showing a perfect fit of the coordinates of the cell types

X: relative size, Y: relative granularity, Z: number of cells

### 3.4.1.2 Cell separation on Percoll gradient

Haemolymph samples from mussel acclimated in the aquarium were collected using the conventional method described in Chapter 2.4.1. The formaldehyde fixed samples were centrifuged on a discontinuous Percoll gradient (2.5.1). In the experiment of Friebel and Renwantz (1995), three layers of cells were obtained: two layers with mixed hyaline and basophilic cell populations and a third layer containing purified eosinophils.

Figure 3.7 presents the flow cytometric analysis of the interfaces of the Percoll gradient. In I and II, two groups of cells are visible. A single patch of cells can be observed in III, this result confirms the observation of Friebel and Renwantz (1995).

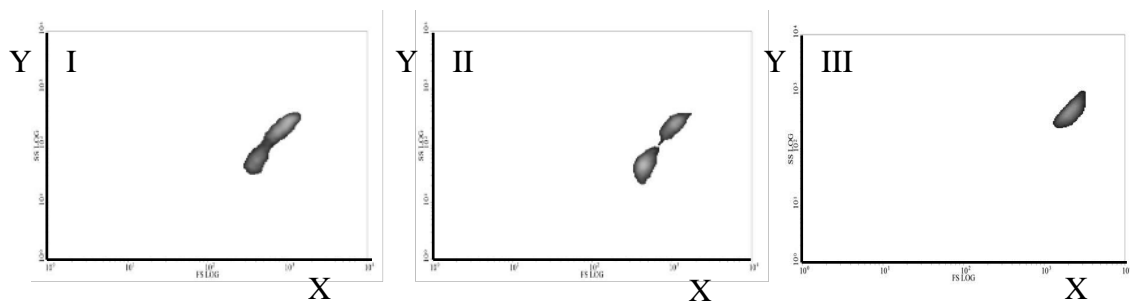


Figure 3.7: Flow cytometric data of cells collected at interfaces of the Percoll gradient. Interface 33%-38% (I), Interface 38%-43% (II). Interface 43%-90% (III). X: relative size, Y: relative granularity



Two overlapping cell populations of I and II were observed. These two layers have different density but correspond to two distinct cell populations regarding their size (X) and cell granularity (Y). The third population, eosinophils (III), are less overlapping. These differences include density, cell complexity and size.

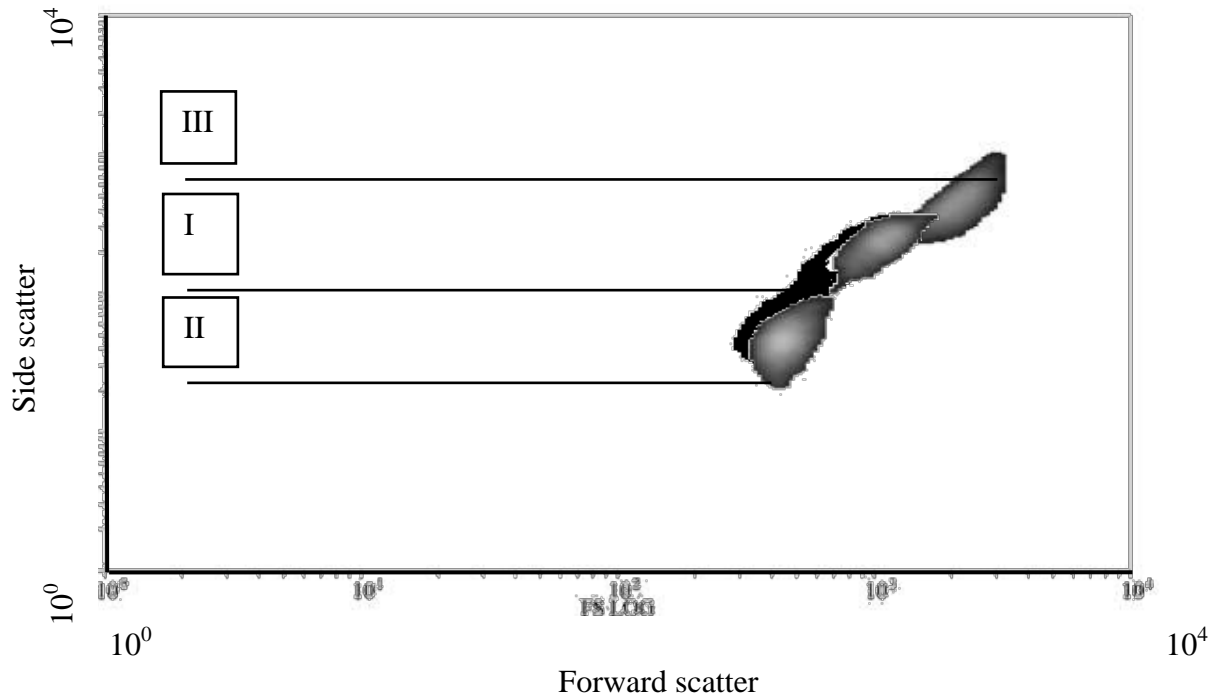


Figure 3.8 : Overlays of flowcytometric charts of cell populations separated on Percoll gradient.  
 (I): Interface 33%-38%; (II): Interface 38%-43%; (III): Interface 43%-90%  
 side scatter: relative granularity, forward scatter: relative size

### 3.4.1.3 Staining techniques in flow cytometry

Fluorescent stain DiOC<sub>6</sub>, staining the mitochondria and the endoplasmic reticulum was used to differentiate circulating haemocyte groups based on the abundance of their organelles. This experiment was to complement the results based on the relative granularity variation observed previously. Two aliquots of fixed haemolymph were analysed by flow cytometry, one unstained and the other stained with DiOC<sub>6</sub> (2.5.4.2). Figure 3.9 shows the overlaid charts of the stained and unstained aliquots.

Three distinct haemocyte populations are observed in the grey and dark charts. In addition, a vertical shift in the fluorescence of stained aliquot trace was observed.

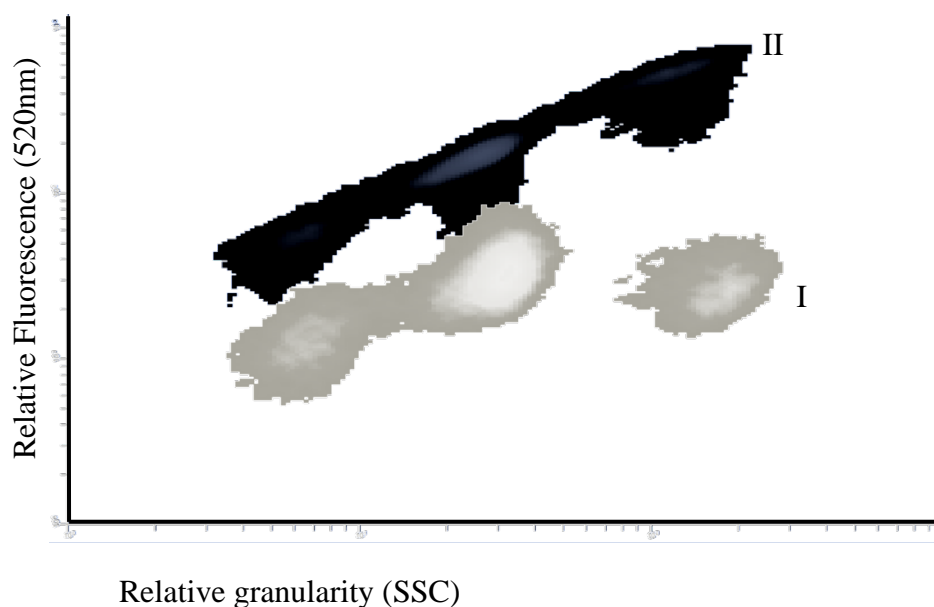


Figure 3.9 : Flow cytometry results of the DiOC<sub>6</sub> staining. Two dimensional representation of the relative granularity and the relative fluorescence of haemocytes of the same sample. I: unstained aliquot, II: stained aliquot.

The following graph presents other aliquots of unstained and stained samples with Wright's stain. The following figure shows overlay of the chart generated with WinMDI software.

We can distinguish three distinct groups on both of the overlaid charts. The two lowest granularity traces of both charts are overlaid on top of each other as the highest granularity traces have, relative to each other, an increase of fluorescence. It is expected that this increase of fluorescence of this last group of cells be due to their staining by the eosin Y. They are likely to be the eosinophils.

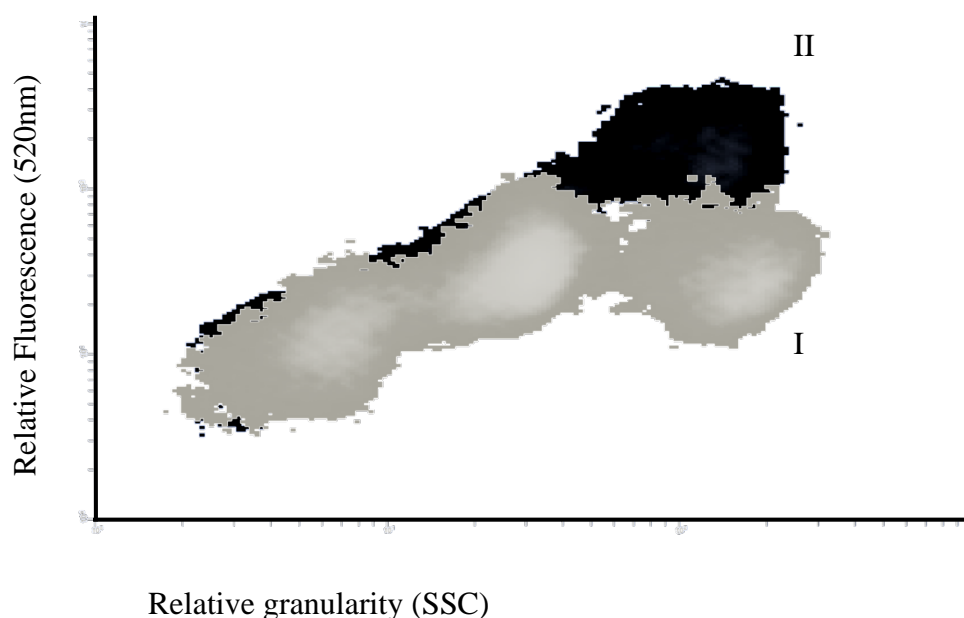


Figure 3.10 : A Flow cytometry result of the Wright's staining.

Two dimensional representation of the relative granularity against the relative fluorescence of the haemocytes.

I: unstained aliquot trace; II: stained aliquot.

### 3.4.2 Direct identification

Cell sorting allowed selective separation of the three cell types from the sample presented in the following graph. In Figure 3.11, each circle represents the gate used for the sorting. In Figure 3.12, the graphs I, II and III represent the rerun of sorted haemocytes, which allowed the double-checking of the sorting process. The cell groups appear well segregated with the exception of the eosinophils where we a tail can be observed, probably due to the physical impact of sorting process.

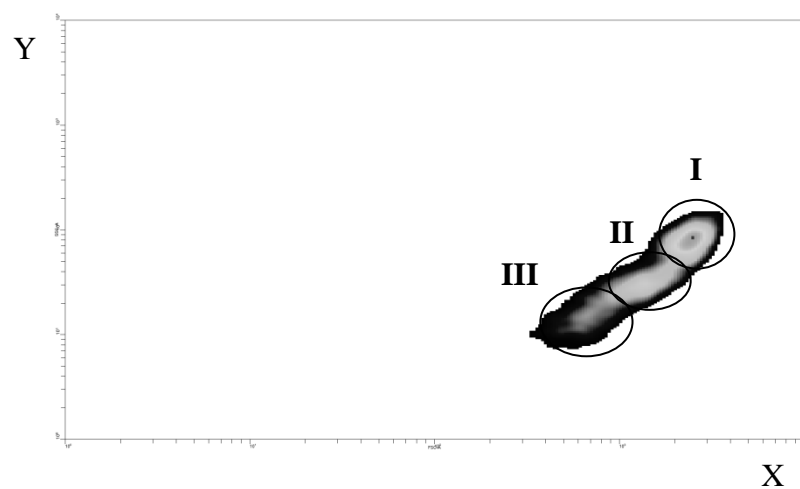


Figure 3.11 : Flow cytometry chart of the sample used for the cell sorting.  
(the circles represent the gates set-up for the sorting parameters),  
X: relative size, Y: relative granularity

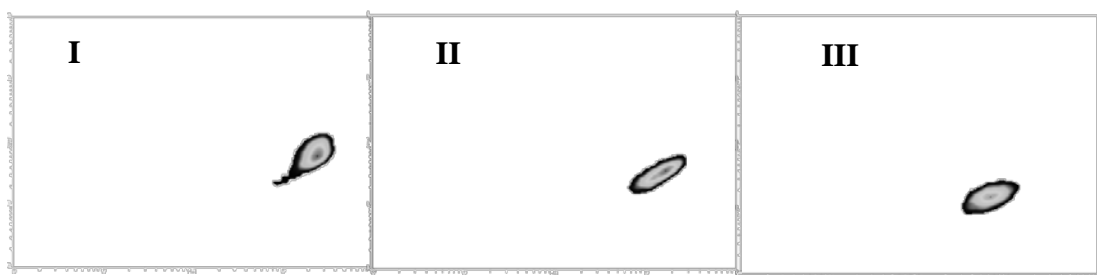


Figure 3.12 : Three charts of the control of the cell sorting effectiveness.  
I: granular cells, II: semi-granular cells, III: agranular cells

Figure 3.13 presents the visual checking of the cell population segregated by cell sorting. The sorted aliquot was stained with Wright's stain and mounted with DepeX mounting solution (BDH Laboratory, Poole, Dorset, UK).

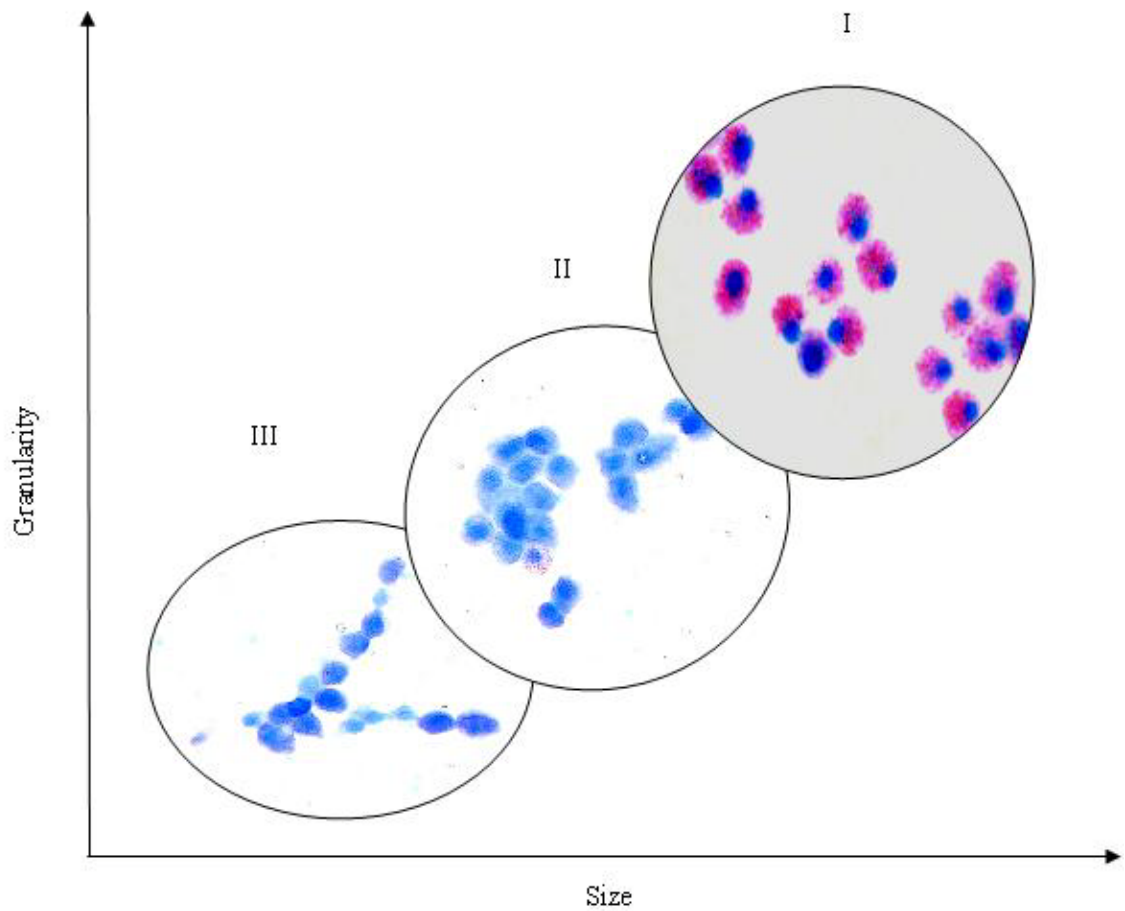


Figure 3.13: Picture of the three cell types sorted by flow cytometry.

I: granular cells: eosinophils, pure populations

II: semi-granular cells: basophils, large majority of basophils, 5-10% of eosinophils

III: agranular cells: hyaline cell, majority of hyaline cell, 5-10% of eosinophils

### 3.5 Behaviour of haemocytes in microfluidics system

The following results are a compilation of experiments using microfluidics systems. This data confirms doubts about the cytopsin preparation qualitative performances.

Cell settlement has remained a problem in the microfluidics system: the cells have the trend to stay at the location of low fluids speed such as the vicinity of edges or walls; agglomerated haemocytes were observed in the central channel and in the side channels, cleaning up was difficult. These problems were overcome later by the treatment of the chip with anti-adhesion solutions.

Figure 3.14 presents the output of central and side channels of the microchip: the left beaker (I) is filled with serum coming from the side channels, while the right beaker (II) is filled with a much more turbid liquid: the concentrated haemocytes.

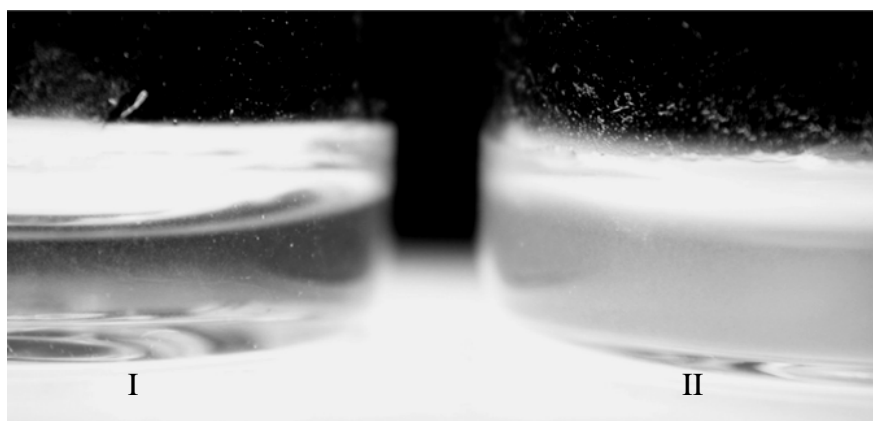


Figure 3.14: Turbidity of concentrated cell sample against the serum sample.  
I: Serum (low turbidity), II: Concentrated cells (high turbidity)

The microscopic study shows the efficiency of the system (Figure 3.15): in (I) a high number of cells are observed, in (II) no or few cells are visible. This investigation allows a qualitative approach of the effect obtained with the microchip, matching with quantitative observations using flow cytometry.

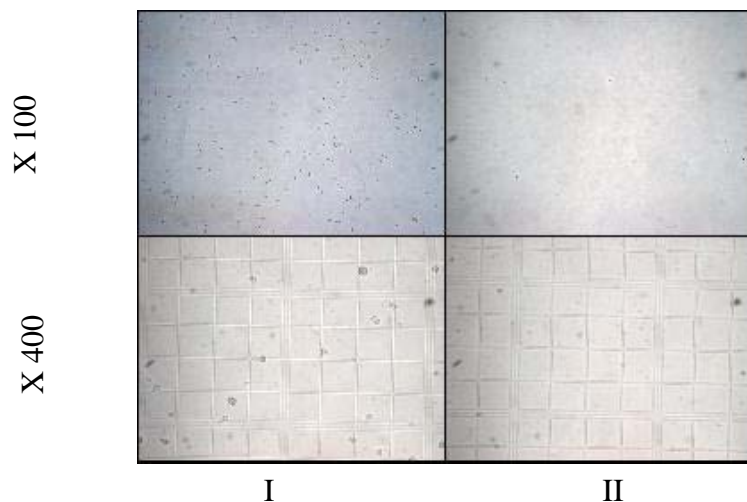


Figure 3.15 : Microscopy observation of the concentrated cells against serum sample. Cell counts of output samples are, in the literature, mainly analysed by bright field microscopy.

Figure 3.16 and Figure 3.17 present the data of different injection speeds of the sample in the microchip. At high speed (10mL/hr), the type of spectrum shown below can be observed:

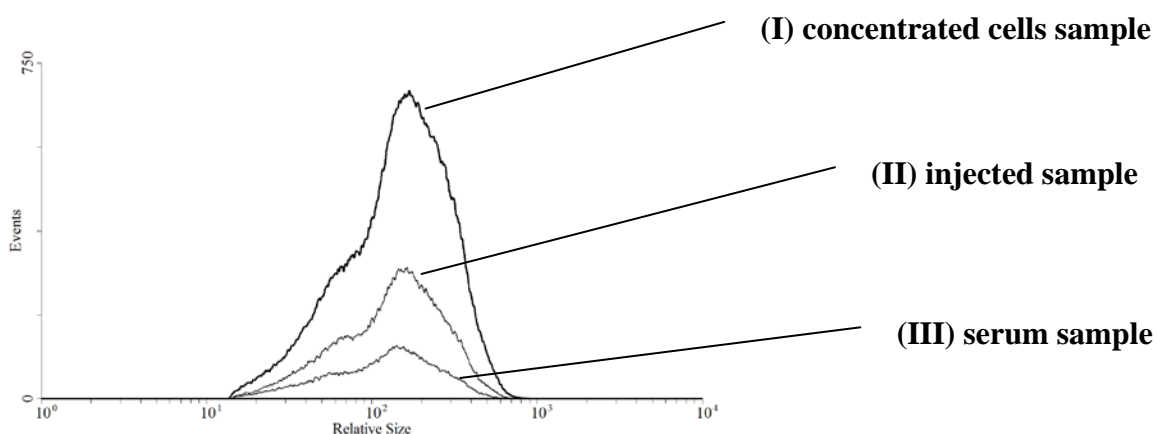


Figure 3.16: Overlay of relative size spectra of the haemolymph sample injected at 10ml/hr.

The three spectra are complementary in their shape and their relative height indicates their relative concentration:  $[\text{serum}] < [\text{injected cells}] < [\text{concentrated cells}]$ .

Figure 3.17 presents also a concentrative effect. In addition, the spectrum of the serum (III) indicates a size-dependent filtration: the trail in the serum spectrum is not complementary to the two other curves, the bigger particles do not pass into the serum, and only the agranular cells do. This result allows us to question the homogeneity of the cytospin. In presence of a microfluidics system (absorbent paper), the cells have a differential behaviour. The observed ring of relatively big cells surrounding the preparation area of a cytospin could be explained (Chapter 3.2.3 ).

The data presented in Figure 3.17 presents an injection' flow rate of 1mL/hr:

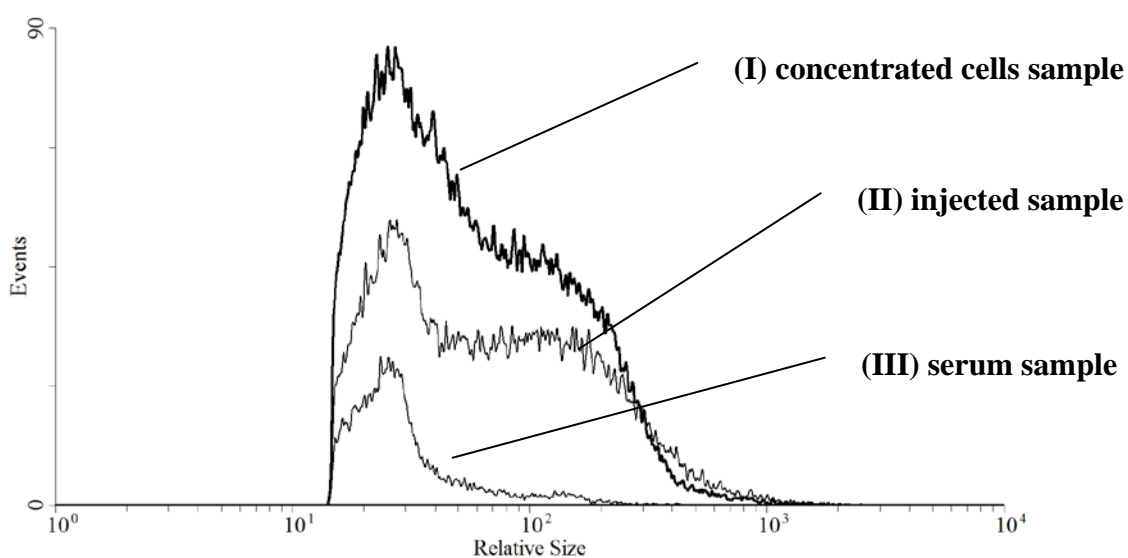


Figure 3.17: Overlay of relative size spectra of the haemolymph sample injected at 1ml/hr.



### 3.6 Discussion

The results indicate a strong impact of the investigation procedures; which could play a role in 43% maximum in the variability of the data. All procedures show advantages and limitations that will be discussed in the following section.

#### 3.6.1 Visual cell count using bright field microscopy and Wright's stain

The results indicate that the systematic error, in the literature, has been greatly underestimated or simply ignored, despite their popular awareness (Goldzahl, 1995). The visual investigation of the THC is strongly limited by two factors. The conventional sampling method induces a maximum potential of 26% uncertainty to the results. In addition, the visual investigation on the improved Neubauer haemocytometer induces a further 7%. The total uncertainty of the method might reach 33% and may hide underlying biological variation. The limited number of counted fields of view investigated, for practical reasons, induces a further bias as the cell suspensions are subject to sedimentation. This limitation can be reduced by more than half by using a precision instrument for the haemolymph sampling and by the precise measurement of the fixation solution volume. THC is still currently in use but the sampling details (such as syringe type, precision, manufacturer) are inadequately, or not, mentioned in *Mytilus* (Ciacci et al., 2009; Parisi et al., 2008) and in other invertebrate studies (Findlay and Smith, 1995; Smith et al., 1995).

The differential count is not as impacted by the sampling method as it uses the relative ratio of haemocyte populations. However, the differential adhesion property of the fixed cells (Vassar et al., 1972) due to their relative size may compromise the homogeneity of the technique as revealed by their differential behaviour in microfluidics systems. It also relies on the judgement of the observer, inducing a none-negligible bias such as on the basophil population that often carries characteristics of the two other cell types. No literature was found regarding the ambiguity of this stain, except for several comments regarding the ambiguity of the cell types (Moore and Lowe, 1977; Rasmussen et al., 1985). The observer bias could possibly be mitigated and quality of the results dramatically improved by using a more discriminating stain. However, this technique is relatively cheap and needs little laboratory equipment. Its use can be justified for small or field laboratories.

### 3.6.2 Evaluation of image analysis

The results of THC using a microscopical visual procedure compared with an image analysis procedure show good correlation. They both suffer from the high uncertainty due to the sampling technique. Image analysis also has a 5% higher uncertainty level compared with visual procedure but it counteracts this drawback by the increase of fields of view investigated and by the number of cells counted. Furthermore, this technology is relatively cheap as the software is free, requires little calculation power, and a simple adapted USB webcam can be used for data acquisition.

Regarding the differential count, image analysis does not allow discrimination between hyaline and basophilic cells. One set of information is lost, but to balance it, the discrimination threshold is more objective, the level of confidence known and the number of counted cells is higher.

The technology is not new and is accessible freely through software such as ImageJ. Commercial applications are available in microbiology for the counting of CFU (e.g.: Oxford Optronix, BioCount Auto, Scan<sup>®</sup> 1200) and other general fields. It is nevertheless easy to develop.

In *Mytilus* research, no comparable use of the technique was found. The use of image analysis was restricted to quantifying the reaction strength in enzymatic reaction (Domouhtsidou and Dimitriadis, 2001; Minier et al., 2000), the size of organelles, cells or organisms (Leonardos and Lucas, 2000; Lowe et al., 1981; Malagoli et al., 2000), and the shape of haemocytes (Caselgrandi et al., 2000; Malagoli et al., 2000). In these studies, good levels of confidence were achieved as they are measuring unidimensional parameters such as length, circumference or darkness of an area. In other studies of more complex systems, such as in larvae identification (Hendriks et al., 2005), 74% identification could be achieved. The confidence of image analysis tools developed in this project are matching the levels observed in the literature.

### 3.6.3 Identification of cell populations in flow cytometry

The results obtained in the indirect methods of correlation have shown the complexities involved in distinguishing the cell types.

The correlation by comparative investigation of cell-type domination samples under bright field microscopy and by flow cytometry indicates a good correspondence in the outputs. More rigorous work was done on *Crassostrea virginica* to compare microscope observation to flow cytometry analysis, and concluded similarly (Ashton-Alcox and Ford, 1998). Nevertheless, these results only give a shallow clue of the correlation of a peak in flow cytometric results with a visual appearance of particular cell types. The use of stains, targeting a precise character of the cells (eosin Y: eosinophilic granules and DiOC<sub>6</sub>: internal organelle membranes), allows a more rigorous approach. They relate to specific features of the cell already observed in bright field microscopy and in electron microscopy (Pipe et al., 1993). Eosin Y allowed a good discrimination of eosinophils. The fixed haemocytes segregation on discontinuous Percoll analysed by flow cytometry is consistent with the literature (Friebel and Renwartz, 1995). Density separation allows a good discrimination of eosinophils. Early flow cytometric studies refer to two cell types (Cao et al., 2003) and later to four cell types (García-García et al., 2008).

These results suggest that hyaline and basophilic populations differ in their characteristics such as density, internal complexity, and size. The continuum between the different cell types could indicate an underlying maturation process from hyaline cells to basophils and to eosinophils. In DNA cell cycle characteristics of haemocytes using DAPI staining, the cells are shown to proliferate in the haemolymph (Bihari et al., 2003) and may indicate the intermediary types observed in this study.

Direct cell sorting has confirmed the previous data and raised further questions about the ambiguity of the intermediary cell types. The characteristics given by the flow cytometer of internal complexity of the cells allows a consistent discrimination of agranular, semi-granular and granular cells. Partial homology links these three groups to the conventional group (hyaline cell, basophils and eosinophils).

Therefore, the denomination of the cell types is dependent on the analytic procedure. Wright stained haemocytes are described as hyaline cells, basophils and eosinophils

under bright field microscopy. Flow cytometric analyses must classify them as agranular, semi-granular and granular cells.

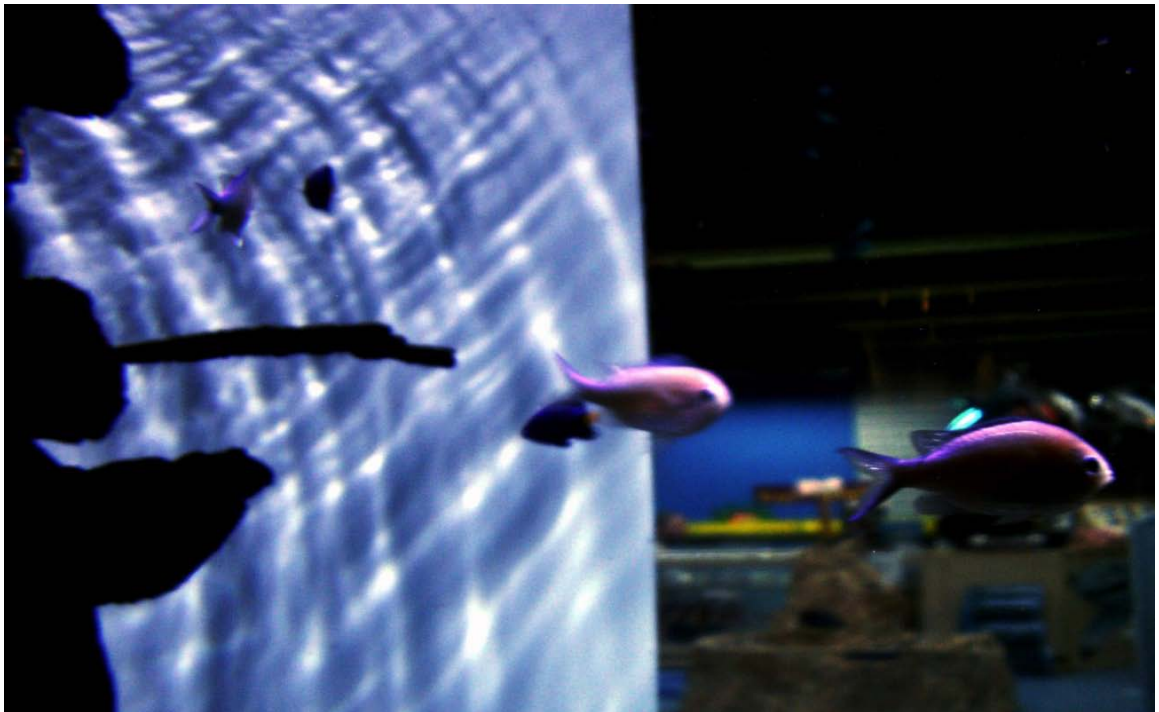
### **3.6.4 Discussion of behaviour of haemocytes in the microfluidics system**

Agranular cells show a differential behaviour in micro-fluidic systems, probably due to their small size. In Figure 3.21, agranular cells have been selectively segregated from the other cell types. As haemocyte circulation in tissue is comparable to the conditions applied in the micro-fluidic experiment (capillaries, low flow rate, and frequent bifurcation), this mechanical behaviour could be a good model to understand how haemolymph and haemocytes conduct their movement in an open vascular system.

This setup has to be considered as a module to a more complex system, where new developments are still to be fully realised (Minc and Viovy, 2004). Other cell separation micro-systems have been developed relying on other principles (Chen et al., 2007; Sai et al., 2006; Sollier et al., 2009) or cell content analysis (Ramadan et al., 2006; Sato et al., 2003; Zhang et al.). Applications of micro-fluidic systems were developed in marine biology for phytoplankton analysis (Benazzi et al., 2007), bacterial analysis (Gilbride et al., 2006; Talbot et al., 2008) and the fish industry (Asensio Gil, 2007). Despite having originally been developed for human blood, the separation device studied in this project revealed itself efficient in *Mytilus edulis* haemocyte investigation.

# Chapter 4

## Variability in circulating haemocytes of *Mytilus edulis*



Title: So Long, and Thanks For All the Fish.

Photo taken at the Sea World Center (Edinburgh, Scotland). The image, unaltered, presents fishes appearing to swim in the void of space. The background resembles earth viewed from space

The photo refers to Douglas Adams' book "The hitchhiker's guide to the galaxy". In this humoristic science fiction novel, the research investigators (Man) are in fact the subject of experiment of an alien researcher (Mouse). This photo states that the point of view impacts radically the understanding of output of an experiment.

## 4 Variability in circulating haemocytes of *Mytilus edulis*

### 4.1 Introduction

Variability induced by the sampling and analysis methods presented in Chapter 3 does not fully reflect intrinsic variation observed in the circulating haemocytes of *Mytilus edulis*. Additional variations are present on three different levels: in individuals composing a geographically restricted population, over time on the scale of a single individual, and in the concentration and ratio of circulating haemocytes.

During the period of study, a large number of populations of *M. edulis* were screened to observe the patterns in wild populations. The investigated populations differed in size (1.5 cm up to 5 cm), abundance (1 individual\*m<sup>-2</sup> up to 10,000 individuals\*m<sup>-2</sup>) or environment (pristine up to high human impact). The parameters investigated were the total haemocyte count (THC) and the cell types (agranular, semi-granular, and granular cells), presented in chapter 3.3.1.

According to (Myrand et al., 2009), variation of allozyme polymorphisms in shore samples may be explained by reproductive mode, larvae settlement, population heterogeneity, or geographical location. *Mytilus* species found in the northern hemisphere, namely *M. trossulus*, *M. galloprovincialis* and *M. edulis*, are known to interbreed and have a viable and reproductive hybrid offspring (Gardner, 1995).

In addition to inter-species', intra-species', and inter-individuals' variation, the variation of circulating haemocytes of a single individual was also investigated. Using a cannulation system, the immune cells of an animal could be followed with minimal stress over long periods. Cell populations were the analysed parameter as the sample volume uncertainty was high and variable: approximately 50µl were sampled using a 1ml syringe; the ease of sampling depended on the sampled individual.

Finally, the results in this chapter will present the origins of variability of the immune parameters of the circulating haemocytes.

## 4.2 Variations in the cell population level

### 4.2.1 Cell types in *Mytilus edulis*

To evaluate qualitatively the range of cell types' variability in *Mytilus edulis*, animals were sampled around the northern United Kingdom using the conventional method (2.4.1). Samples were analysed by flow cytometry. Haemolymph samples of 148 individuals acclimatised in the aquarium for 3 days were characterised to determine cell type frequency.

Figure 4.1 illustrates the diversity of cell groups' spectra observed in *M. edulis* haemocytes. On the base axis, X represents the relative size, Y the relative granularity and Z the number of cells. As previously described, three types of cells are usually expected in different number and proportions. The variability observed in Figure 4.1 suggests that assumptions such as equivalent cell populations between sites and individuals used in the literature have been overestimated. Graphs I and II represent mussels sampled from Blackhall (near Newcastle, in October 2006). Graph III represents a sample extracted in the laboratory from a mussel coming from Cramond (Edinburgh, May 2006). Finally, graph IV represents a sample extracted directly from a mussel at the shore site (Cramond). In samples analysed, the frequency of observed cells types are: spectrum of type III (68%) > spectrum of type II (20%) > spectrum of type IV (9%) > spectrum of type I (3%). In addition, graph IV represents a second population of basophilic semi-granular cells. This cell population has been confirmed and their activity described (García-García et al., 2008).

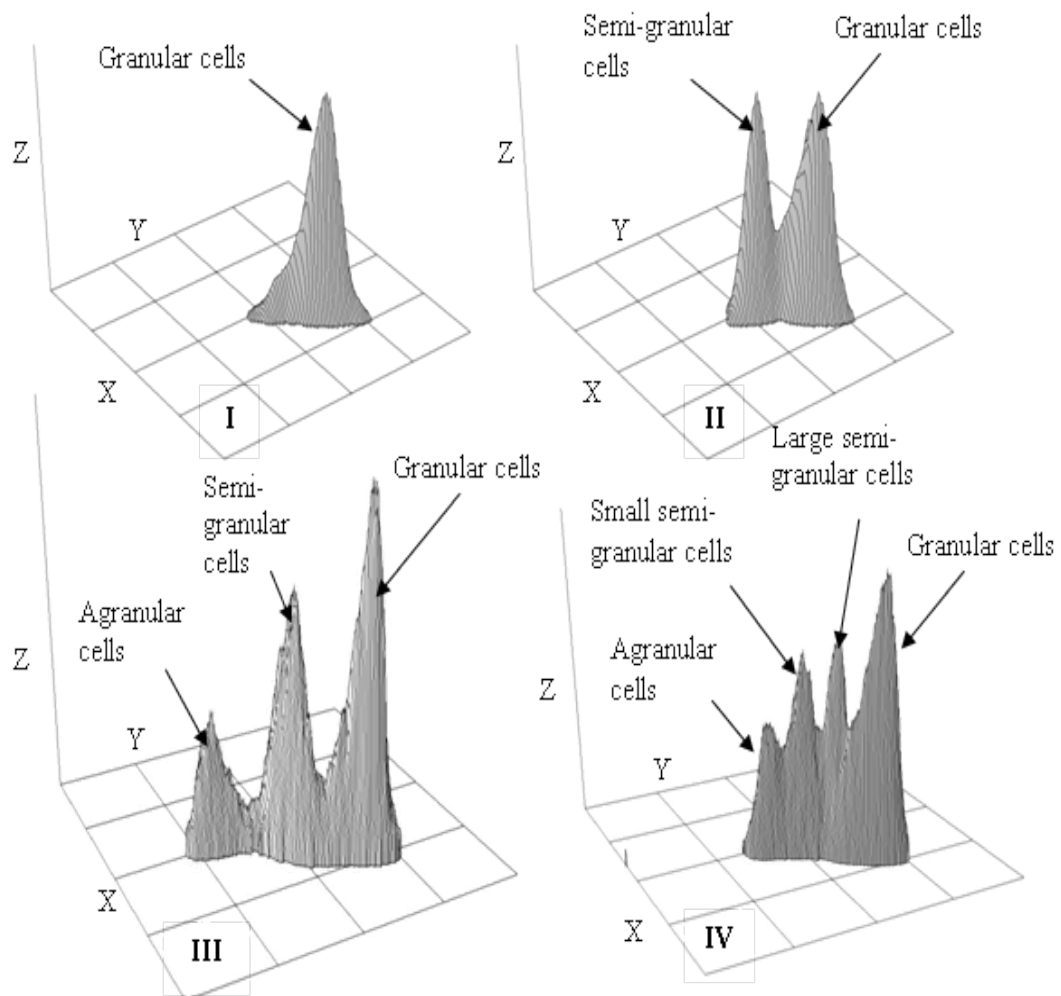


Figure 4.1 : Graphic representation of the cell group variability of the mussel. X is the size scale, Y the relative cell complexity, and Z the number of cells.  
 I: spectrum type I, Shores of Blackhall (near Newcastle, in October 2006)  
 II: spectrum type II, Shores of Blackhall (near Newcastle, in October 2006)  
 III: spectrum type III, Cramond (Edinburgh, May 2006)  
 IV: spectrum type IV, Cramond (Edinburgh, May 2006)



A fifth cell type has been identified on a cannulated Cramond mussel. This is similar to the agranular cell, but slightly bigger. Nothing yet is known about its roles or origin.

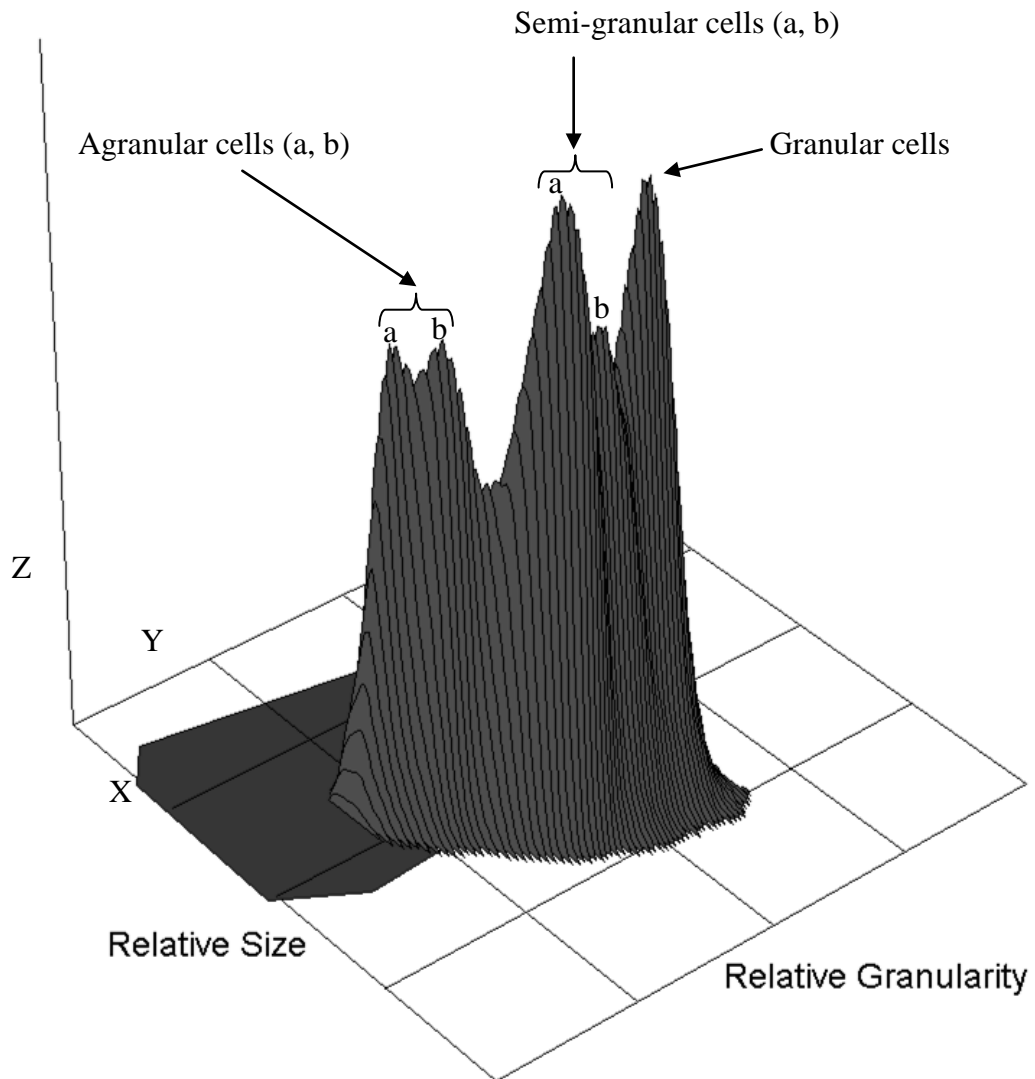


Figure 4.2 : Unusual spectrum cell type of the mussel immune system, spectrum type V. X is the size scale, Y the relative cell complexity, and Z the number of cells. The dark area is the representation of the gate applied to clean up the background noise.

### 4.2.2 Variation of THC and haemocyte types

To investigate the potential impact factor of the THC on the ratio of its haemocyte types, a set of 50 mussels was collected from Cramond and left to acclimatise in the aquarium for a minimum of 3 days in aerated full seawater. The animals were bled using the conventional method and their haemolymph was analysed using flow cytometry processing each sample for 110 seconds. As the running time was identical, the number of analysed cells is relative to their concentration.

Figure 4.3 represents the percentage of cell types against the number of events. A trend line was determined for the three cell types. The coefficient of each trend is tending to zero; no relationship can be implied between THC and the proportion of the different cell types.

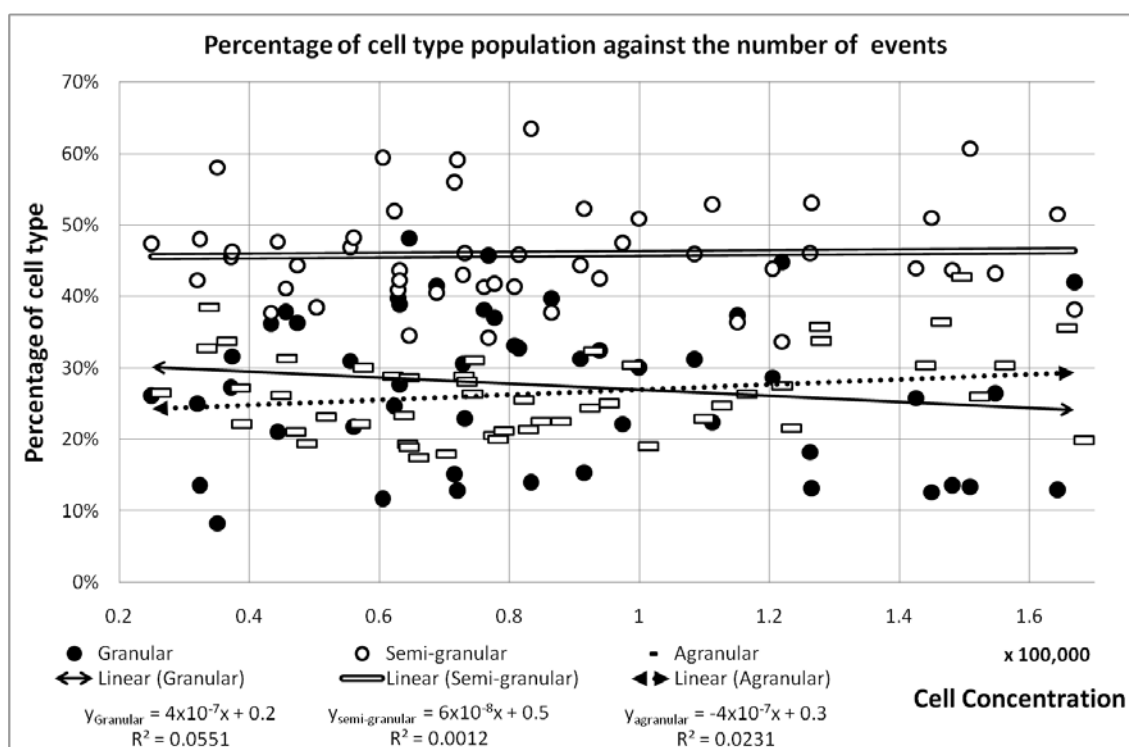


Figure 4.3 : Cell count against the cell type by flow cytometry (N=50).

The number of events equals the number of cells detected and analysed by the flow cytometer. This value is relative to the concentration of haemocytes in the sample, as the time and speed of the analysis was identical for each analysis.

### 4.3 Inter-individual variability in circulating haemocytes of *Mytilus edulis*

To evaluate potential links between changes in the circulating haemocytes and environmental parameters (e.g., wave exposure, predation, animal density), ten individuals of *Mytilus edulis* were sampled on site and general shore observations were recorded in parallel with haemocyte samples collected at various sites around Scotland.

#### 4.3.1 Results from environmental sampling

##### 4.3.1.1 Outer Hebrides sampling results

Figure 4.4 shows an aerial view of the Isles of Harris, Lewis and the Uists, with sample sites from June 2007 marked with a pin. The selected mussels and their environments were recorded by photographic means. Two examples of photographs of sampled mussels are presented in Figure 4.5.

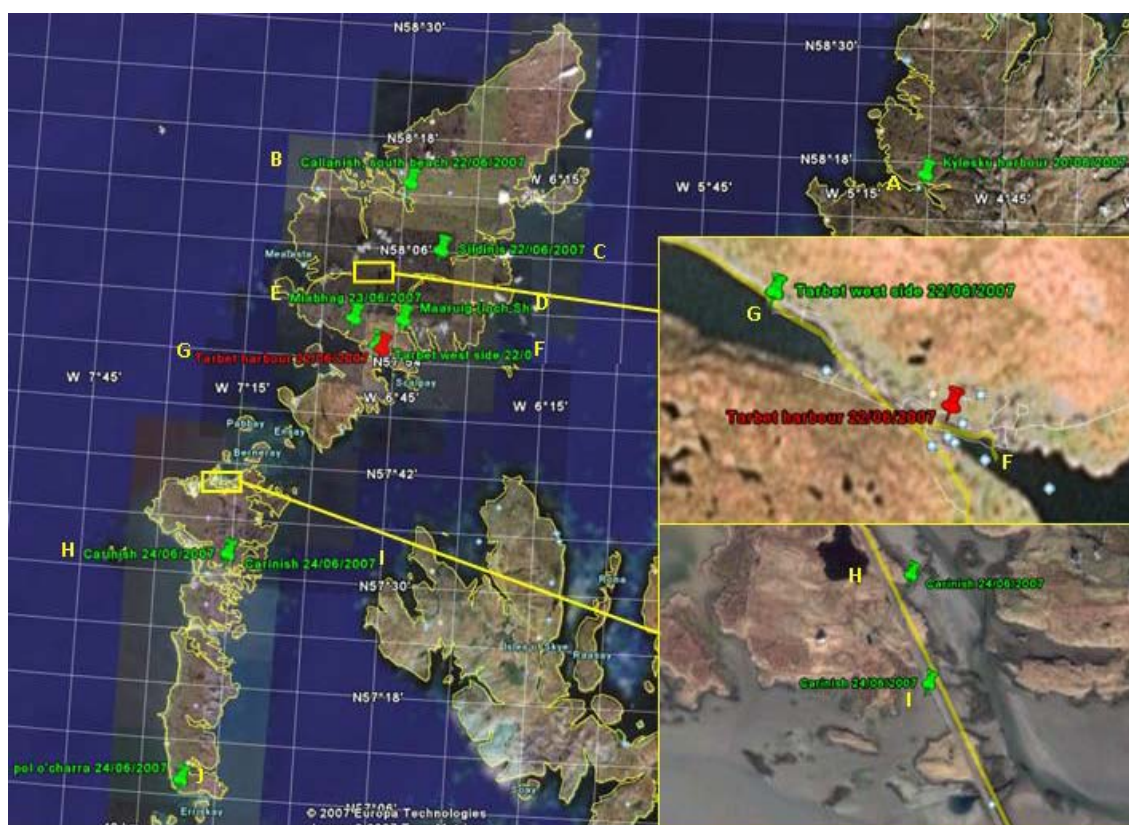


Figure 4.4 : Sampling sites on Harris, Lewis and the Uists (Outer-Hebrides, Scotland, UK).  
Sources: Google Earth© 5.0.11733.9347

The table presents environmental data recorded from the Outer Hebrides during the period of the 20<sup>th</sup> to 24<sup>th</sup> of June 2007.

Table 4.1: Environmental observations of each sampling site.

*Fucus spiralis*: F, *Ascophyllum nodosum*: A, S: sheltered, S,VS: sheltered to very sheltered  
The sites A to J are located on the map (Figure 4.4). The exposure level was interpreted from factors such as sedimentation, local geography, or observable damages on algae. Suspected stress was inferred from direct evidence such as pipe outputs, boat traffic or artefacts of human activity (fishing nets and boxes, car batteries, plastics). The biological environment was observed in the immediate vicinity of the sampled mussels, describing only the dominant species. In the case of predation, the dogwhelk (*Nucella lapillus*) was reported only if found on the shell of mussels.

Site	Site name	Sampling date	Sample size	Exposure	Suspected stress	Predation	Algal coverage	Site observation
A	Kylesku harbour	20/06/2007	10	S VS	untreated waste water, chronic oil/diesel spills from ship, metal (Fe)	<i>Nucella lapillus</i>	F A	
B	Callanish, south beach	22/06/2007	10	S VS	untreated waste water oil/diesel (low)		F A	
C	Sildinis	22/06/2007	10	S VS	untreated waste water chronic oil/diesel spills from ship (low)		F A	
D	Maaruig (loch Shiphoint)	22/06/2007	10	S	none appreciable		F A	See Fig. 4.6
E	Miabhag	23/06/2007	10	S VS	none appreciable		F A	low mussel density
F	Tarbet harbour	22/06/2007	10	S	untreated waste water oil/diesel from shipping		F A	See Fig. 4.6
G	Tarbet west side	22/06/2007	10	S	untreated waste water oil/diesel (low)	<i>Nucella lapillus</i>	F A	small <i>Mytilus</i> (Fig. 4.5)
H	Carinish	24/06/2007	10	S VS	none appreciable		F A	
I	Carinish	24/06/2007	10	S VS	none appreciable		F A	very low density
J	Pol o'charra	24/06/2007	10	S	untreated waste water (low)		F A	

Appendix III presents a striking example of two contrasting sampling sites. On the left hand side is displayed the pristine coast of Maaruig (Loch Shiphoirt, site D) in opposition to the heavily impacted shore of Tarbet harbour on the right hand side (site F), presenting strong anthropogenic activities.

The size of the individuals was variable, from 5-6cm in length for most sites and from 1.5-3cm for site G.

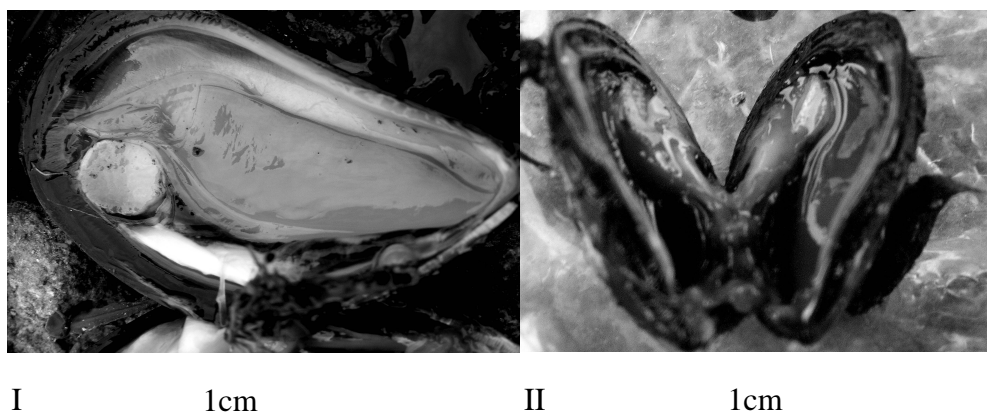


Figure 4.5: Recorded pictures of the sample mussels and their scale. The mussel from picture I was sampled in site D, the mussel from picture II was sampled in site F. Both corresponding environments are presented in Appendix III.

Figures 4.6. and 4.7 depict the variability of average haemocyte populations analysed from ten individuals for the sampled sites A through J, respectively. Mean values oscillate by 19% for agranular cells, 40% for semi-granular cells and 46% for granular cells. The standard deviation varied from 8% to 20%. Site A and B have comparable immunological spectrum, site B was described as low potential impact but predation was observed in site A as well as in close proximity to untreated waste water. On very dissimilar immune spectrum such as site C and F, comparable stress was recorded. Seven percent of the individuals show evidence of reproductive status (spermatozoa in haemolymph), the majority of which occur in site G. The sites F and G, as well as H and I (the latter almost identical in their immune spectra), are geographically very close (less than 300 meters apart; compare with zoomed areas in Figure 4.4), but they belong to different water bodies (west/east side). The variation in immune spectra could not be correlated with the observed parameters described in Table 4.1, such as wave exposure, human activity, mussel density, size range or predation.

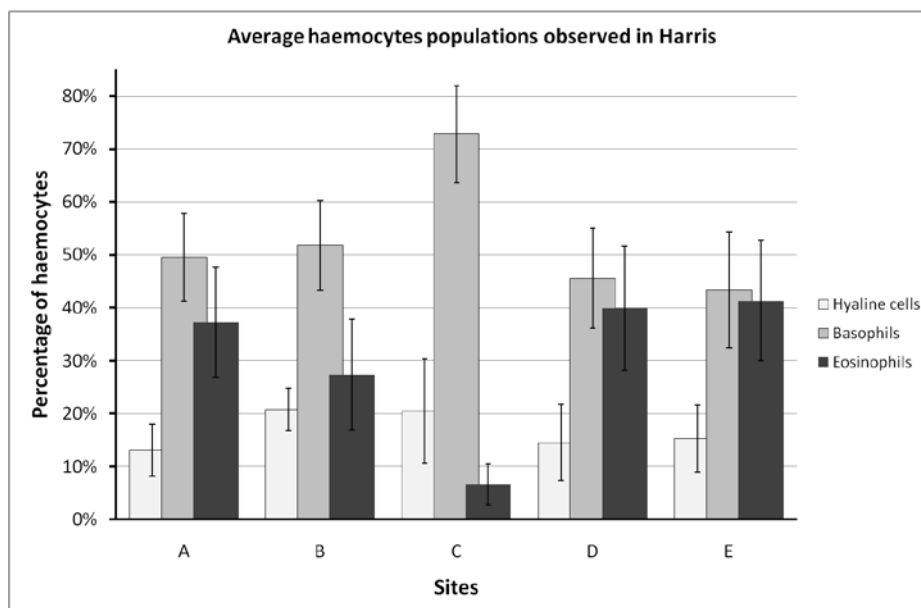


Figure 4.6 : Variation in circulating haemocyte types observed in Harris (Outer Hebrides, Scotland, UK).

Ten individuals sampled from sample sites A - E, respectively. Samples were measured by flow cytometry, data analysed using WinMDI 2.9 and the error bars represent the standard deviation .

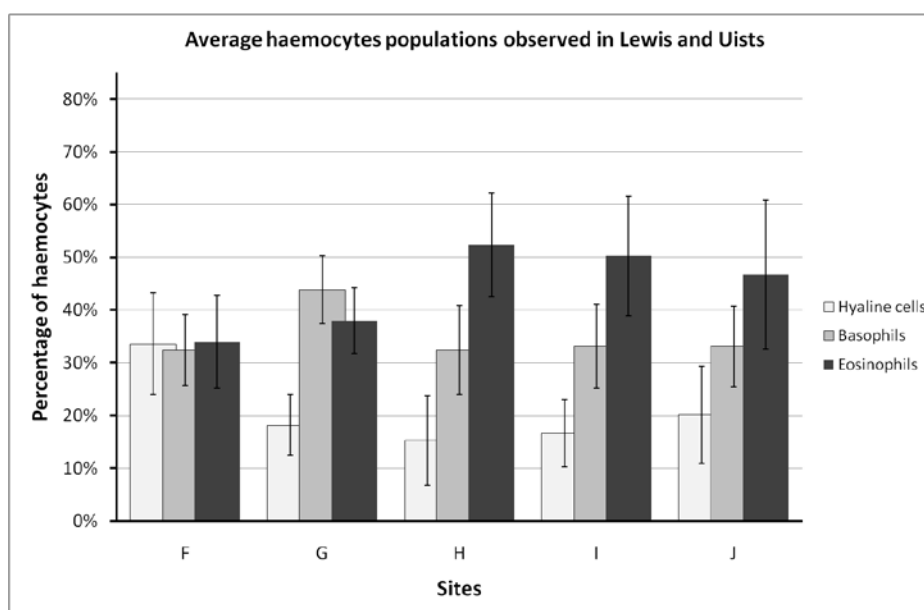


Figure 4.7: Variation in circulating haemocyte types observed in Lewis and Uists (Outer-Hebrides, Scotland, UK).

Ten individuals sampled from sample sites F – J, respectively.

Samples were measured by flow cytometry, data analysed using WinMDI 2.9 and the error bars represent the standard deviation (N=10).

## 4.3.1.2 West coast sampling results

Figure 4.8 presents the data acquired from a further experiment, conducted on the west coast of the mainland of Scotland (Figure 4.9) during the period of the 24<sup>th</sup> to 26<sup>th</sup> of March 2007. The size of the sampled individuals ranged from 3-5cm in length. Ten percent of the samples were contaminated with spermatozoa, all from *Bellochantuy*.

We observe that the ratio of the different cell types is more homogenous than seen in the previous example (4.3.1.1) from Harris, Lewis, and the Uists. Individual mean values oscillated by 6% for agranular cells, 12% for semi-granular cells and 6% for granular cells. The standard deviation varied from 12% to 25 %.

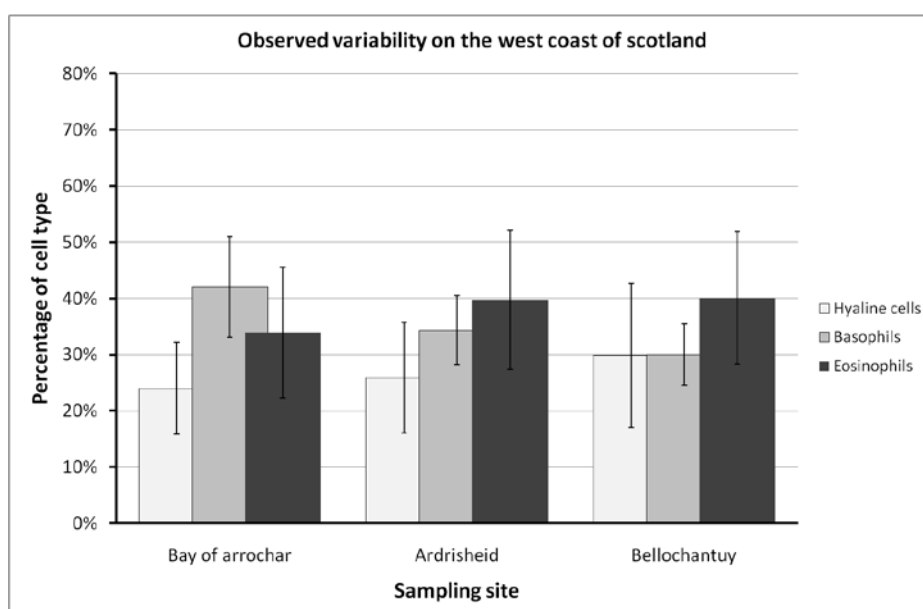


Figure 4.8: Circulating haemocytes population variation observed in Argyll (Scotland, UK). Samples were measured by flow cytometry, data analysed using WinMDI 2.9 and the error bars represent the standard deviation (N=10).

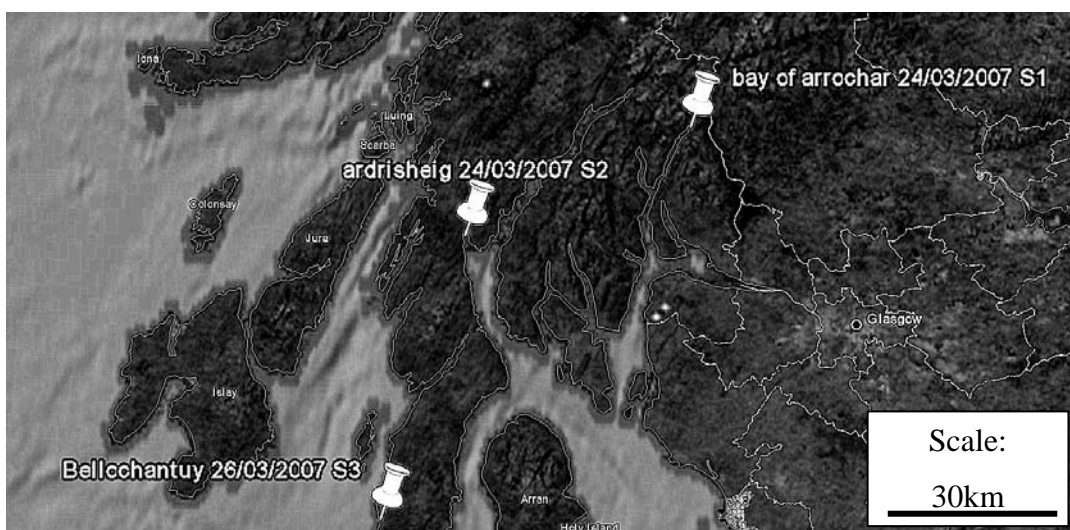


Figure 4.9: Sampling sites in Argyll (Scotland, UK).  
Sources: Google Earth© 5.0.11733.9347

### 4.3.2 Results from laboratory sampling

*Mytilus edulis* were collected from Cramond and left to acclimatise for 3 days in April 2007 and June 2008. In both cases, fifty individuals were sampled by the conventional procedure. Haemocyte populations were determined by flow cytometry. Both populations were collected from the exact same location.

In the population sampled in April 2007, 60% of the individuals showed evidence of gametes in their haemolymph, as opposed to only 30% in the individuals sampled in June 2008. The cell type ratio is equivalent regarding the hyaline cells, but ratio of basophilic cells and eosinophilic cells are reversed. In regard of the number of individuals with gametes in the haemolymph, the difference observed could be attributed to the sexual status.

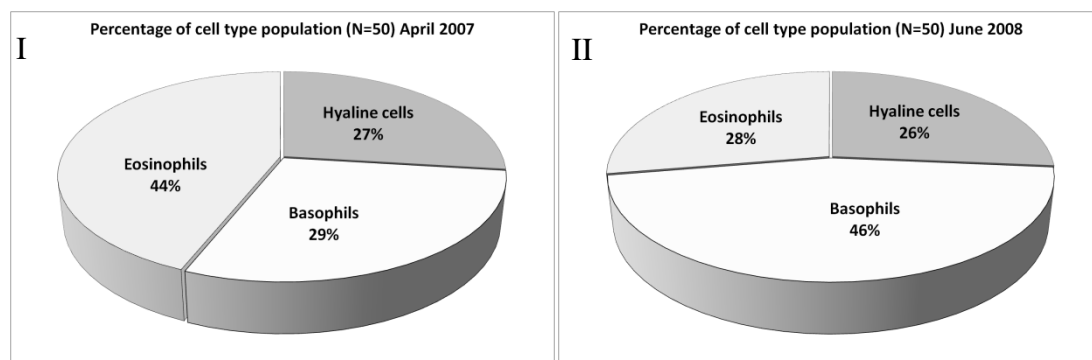


Figure 4.10: Population of haemocytes observed in aquarium-kept organisms. Graph I represents the data analysed by flow cytometry of 50 individuals sampled in April 2007. Graph II represents the data analysed by flow cytometry of 50 individuals sampled in June 2008.



#### 4.4 Individual variability in of *Mytilus edulis* circulating haemocytes

##### 4.4.1 Position of the adductor muscle with regards to the mussel size

The position of the adductor muscle was measured on seven mussels sampled in Cramond. This was done in order to place the cannula accurately (2.2.3) in the adductor muscle.

Figure 4.11 represents the relative position of the adductor with respect to the size of the mussel, thus allowing precise positioning of the cannula. Figure 4.11 also led to the creation of a tool allowing quick and reliable positioning of the drilling (Figure 4.12).

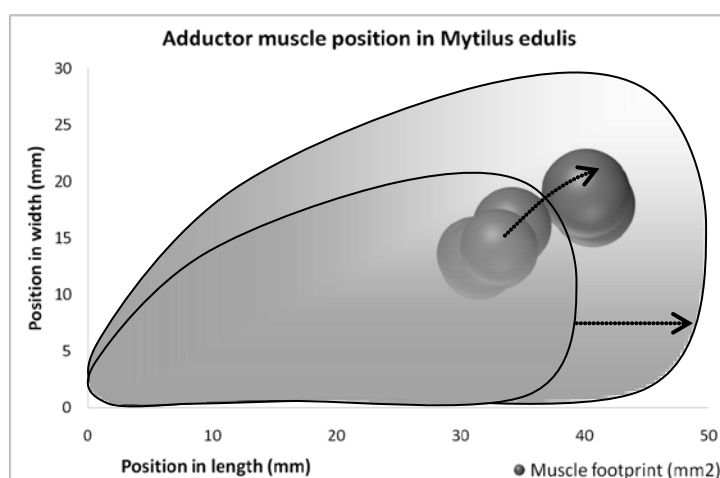


Figure 4.11 : Relative position of the adductor muscle. The coordinates were taken relative to the tip of the narrow end of the organism. The mussels were euthanatized as described in Chapter 2.6.

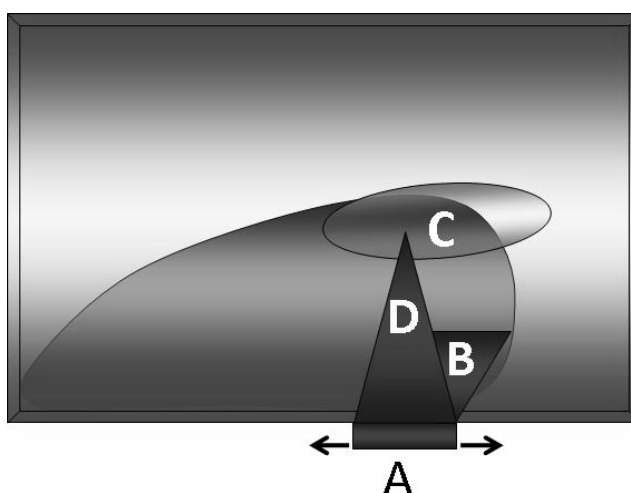


Figure 4.12 : Drilling positioning tool.

The positioning tool was made from the cover cap of a micropipette tips' plastic box. A Dremel drill, mounted with a cutting disk, was used to cut a rail for the mobile part (A) that slides laterally. The tip B was adjusted to the edge of the shell. In the hole C, the precise position of the adductor muscle is given by the tip of D.

## 4.4.2 Individual variation of haemocyte populations

### 4.4.2.1 Variations observed over 2 weeks

In view of the variation observed over a period of 15 months in the large sample sets from the Cramond location, two questions arose: Is this variation due to the time period chosen, or could this variation be attributed to individual variation? To test these two hypotheses, four cannulated mussels were individually sampled twice a day for 13 days to determine the relative variations of their immune cell types. Fifty microlitres of haemolymph were withdrawn from the adductor muscle through the cannulation on each sampling occasion. The cells were fixed in a formaldehyde buffer as they were sampled. The cells were analysed by flow cytometry, and the data analysed with WinMDI 2.9.

The graphs presented in Figure 4.13 show large variations in the three cell types. Over 13 days, a variation from 37% up to 58% can be observed in the agranular cell population. In the semi-granular cell populations, variation ranges from 23% up to 58%, and in the granular cells, from 25% up to 34%. Therefore, we measured a large variation in every sampled individual over a period of 13 days.

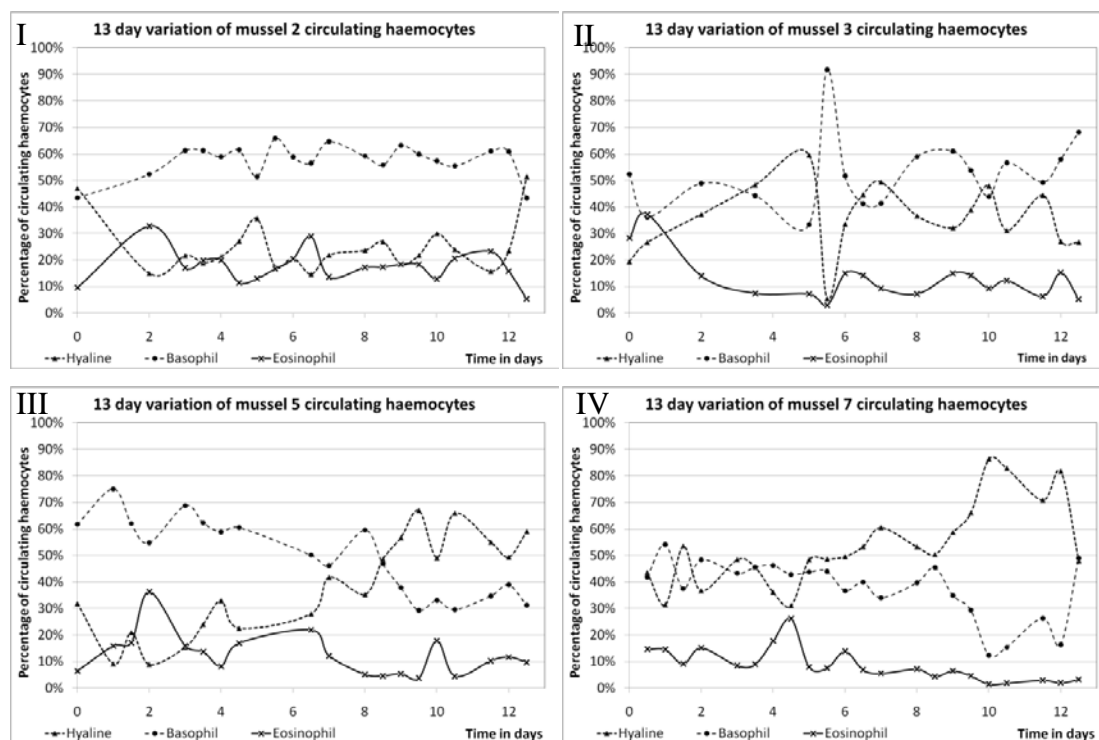


Figure 4.13: Measured variation of haemocyte populations over 13 days. Graph I – IV present the variation of haemocyte cell type populations in mussels 2, 3, 5, and 7, respectively.

## 4.4.2.2 Variations observed over five days

Due to the strikingly large variation observed over the 13-day time period, a further experiment was set up to see whether such results could be reproduced. A set of mussels were individually sampled twice a day for five days. Fifty microlitres of haemolymph were withdrawn from the adductor muscle through the cannulation. The cells were fixed in a formaldehyde buffer as they were sampled. The cells were analysed by flow cytometry, and the data analysed with WinMDI 2.9.

On the graphs presented in the Figure 4.14, large variations are observed in the three cell types. Over the five days, a variation from 27% up to 44% could be observed in the agranular population. In the semi-granular population, variation ranged from 22% up to 34%, and in the granular cells, from 2% up to 21%.

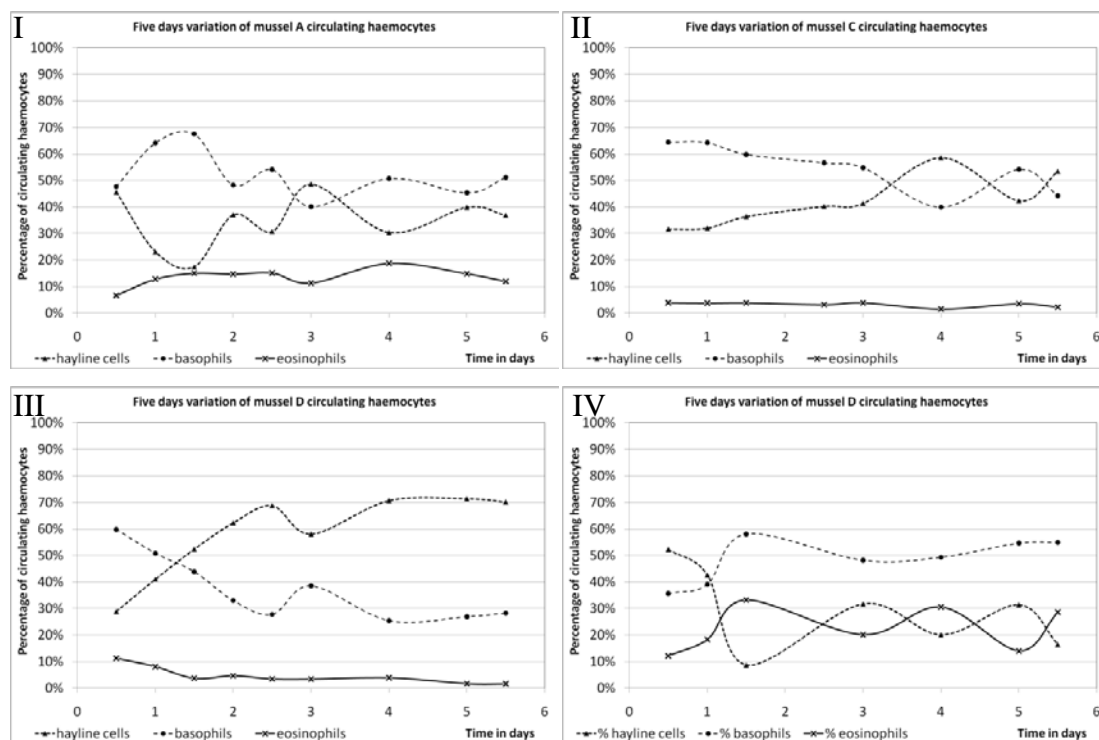


Figure 4.14: Measured variation of haemocyte populations over 5 days.

Graph I presents the variation of haemocytes populations in mussel A variations: agranular cells (31%), semi-granular cells (27%) and granular cells (12%).  
 Graph II presents the variation of haemocytes populations in mussel C variations: agranular cells (27%), semi-granular cells (25%) and granular cells (2%).  
 Graph III presents the variation of haemocytes populations in mussel D variations: agranular cells (42%), semi-granular cells (34%) and granular cells (10%).  
 Graph IV presents the variation of haemocytes populations in mussel E variations: agranular cells (44%), semi-granular cells (22%) and granular cells (21%).

## 4.4.2.3 Variations observed over 12 hours

From the two previous experiments, we observed that the fluctuations are present in each individual. To yet increase the resolution of the time period, a set of mussels were individually sampled hourly for 12 hours. Fifty microlitres of haemolymph were withdrawn from the adductor muscle through the cannulation. The cells were fixed in a formaldehyde buffer as they were sampled. The cells were analysed by flow cytometry, and the data analysed with WinMDI 2.9.

On the graphs presented in the Figure 4.15, large variations are observed in the three cell types. Over the 12-hour period, the agranular population varied from 6% up to 26%, the semi-granular population ranged from 22% up to 27%, and the granular cells from 21% up to 41%.

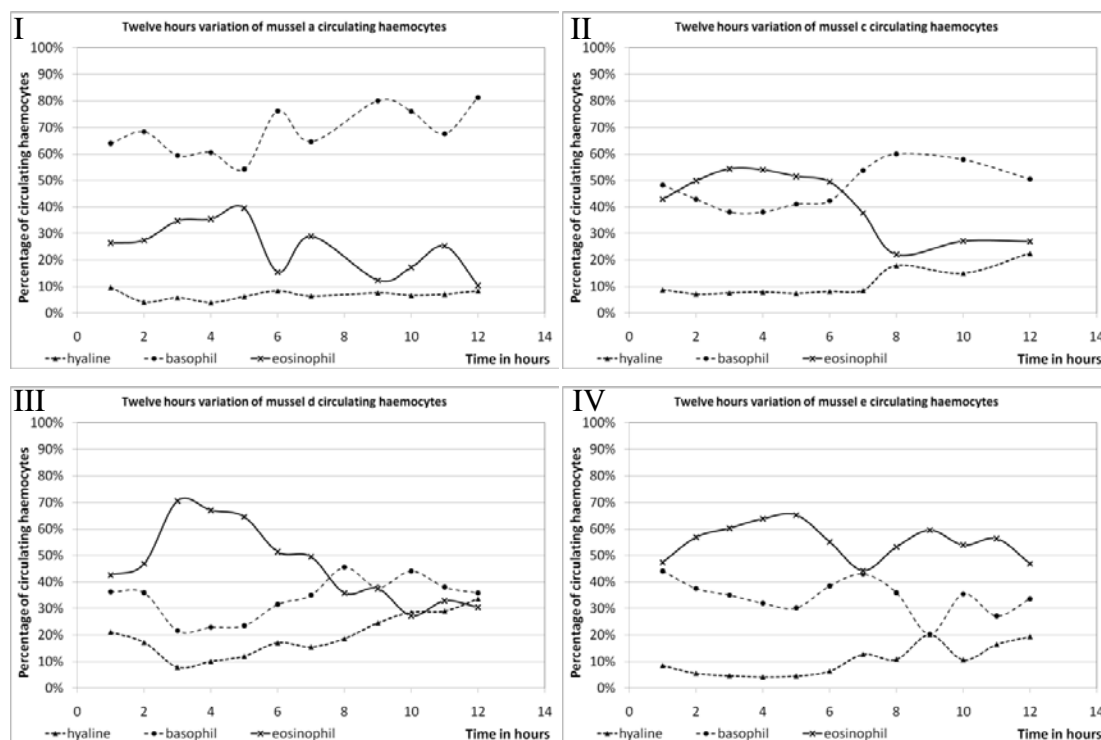


Figure 4.15: Measured variation of haemocyte populations over 12 hours.

Graph I presents the variation of haemocyte populations in mussel a variations: agranular cells (6%), semi-granular cells (27%) and granular cells (29%).  
 Graph II presents the variation of haemocytes populations in mussel c variations: agranular cells (15%), semi-granular cells (22%) and granular cells (32%).  
 Graph III presents the variation of haemocytes populations in mussel d variations: agranular cells (26%), semi-granular cells (24%) and granular cells (43%).  
 Graph IV presents the variation of haemocytes populations in mussel e variations: agranular cells (16%), semi-granular cells (23%) and granular cells (21%).

## 4.5 Investigation of a potential haemocyte reservoir in *Mytilus edulis*

### 4.5.1 Observation of the *Mytilus edulis* mantle

In view of the results obtained on the hourly immune cell fluctuations, cell replication cannot be contemplated as the only factor of cell type variations. As the time delay is so short, the most likely hypothesis would be that the cells are stored. To test this hypothesis, the tissue of *Mytilus edulis* was investigated using the same stain (Wright stain) as the one used in the differential count bright field microscopy procedure. Therefore, the body mass of *M. edulis* was explored for potential immune cell reservoirs. The mantle makes up a significant part of the soft tissue of *Mytilus edulis*. This tissue was investigated to track haemocyte infiltration. The organisms were kept under normal condition, but were not fed. A set of ten mussels were euthanized and their tissues dissected. The tissue sections were prepared as presented in chapter 2.3. The following figures are the compilation of images taken at 100x magnification under bright field microscopy, detailing the morphology of the mantle; details of certain areas are inserted for a better visibility. Figure 4.16 to

Figure 4.19 sequentially present the patterns of haemocyte infiltration within the mantle. The general histological data and zonation of eosinophils (red line) are outlined in Figure 4.16. The tissues are coloured in blue. We can observe the strongest staining on the teguments.

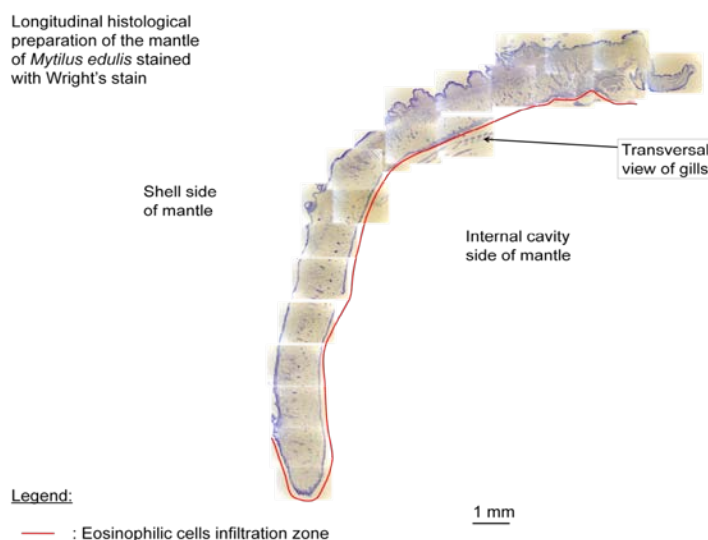


Figure 4.16: *Mytilus edulis*' mantle from 23 fields of view under bright field microscopy. The schematic representation of the blue mussel (not to scale) presents the location of the investigated area.

Figure 4.17 shows the mantle edge with its muscular features. Eosinophils are clustered in the teguments of the lumen of the internal cavity. These cells appear to extend pseudopods through the epithelial cells into the lumen. An average of 17 eosinophils per 100  $\mu\text{m}$  is observed on the magnified areas.

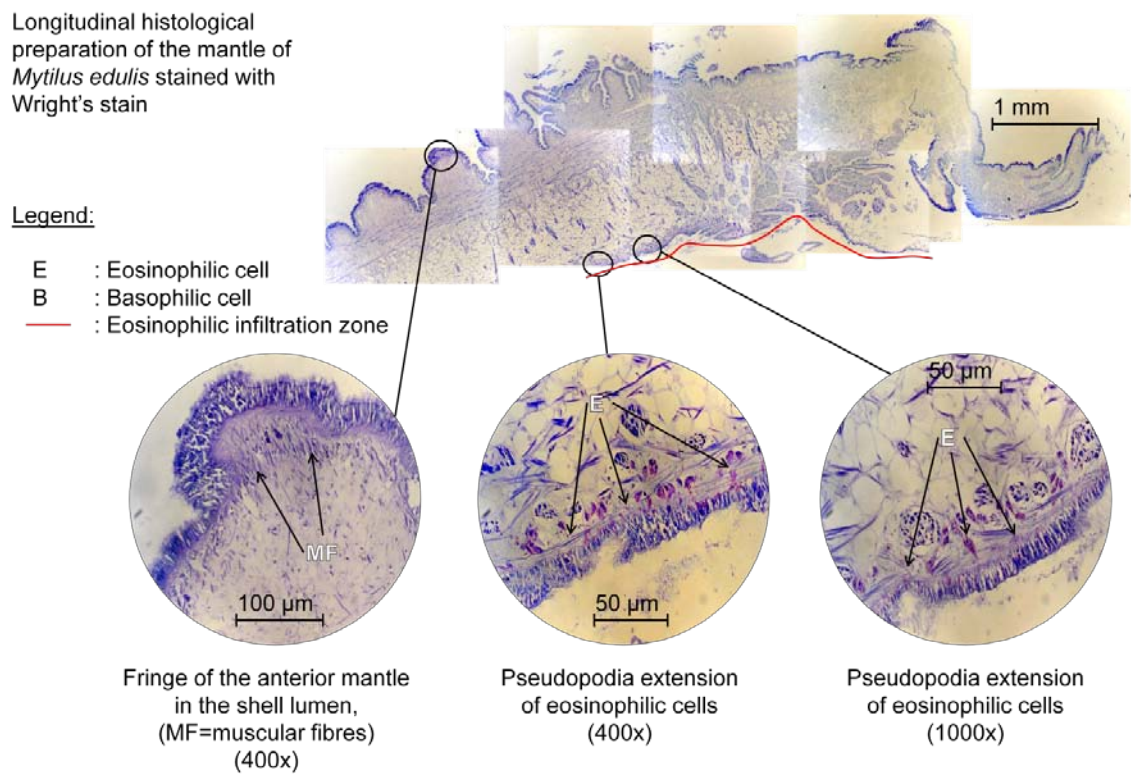


Figure 4.17: *Mytilus edulis*' mantle from 11 fields of view under bright field microscopy. The density of eosinophils is 17 cells per 100  $\mu\text{m}$ .

Figure 4.18 shows the median area of the mantle. Eosinophils are still present clustered towards the internal cavity, and basophils can be seen in the parenchyma. An average of 20 eosinophils per 100  $\mu\text{m}$  is observed on the magnified areas.

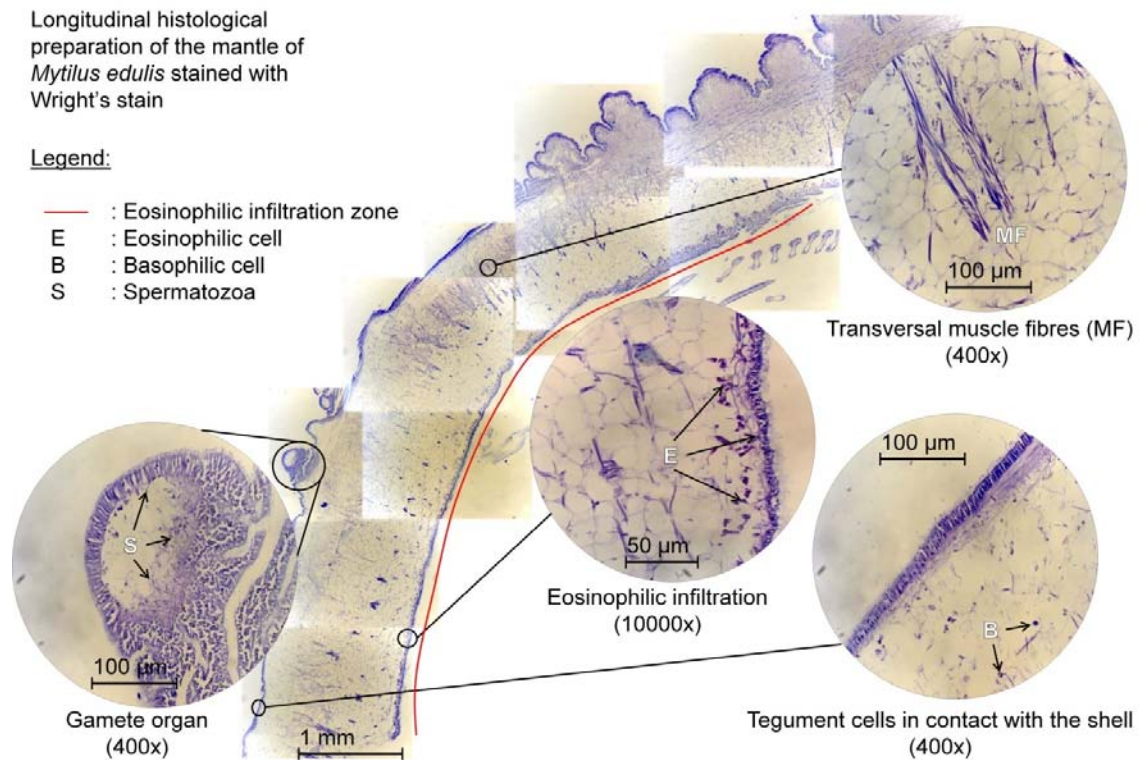


Figure 4.18: *Mytilus edulis*' mantle from 11 fields of view under bright field microscopy. The density of eosinophils is 20 cells per 100  $\mu\text{m}$ .

Figure 4.19 shows the ventral part of the mantle, which has a similar pattern of haemocytes infiltration as Figure 4.16, Figure 4.17 and Figure 4.18. An average of 15 eosinophils per 100 $\mu\text{m}$  is observed on the magnified areas.

In a qualitative calculation, averages of 15 eosinophils are found every 100 $\mu\text{m}$  on a thickness of 10 $\mu\text{m}$  on the inner cavity tegument. The average surface area of the mussel mantle is twice 50 mm in length and 20 mm in width, thus a surface of 40,000 $\mu\text{m}$ \*20,000 $\mu\text{m}$ \*2=2,000,000,000 $\mu\text{m}^2$  or  $2 \times 10^9 \mu\text{m}^2$ ). Assuming homogenous repartition of eosinophils at a density of 15 cells per  $10^3 \mu\text{m}^2$ ,  $15 * 2 \times 10^9 / 10^3$  (or  $3 \times 10^7$ ) eosinophils could be expected to infiltrate the mantle under normal conditions.

Longitudinal histological preparation of the mantle of *Mytilus edulis* stained with Wright's stain

Legend:

- E : Eosinophilic cell
- B : Basophilic cell
- : Eosinophilic infiltration zone

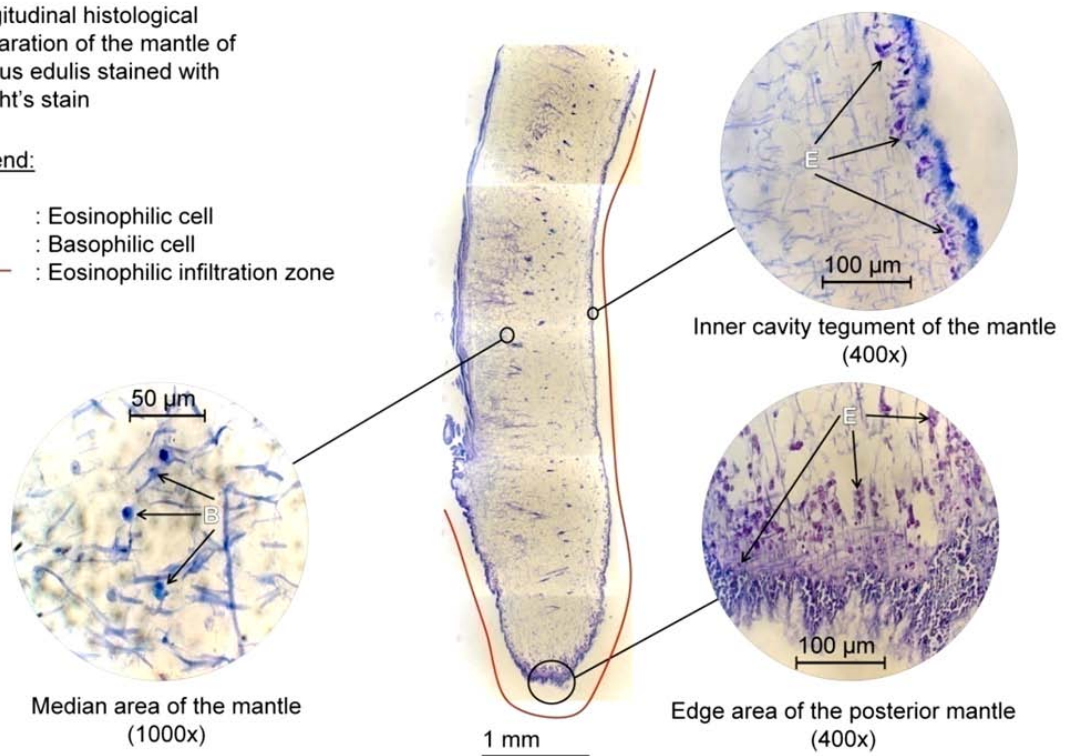


Figure 4.19: *Mytilus edulis*' mantle from 5 fields of view under bright field microscopy. The density of eosinophils is from 10 up to 20 cells per 100 $\mu\text{m}$ .



### 4.5.2 Observation of the visceral mass of *Mytilus edulis*

The visceral tissue was studied to investigate the infiltration of haemocytes. The following figures (4.20 and 4.21) present data images taken at 100x magnification under bright field microscopy. These show the morphology of digestive tissue; it has been divided into two parts to allow for better visibility.

Figure 4.20 shows the general outline of the histological section and the zonation of eosinophils. These cells are side-by-side and closely associated with the gut epithelium. No approximation of the haemocyte number was possible, as the organ is convoluted and its dimension not measurable.

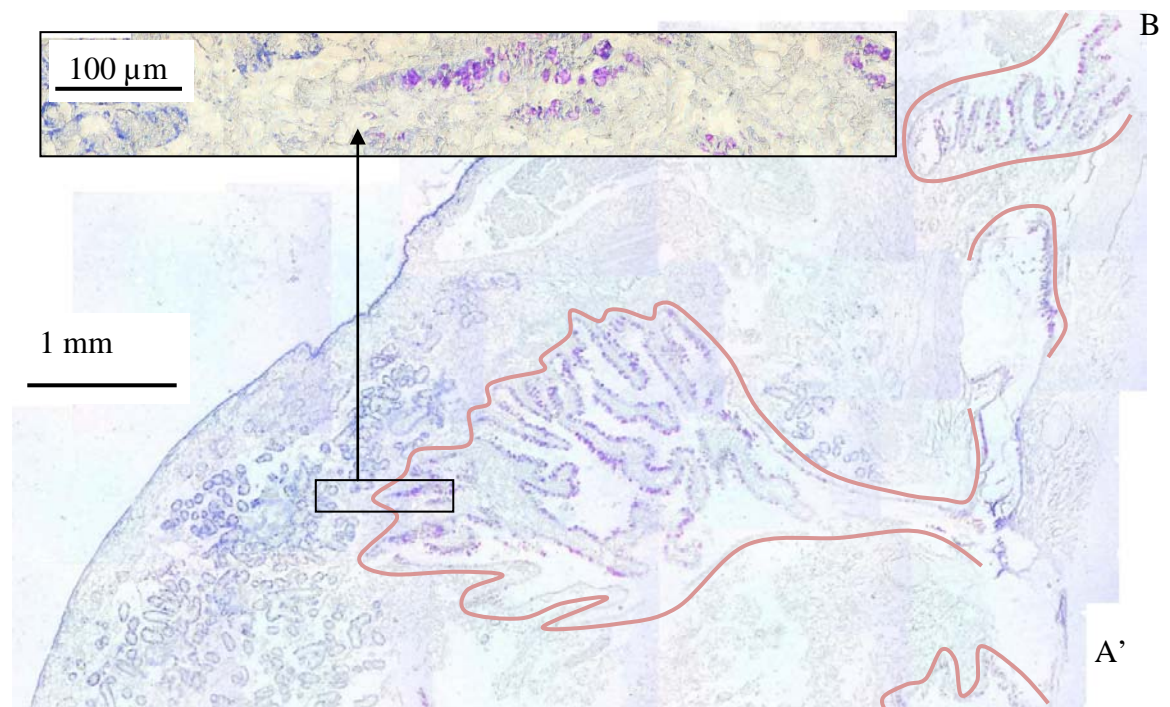


Figure 4.20: *Mytilus edulis*' visceral mass from 20 fields of view under bright field microscopy. The highest density of eosinophils (—) is found in association with the gut epithelium.

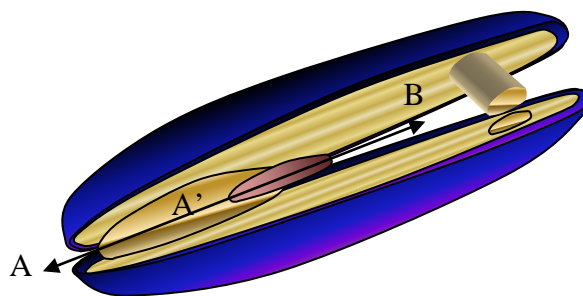


Figure 4.21 (A' - B) continues to present the general outline of the histological section and the zonation of eosinophils shown in Figure 4.20 (A - A'). These cells are side-by-side and closely associated with the gut epithelium and the labial palp. No approximation of the haemocyte number was possible, as the organ is convoluted and its dimension not easily measurable.

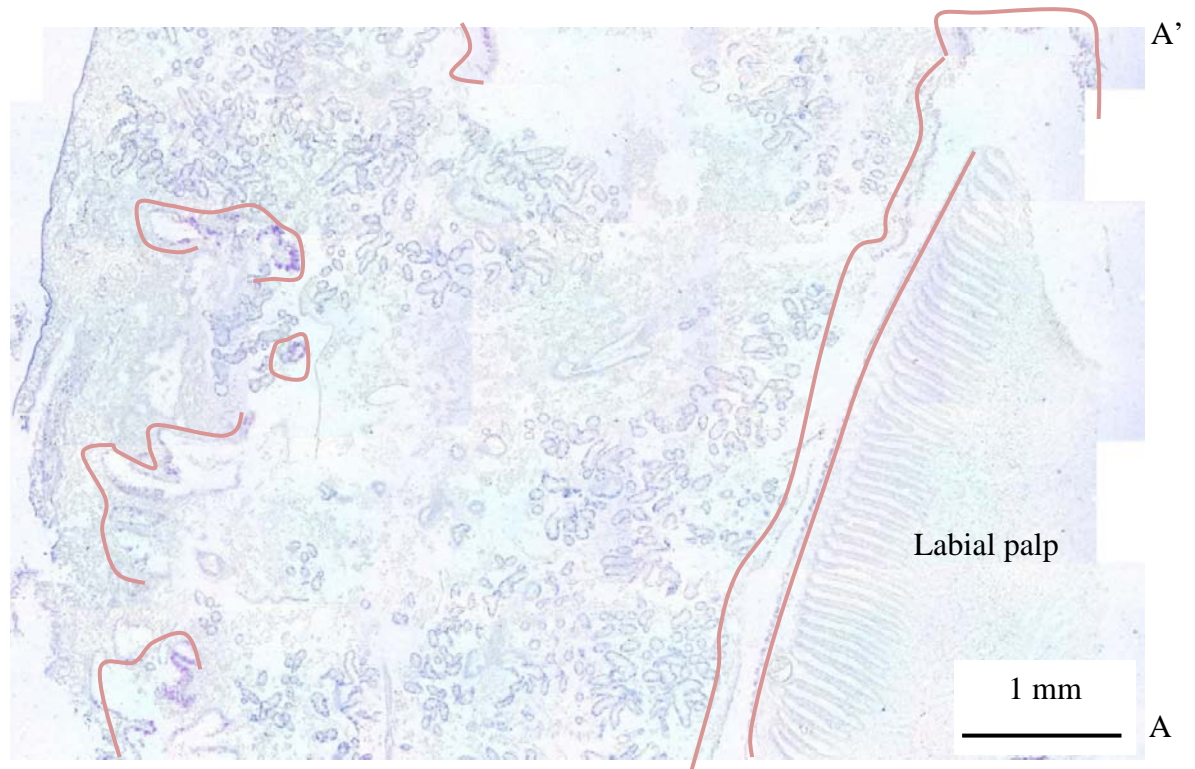
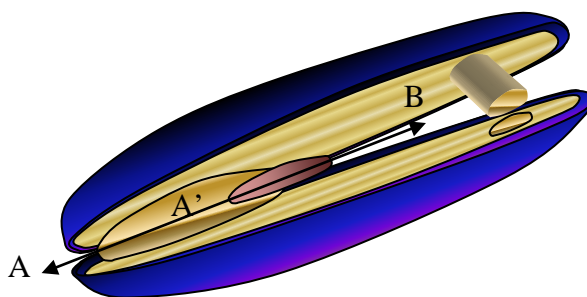


Figure 4.21: *Mytilus edulis*' visceral mass from 30 fields of view under bright field microscopy. The highest density of eosinophils (—) is found in association with the gut epithelium and with palp epithelium.



### 4.5.3 Observation of the gills tissue of *Mytilus edulis*

The gills tissue was studied to investigate haemocyte infiltration. Figure 4.22 is the compilation of the images taken at 100x magnification under bright field microscopy. Eosinophils and basophils were found in high number in the gill lamellae, eosinophils in close association with the epithelial cells and the basophils in the interstitial area. No approximation of the haemocyte number was possible, as the organ is convoluted and its dimension not appreciable.

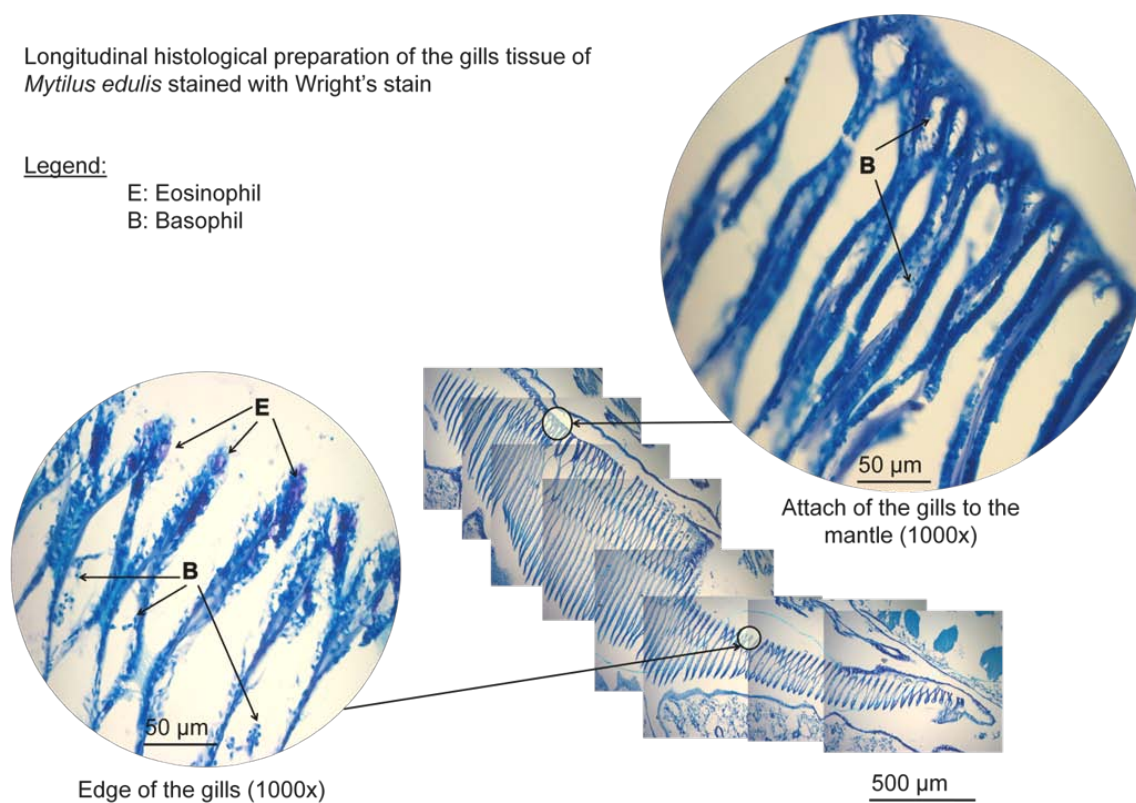


Figure 4.22: *Mytilus edulis*' gills from 8 fields of view under bright field microscopy. Eosinophils are found in association with the gills lamella epithelium, and basophils in the interstitial space in the lamella.

## 4.6 Discussion

### 4.6.1 Variations in the cell population level

The results of this population investigation have shown an unexpected variation of the different cell types in their ratio, but also in the number of cell types that comprise the haemocytes. In a random sample, the three typical cell populations are encountered, but at a lower frequency, entire cell groups are missing from the circulating haemolymph; in other cases, one or two unusual groups can be identified. To mitigate the impact of the cell type variation, the pooling of samples has been used for enzymatic assays (Coles and Pipe, 1994; Pipe et al., 1993; Winston et al., 1996), gene expression (Canesi et al., 2008; Costa et al., March 2009 ; Li et al., 2008a) and immune assays (Grundy et al., 1996). Other studies have been taking into account the cells ratio to normalise the results per individuals (Dyrynda et al., 1998; Wootton et al., 2003).

The data indicate ubiquitous variation of THC throughout the samples (field, aquarium controls and treated organisms), up to a factor of 50. This finding is also presented where the relative variability ranges from  $3 \times 10^5$  up to  $3 \times 10^6$  (Parisi et al., 2008). This variation in the controls shows no relation to the type of haemocyte population. These THC variations in normal conditions have also been recorded in other genera such as in *Eledone cirrhosa* (Malham et al., 1998), and in *Ruditapes philippinarum* (Ford and Paillard, 2007).

As presented in Chapter 3, the THC variation could be partly explained by the sampling procedure itself. Similar variations are observed in other bivalve species such as *Crassostrea virginica* with 68% and *C. gigas* with 51% variations in THC (La Peyre et al., 1995). Nevertheless, the sampling method can only be held accountable for a 31% of the observed variation. The further variation may be explained by the inter-individual variability.

#### 4.6.2 Inter-individual variability in circulating haemocytes of *Mytilus edulis*

Sampling results from the Outer Hebrides, the West coast, and from other sites show variations similar to those observed in the aquarium control. Given that the observer has no clues on the close or remote events occurring in the sampling area, any conclusion extracted from the data should be made with great care. The impact of physical stress such as air exposure, mechanical stress, high temperature and extreme salinity conditions are often hard to assess but have been shown to be significant (Fagotti et al., 1996; Grundy et al., 1996; Malagoli et al., 2007; Thompson et al., 1978). In addition, the micro-floral environment cannot be assessed in field circumstances despite its recognised impact (Lane and Birkbeck, 1999). Therefore, no correlation can be established from environmental data to anticipate immunological parameters, unless the challenge is of a dramatic scale, e.g. oil spill. In such a case, other eco-toxicological studies would be more appropriate, as eco-immunological methods are costly.

The data collected in the laboratory environment show a similar inter-individual variability. Since environmental factors such as light period, temperature, salinity, and predation are controlled in the laboratory, yet the haemocyte populations show a similar degree of numerical variation to those observed in the field samples, it is likely that these haemocyte concentrations and cell types' ratio variations are intrinsic to the organism.

Furthermore, spermatozoa were observed in haemolymph samples. No literature reports this observation. Contamination of the needle tip during the sampling cannot explain the levels of spermatozoa observed (up to 60% of the total cell population of the sample). It is reported that larger eosinophilic cell populations infiltrated in the mantle tissues are observed at the end of the reproductive cycle, and are involved in the gonads resorption (Bayne, 1976).

### 4.6.3 Individual variability of *Mytilus edulis* circulating haemocytes

Experiments on the variation in haemocyte cell type populations within a single individual are, when conducted over short time periods, striking for its degree of variability. Impact of tidal cycles have been recorded on the tissue level (Tremblay and Pellerin-Massicotte, 1997), on the enzyme regulation (Letendre et al., 2009; Letendre et al., 2008), and on gene regulation (Gracey et al., 2008). Similar immune cell variations, attributed to circadian cycles, have been observed in individuals of *Eledone cirrhosa* (Malham et al., 1998), in *Ruditapes philippinarum* (Ford and Paillard, 2007), and in zebra fish leukocytes (Kaplan et al., 2008).

This individual immune fluctuation over very short periods adds to the unreliability of single sampling points from field data. Furthermore, it also indicates that circulating haemocytes are not representative of the total immune cell population. These sudden fluctuations cannot be explained only by duplication of the immune cells. Other cell mechanisms are at work, such as cell reservoirs or cell infiltration into the tissues.

### 4.6.4 Investigation of a potential haemocyte reservoir in *Mytilus edulis*

The eosinophils appear ubiquitous in the investigated tissues (mantle, visceral mass, gills), but they are mainly associated with epithelial cells. Histological work on the adductor muscle and on the foot showed no eosinophils.

Basophils appear to be in lower number and are more scattered in the parenchyma tissues or in the internal space of the gills' lamella. They also have been seen in the adductor muscle in unpublished data.

In control organism, 25% of circulating cells are eosinophils, an average of  $5 \cdot 10^4$  eosinophils per millilitres. The number of infiltrated eosinophils ( $3 \cdot 10^7$  cells) is significant in regard to the circulating ones. Their mobilisation could explain the observed variation of the eosinophils in circulation, but the underlying mechanisms are unknown.

# Chapter 5

## Induced variability in the *Mytilus edulis* immune system



Title: Perspective.

This photo presents blue mussels a moment after their cannulation, the glue fixing the setup is left to harden. All mussels seem identical, organised and standardised. Yet, this impression is shattered by the detailed cellular study of their immune system, this system being one of the pillars of the biological self. This image introduces the chapter, which will put into perspective the dramatic variability of individual variation of immune parameters. It sets the difficulty to relate an observation to a causal link between observed immune parameters and a potential stress.

## 5 Induced variability in the *Mytilus edulis* immune system

### 5.1 Introduction

In the previous experimental chapter, the variability in the number and type of cells of the immune system has been identified as induced by the experimental bias, and by the nature of the organism itself. The experimental bias can be mitigated by the use of more accurate tools as well as the use of percentages that remove the problem of sampling variability. The variability induced by the organism, although described, has not yet been fully understood. This chapter will focus on testing the possible sources and causes of the observed variability. The sources of variation expected in the natural environment can be of biological and physical nature, but as unveiled in the previous chapter, the variation of the haemocyte population can be observed over very short time scales, underpinning another mechanism of differential haemocyte storage capacity.

As the circulating haemocytes are largely fluctuating in their number and relative ratio, the tissues of *Mytilus edulis*, such as gills, mantle, visceral mass or adductor muscle, were investigated in light of their “reaction” to physical, chemical, and biological stress.

The haemocytes are also involved in tissue damage restoration (Kádár, 2008; Kadar et al., 2008; Pauley and Heaton, 1969). In order to assess the stress *Mytilus* experiences by exposure to barium sulphate, a chemical used in offshore drilling mud, its impact on the gill tissues, guts and on the immune system was investigated.

Bacterial challenge mitigation is one of the main activities of the immune system. It is reported that *Mytilus* is colonised by a large number of bacteria (conference communication, Margulis, 2008) and some have reported that bacteria are found in the haemolymph of healthy organisms (personal communication, P. Roch, Montpellier II University, 2007). These interactions may be another key factor of variability of the circulating haemocyte populations. To test this impact, Chapter 5.3 will explore this form of biological stress.

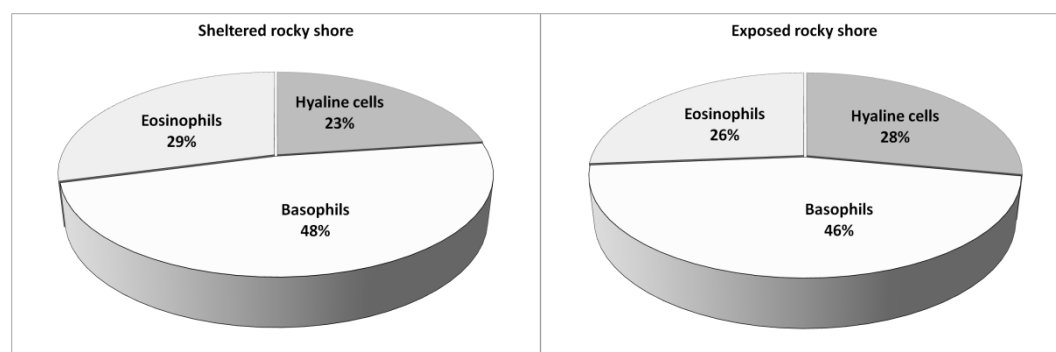


## 5.2 Impact of physical stress:

### 5.2.1 Impact of wave exposure on circulating haemocyte ratio

To test the impact of wave exposure on field organisms, ten mussels were sampled from the sheltered bay of Dunbar (Scotland) and ten others from the adjacent rocky shore on the 26/03/2007, using the conventional procedure (2.4.1). The samples were analysed by flow cytometry.

Figure 5.1 presents the percentage of the circulating haemocytes from organisms sheltered from (left), and exposed to (right), wave action. The standard variation is presented below the figure and its values indicate that the two wave exposure regimes had little or no impact on the cell ratio or the fluctuation.



#### Standard variation

N=10	Standard variation		
	Hyaline cells	Basophils	Eosinophils
Sheltered rocky shore	8%	10%	8%
Exposed rocky shore	9%	7%	7%

Figure 5.1: Percentage of haemocytes in exposed and sheltered mussels.

### 5.2.2 Impact of air exposure on circulating haemocyte ratio

A set of mussels acclimatised in the aquarium were kept either immersed in aerated, filtered seawater in a 50 litre plastic tank or in an empty 50 litre tank in the same condition of light and temperature for a period of five days. Five immersed and five air-exposed mussels were sampled morning and afternoon by conventional procedure then were placed back in another tank.

Figure 5.2 and Figure 5.3 present the percentages of circulating haemocytes in the two treatments; a large standard variation is observed. Immune parameters fluctuation are equivalent in the immersed and air-exposed groups until day 3, then the eosinophil populations decrease in mussels kept out of water in comparison with immersed animals.

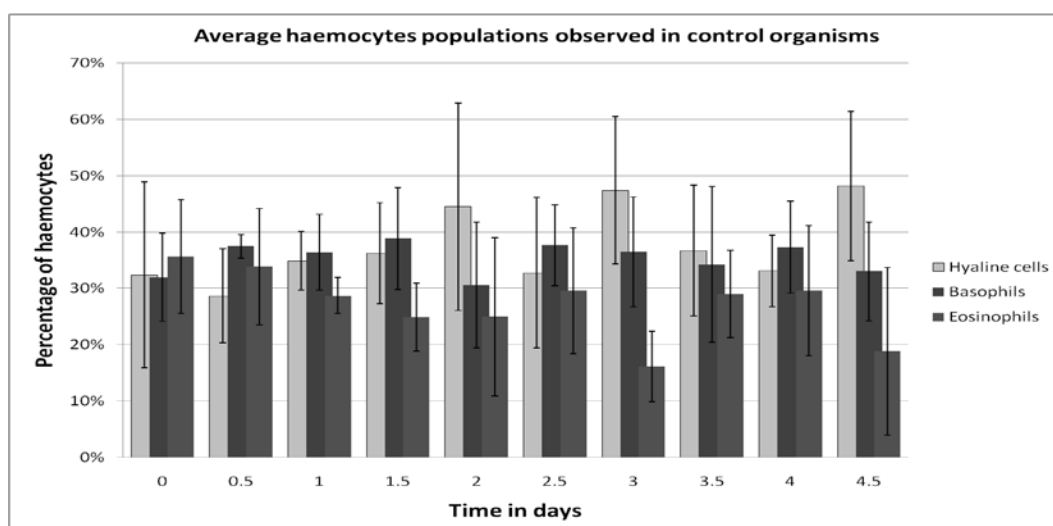


Figure 5.2: Percentage of haemocytes in mussels immersed in seawater over five days. N=5

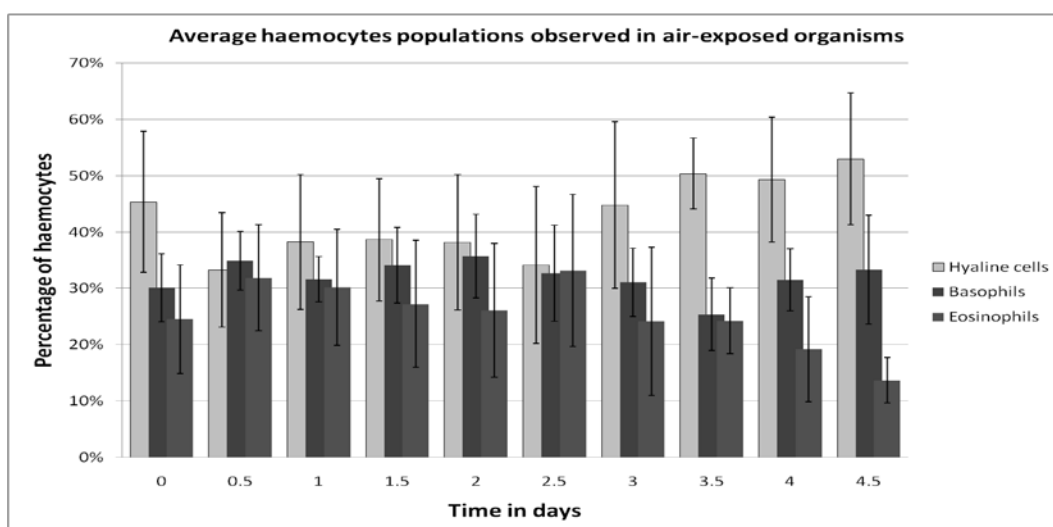


Figure 5.3: Percentage of haemocytes in non-immersed mussels over five days. N=5

### 5.2.3 Impact of iron oxide coverage on circulating haemocyte ratio

In North East England, 8km North of Hartlepool, mine water outfall is streaming on the rocky shore (Figure 5.4). The acidity of the underground water corrodes the iron structure of the mine and when the water reaches the surface, iron ions precipitate, covering the vicinity of outfall over 50 meters. Mussel mats growing on the iron-covered area, and mussels from a control site 100 meters south, were sampled twice in the course of four days on site using the conventional procedure. The samples were analysed by flow cytometry.

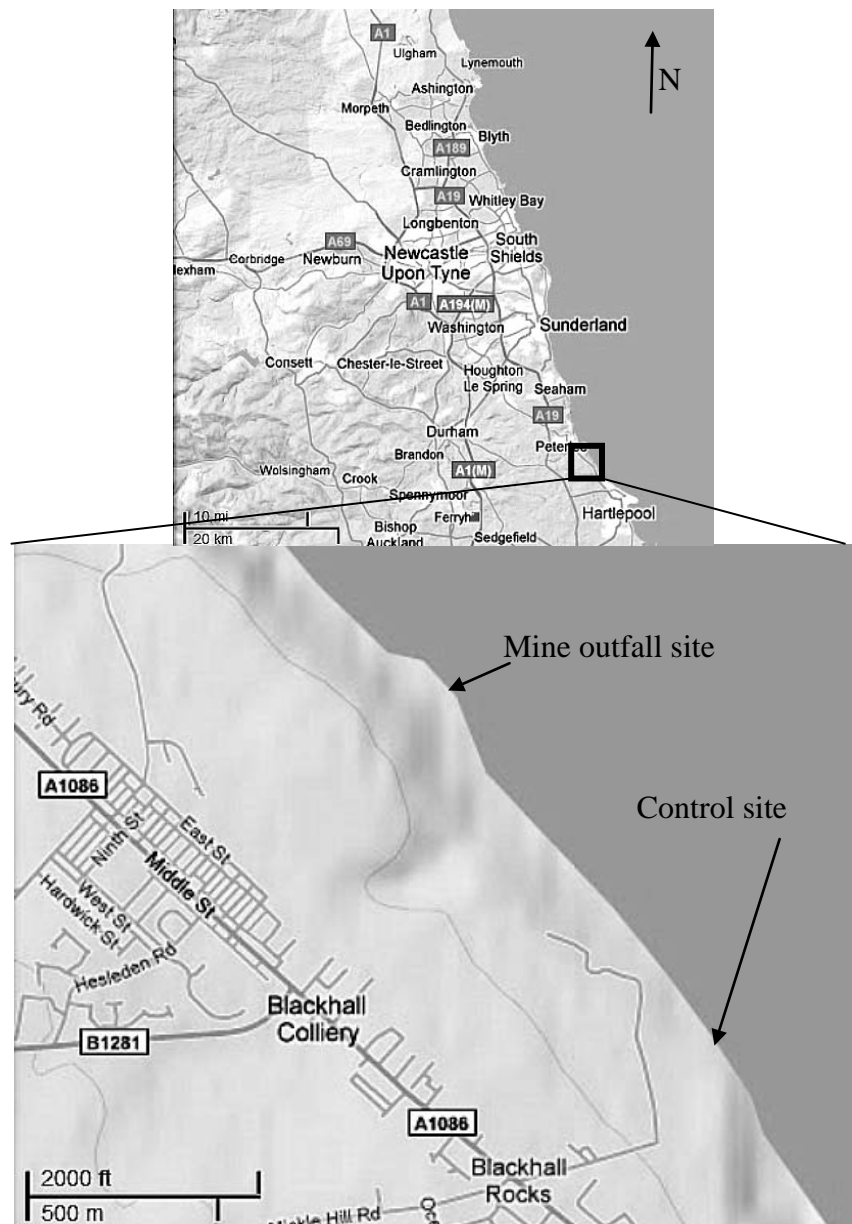
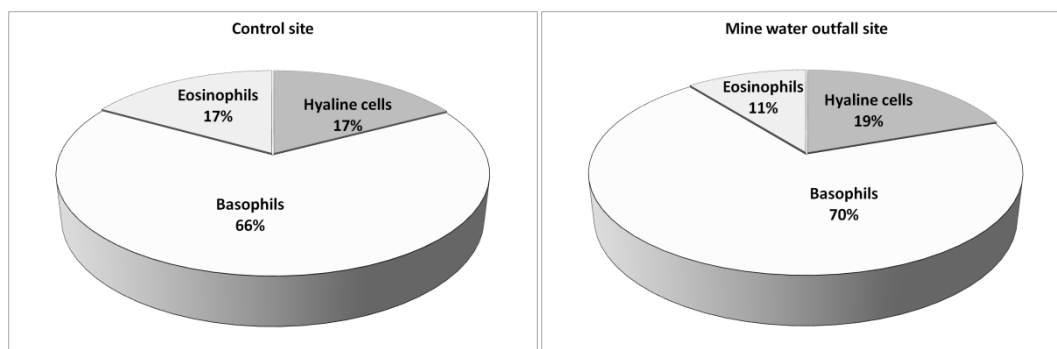


Figure 5.4: Sampling sites in Blackhall (UK).  
Sources: Google Map ©

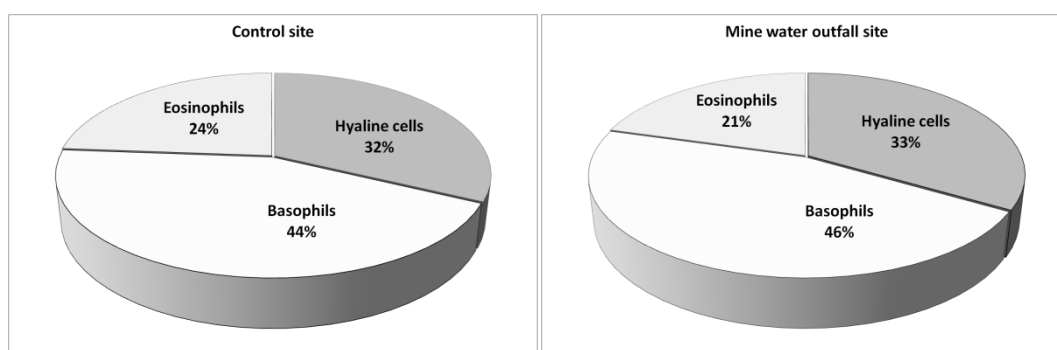
Figure 5.5 presents the comparison between percentages of circulating haemocytes from the two locations at the first sampling (17/09/2006), and Figure 5.6 shows that found during the second measurement (20/09/2006). A difference in the basophils dominance from the two sampling dates can be seen but no difference from the sampling location.



## Standard variation

	Hyaline cells	Basophils	Eosinophils
Control site (N=27)	11%	7%	8%
Mine outfall (N=9)	12%	6%	9%

Figure 5.5: Haemocyte percentages on the 17/09/06.



## Standard variation

	Hyaline cells	Basophils	Eosinophils
Control site (N=15)	8%	8%	8%
Mine outfall (N=30)	12%	8%	9%

Figure 5.6: Haemocyte percentages on the 20/09/08.

### 5.2.4 Barium sulphate

Having found little or no evidence of impact of the iron oxide smothering on the circulating immune system of *Mytilus edulis*, another experimental setup was developed, exposing the organism to barium sulphate. This experiment was expected to be more deleterious to the organism in two ways: First, in that the applied quantity was high, and second, that its effect on the tissue was known to be extremely abrasive (Maia Strachan, personal communication, 2007). Treated organisms were exposed for 5 days to daily continuous 2mm coverage of barium sulphate particles as described in Chapter 2.7.

#### 5.2.4.1 Impact of barium on the gill' tissues, surgical window

##### Tolerance of the surgical window by the organism

The surgical window, described in Chapter 2.4.3, was well tolerated by the organisms, as their feeding patterns were unchanged (unpublished data) and long viability was achieved. The complete recovery of the organism was observed after a 5-month period; when re-growth had closed the observation hole entirely. This observation correlates with *M. edulis* recovery studies (Kádár, 2008; Kadar et al., 2008).

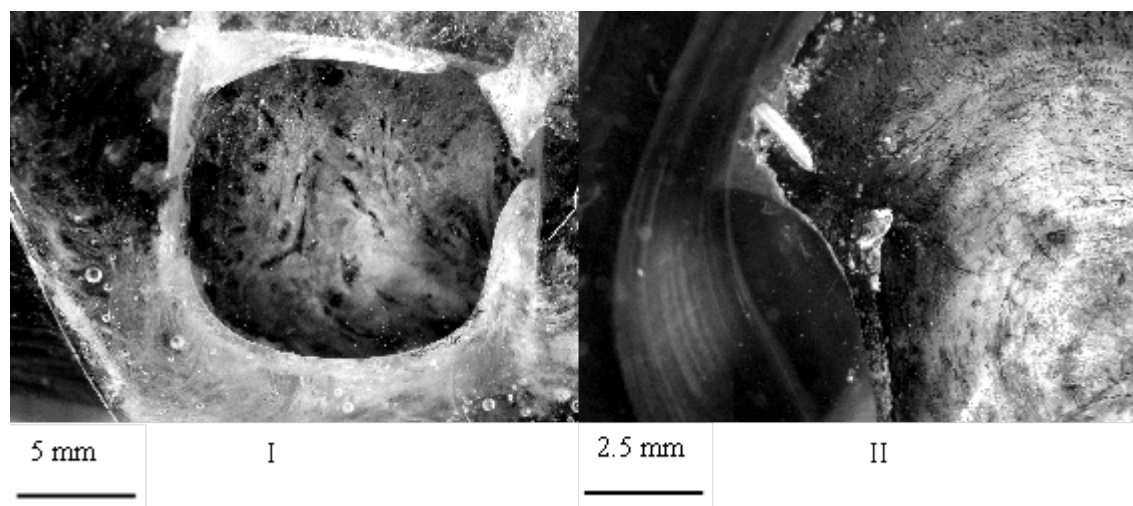


Figure 5.7: Macro picture of a fully re-grown shell.

I: outside view of the shell regrowth, the brittle membrane is cream to brown in colour, with dark brown to black patterns.

II: inside view of the shell regrowth, the newly formed shell covers about twice the original hole and offers series of concentric striations of regrowth. The colour, initially brown, turns to light brown at its centre.

### Gill damage observed on *Mytilus edulis*

The impact of barium on a macro scale has been investigated using 15 organisms with a surgical window, collected in Cramond and acclimatised for three days in the aquarium. It allowed the visualization of the erosive activity of the barite on the delicate structure of the gills, thus affecting both their structure and integrity.

In Figure 5.8 II, the faint line is the barium sulphate trapped by the gill mucus that will later be excreted as pseudo-faeces. The two main damages observed on the treated gills (right picture) are large invaginations on the fringe and disrupted and irregular connective lines (white arrows).

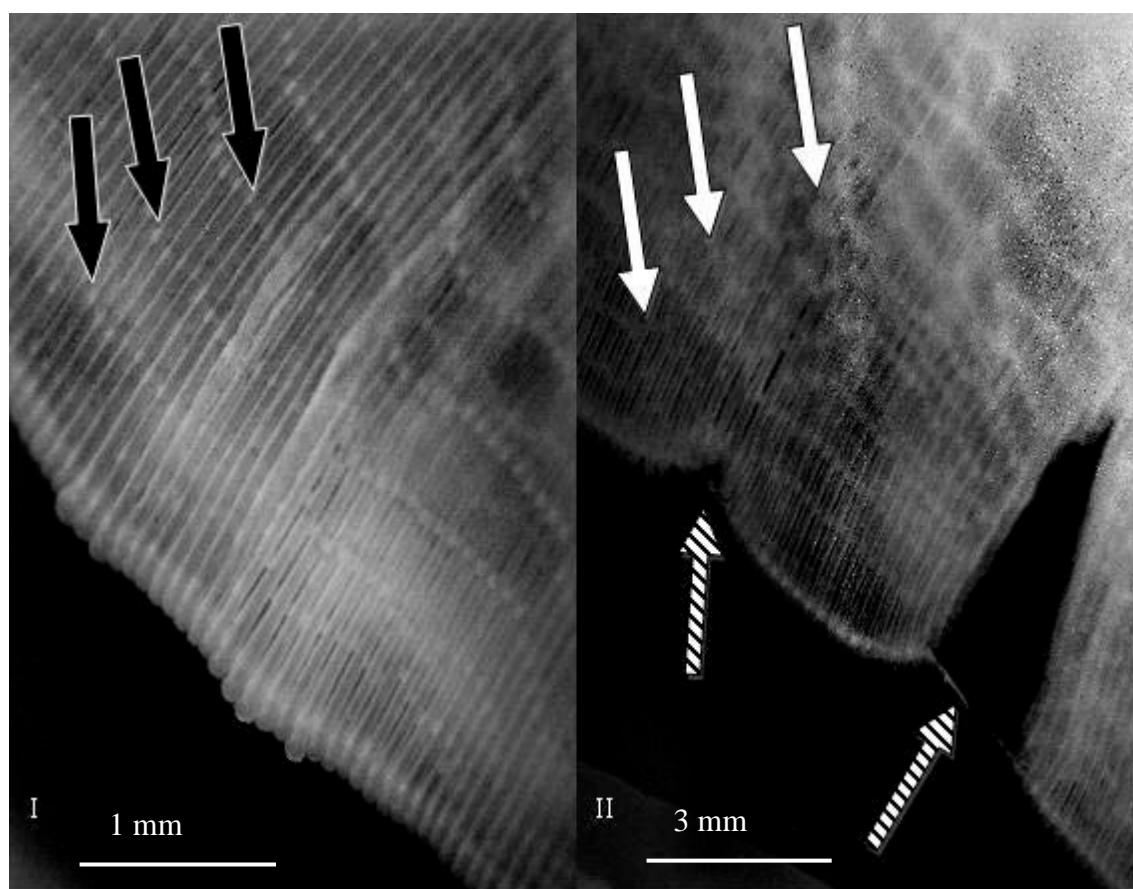


Figure 5.8: Pictures of impact of barium sulphate on gills of *Mytilus edulis*.

I: control organism, the gills' lamellae are regular and the connective tissues (black arrow) are regular.

II: treated organism, the gills' lamellae are split (stripy arrows) and the connective tissues (white arrows) are irregular. The striped arrows indicate barium sulphate trapped in gill mucus.

### Gill damage observed on *Modiolus modiolus* (Horse mussel)

To explore whether the impact of barium on a macro scale can similarly be traced in the gills of a different species of bivalve, *Modiolus modiolus* was chosen to undergo the same treatment. The sample size was increased to 20 organisms, all mounted with a surgical window. The damages observed previously on *Mytilus edulis* were also present in *Modiolus modiolus*. In addition, large scar tissues appeared sporadically (Figure 5.9 II).

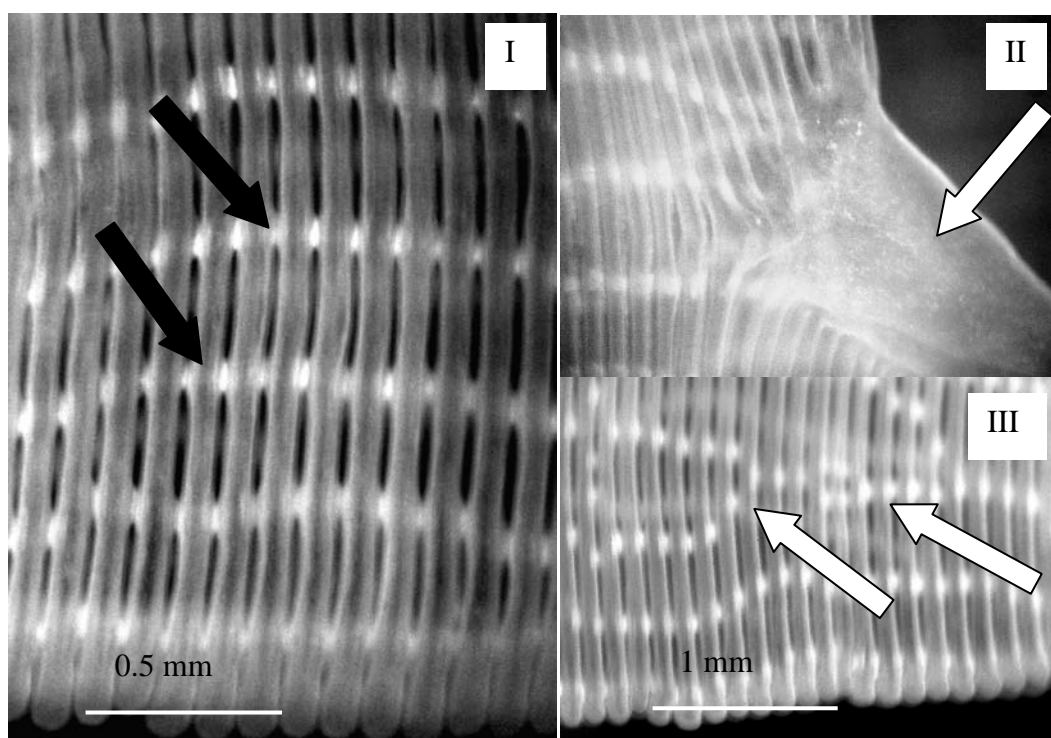


Figure 5.9: Pictures of impact of barium sulphate on gills of *Modiolus modiolus*.

I: control organism, the gills' lamellae are regular and the connective tissues (black arrow) are regular.

II: treated organism, scar tissues on the lamellae (white arrows).

III: treated organism, the connective tissues (white arrows) are irregular.

#### 5.2.4.2 Impact of barium sulphate on *Mytilus edulis*, histological scale

To introduce the immunological study, exposed tissues (gills, intestines) were searched for evidence of damage and immune cell infiltration. The immunological study was done on *Mytilus edulis* for practical reasons, and the immune parameters were studied in *M. edulis* (wild and farmed samples) and in *Modiolus modiolus*.

#### Damage of barium sulphate on the gill tissues

Control organisms show a thin basal lamina of the gill lamellae (Figure 5.10 I). Basophils are observed in the internal lumen of gill lamellae, eosinophils at the top of the lamellae, and the gill cilia are long and bushy.

In treated organisms (Figure 5.10 II), no or very few basophils are visible, eosinophils are present in high numbers and scattered along the lamellae. The basal lamina appears thickened, and the gill cilia are short and damaged. Particles of barium sulphate are embedded in the inter lamella space and can be found inserted into the epithelium.

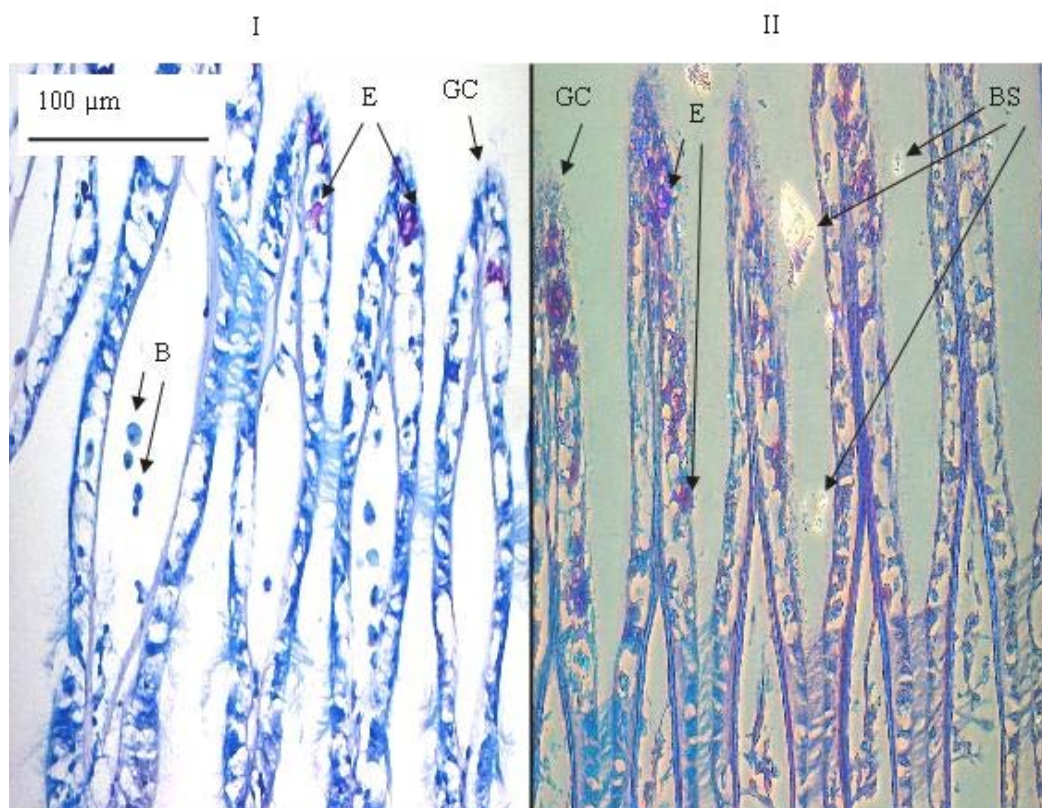


Figure 5.10: Transverse section of *Mytilus edulis*' gills under bright field microscopy.  
 I: control organism, basophils (B) in the internal lumen of gill lamella, eosinophils (E) located at the top of the lamella, gill cilia (GC) long and bushy .  
 II: treated organism, no basophils visible, eosinophils (E) in high numbers , gill cilia (GC) short and damaged, barium sulphate (BS)



### Damage of barium sulphate on digestive tissues

Control organisms (Figure 5.11 I) show normal stomach walls and thin digestive cecum walls, a low or localised eosinophil infiltration, often associated with the epithelium.

In treated organisms (Figure 5.11 II), the stomach walls are thinner and the digestive cecum walls are thickened. Large amounts of eosinophils are found in the interstitial tissues and also the lumen. Particles of barium can be identified clearly, as they are very refractant to the light.

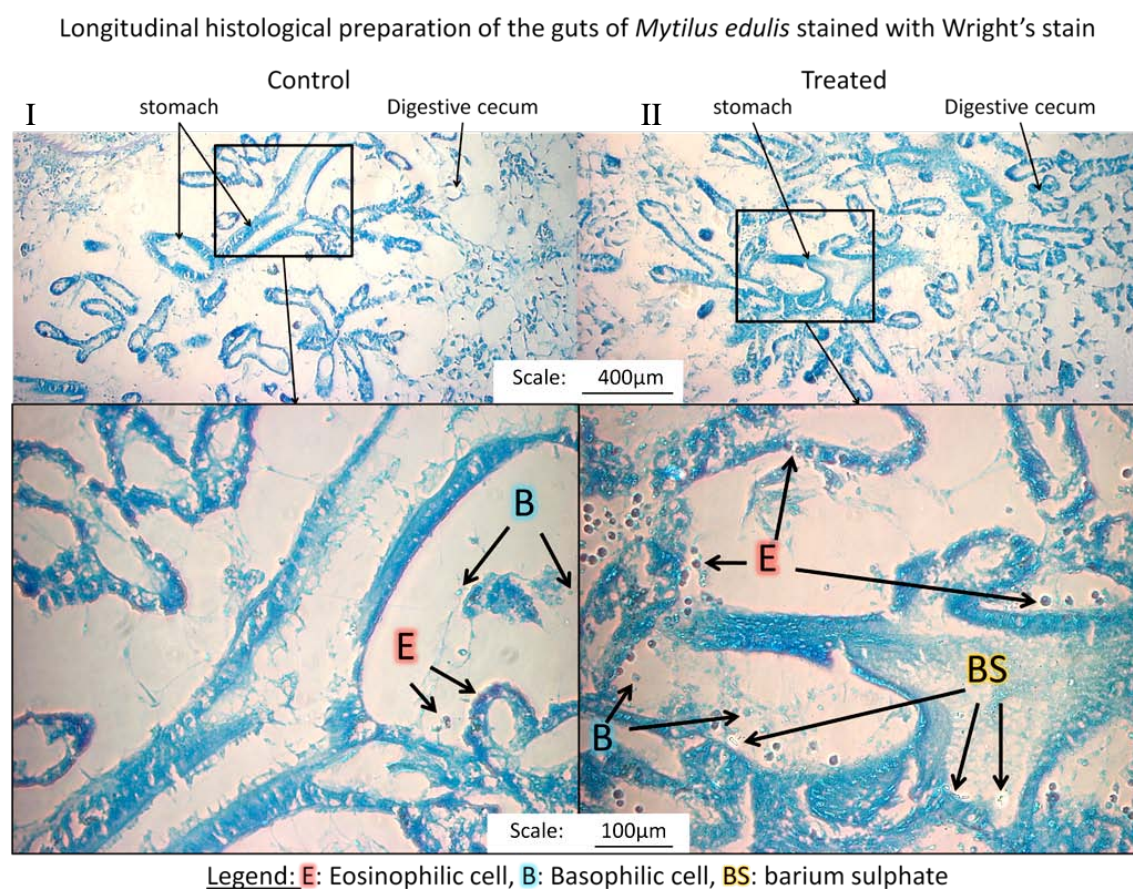


Figure 5.11: Section of the visceral mass of *Mytilus edulis*.

I: control, few haemocytes observed and eosinophils mainly in association with the gut epithelium.

II: treated, haemocytes infiltrated in the surrounding tissues of the guts and within the guts tract, barium sulphate is observed in the guts lumen.

### 5.2.4.3 Impact of barium: the circulating immune system

In addition to the tissue investigation, circulating haemocytes were investigated in cannulated, wild and farmed mussels of *Mytilus edulis*, as well as in *Modiolus modiolus* (Horse mussel), to measure their potential fluctuation when exposed to physical stress. To assess the influence of the mussel adaptation to its environment in its development, farmed mussel and Cramond mussel were exposed to barium sulphate. In this case, farmed mussels were grown on ropes in Scottish loch where the potential exposition to wave action and sand erosion were much reduced. Cramond mussels were grown on an exposed shore at the vicinity of a sand bank.

#### Impact of barium sulphate on cannulated mussels

Fifty microlitres of haemolymph were sampled daily from the cannula on control and treated animals, and analysed by flow cytometry. The cannula was still under development, and not all data were useable. The barium had a highly deleterious effect on the survival of cannulated mussels. Nevertheless, the data indicate an impact of barium sulphate stress by the decrease of circulating eosinophils and an increase of hyaline cell populations.

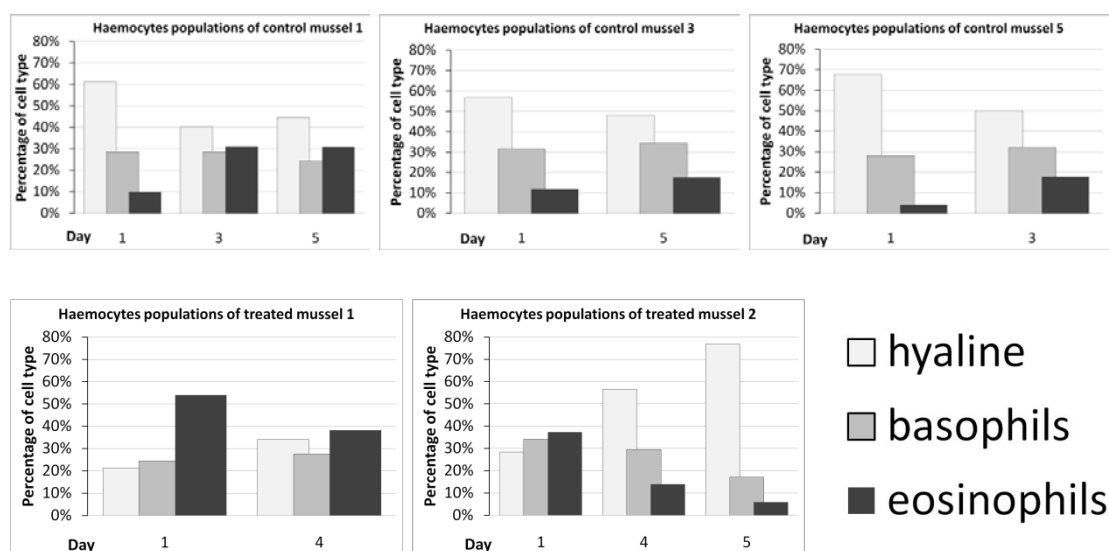


Figure 5.12: Percentages of circulating haemocytes in control and barium sulphate treated cannulated mussels.

In control mussel 1, 3, and 5, the percentages of eosinophils are slightly increasing and the hyaline population decreasing.

In treated mussels 1 and 2, decreases in eosinophils and increases in hyaline cell populations are observed.

## Impact of barium sulphate on Cramond mussels

The same five control and treated individuals were sampled daily over five days. Five hundred microlitres of haemolymph were sampled from the adductor muscle using the conventional method and analysed by flow cytometry. Control data (Figure 5.13) show increased hyaline cell populations (+31%, +/-5%), no significant change in basophils (0%, +/-4%), and a decrease in circulating eosinophil (-30%, +/-5%). Treatment data show increased hyaline cell populations (+27%, +/-6%), no significant change in basophils (-3%, +/-5%), and a decrease in circulating eosinophil (-24%, +/-6%).

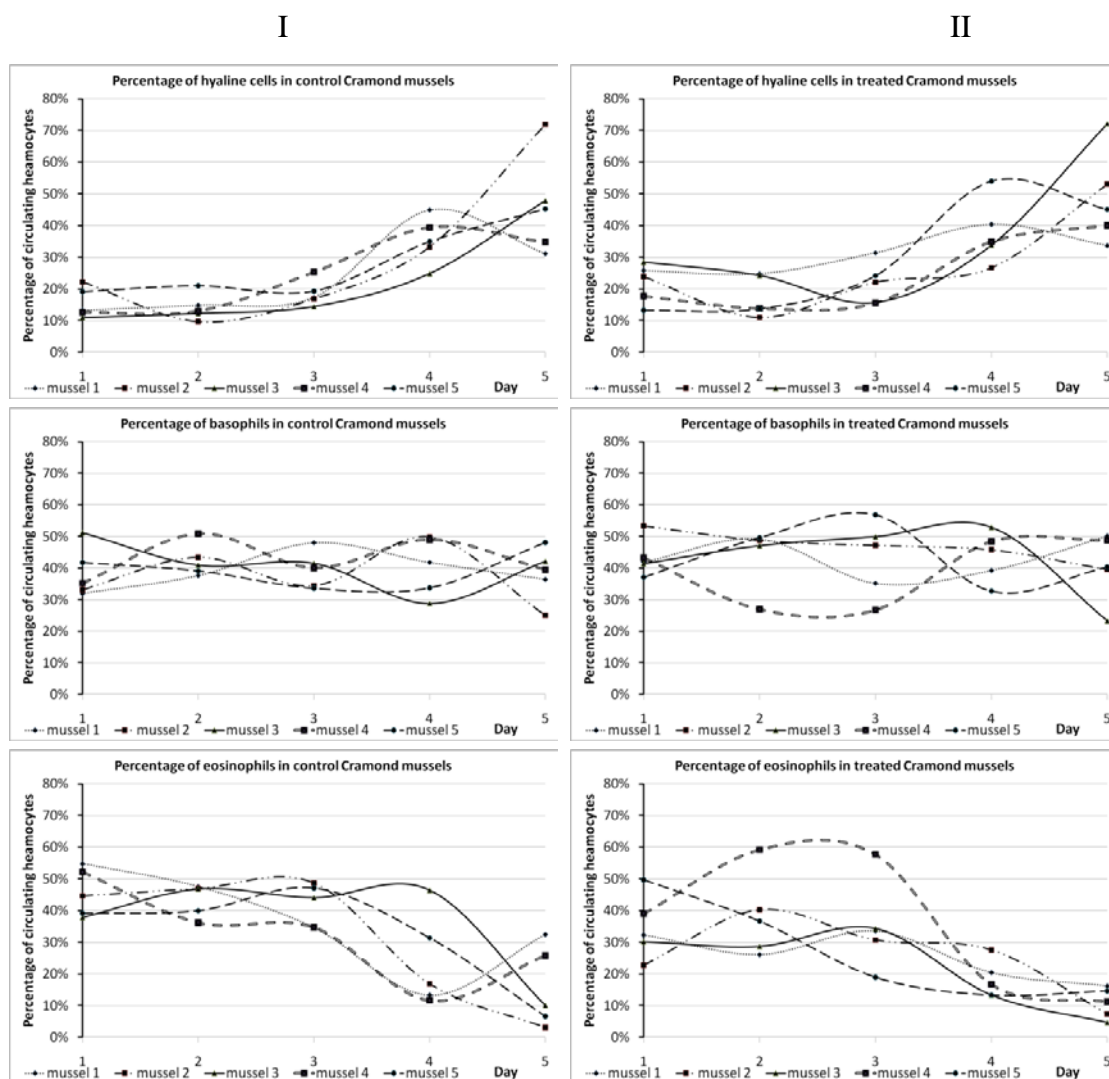


Figure 5.13: Change in circulating haemocyte populations of Cramond mussels over five days. I control, II treatment. In I and II, a similar pattern of inter-individual variability is observed; also appreciable are equivalent motifs of increase (hyaline cells), regularity (basophils), and decline (eosinophils).

## Impact of barium sulphate on farmed mussels

The same five control and treated individuals were sampled daily over five days. Five hundred microlitres of haemolymph were sampled from the adductor muscle using the conventional method and analysed by flow cytometry. Control data show increased hyaline cell populations (+26%, +/-6%), no significant change in basophils (-1%, +/-5%), and a decrease in circulating eosinophil (-25%, +/-5%). Treatment data show increased hyaline cell populations (+21%, +/-3%), no significant change in basophils (-3%, +/-3%), and a decrease in circulating eosinophil (-25%, +/-2%). However, no difference was observed in the haemocytes ratio between farmed and Cramond mussels.

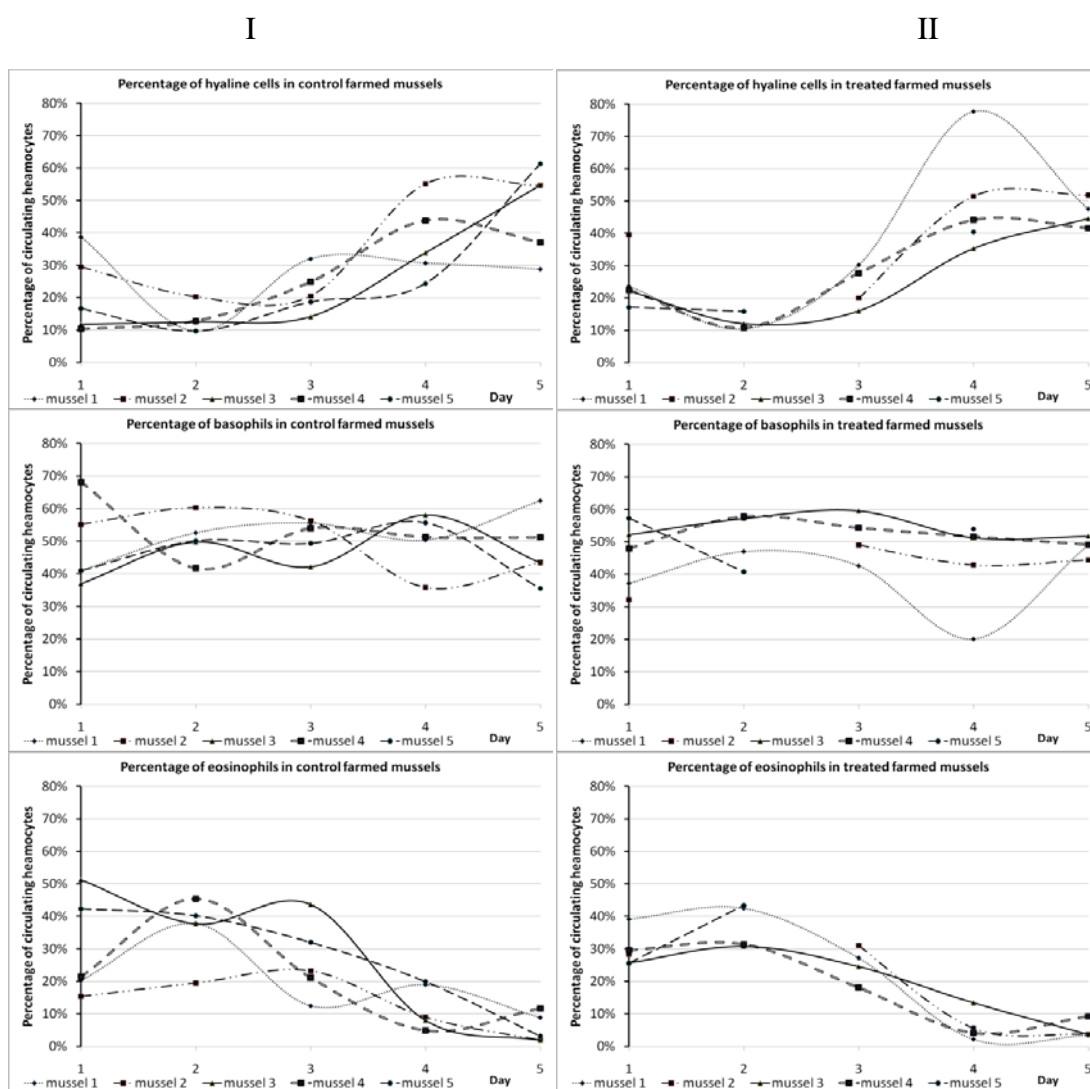


Figure 5.14: Change in circulating haemocyte populations of farmed mussels over five days. I control, II treatment. In I and II, similar pattern of inter-individual variability is observed; also, equivalent motifs of increase (hyaline cells), regularity (basophils), and decline (eosinophils) are observed.

## Impact of barium sulphate on horse mussels

The same five control and treated individuals were sampled daily over five days. Seven hundred and fifty microlitres of haemolymph were sampled from the adductor muscle using the conventional method and analysed by flow cytometry. Control data show increased hyaline cell populations (+31%, +/-3%), no significant change in basophils (-2%, +/-2%), and a decrease in circulating eosinophil (-29%, +/-3%). Treatment data show increased hyaline cell populations (+40%, +/-3%), a slight decrease of basophils (-13%, +/-2%), and a decrease in circulating eosinophil (-27%, +/-2%).

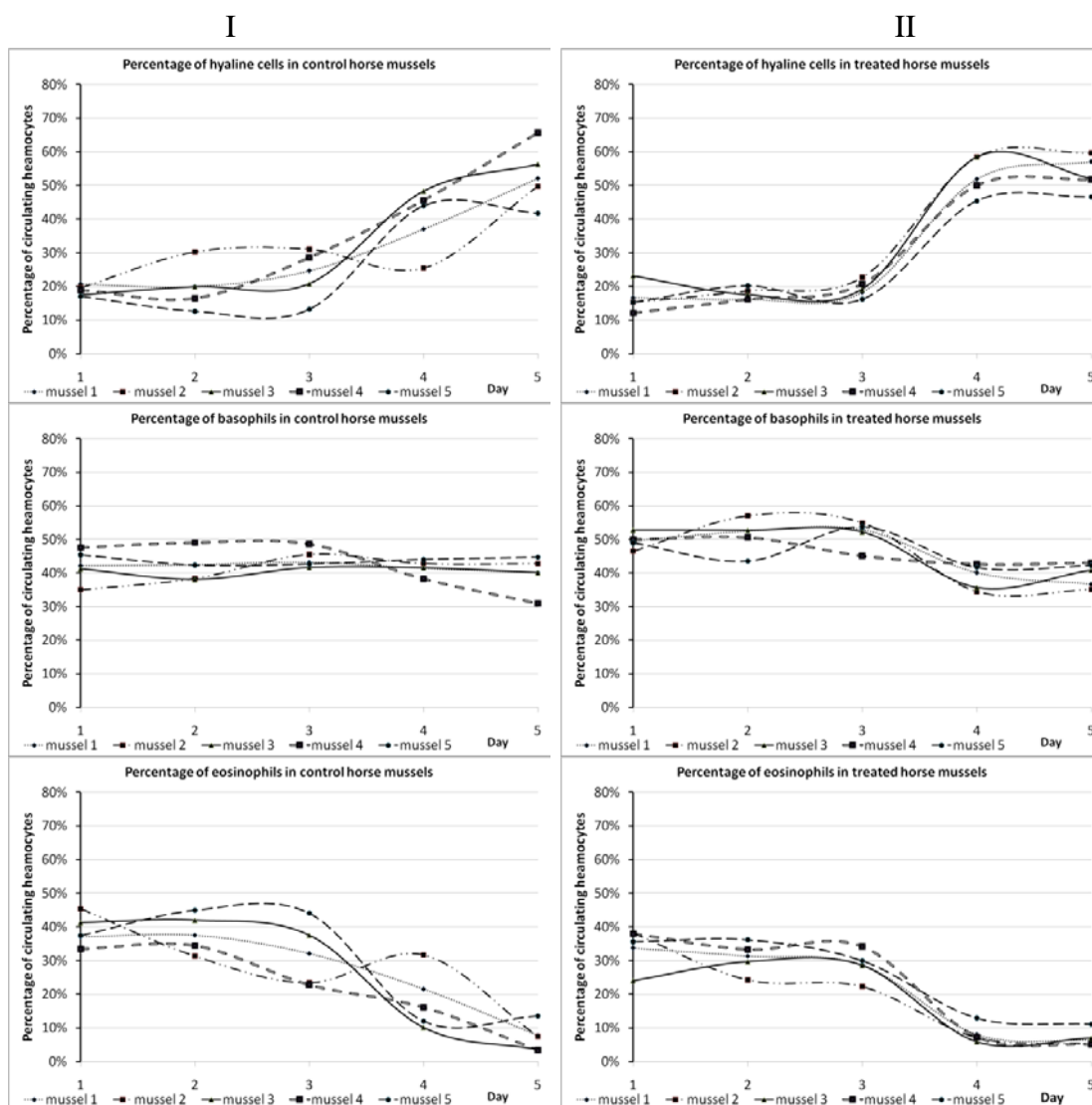


Figure 5.15: Change in circulating haemocyte populations of horse mussels over five days. I control, II treatment. In I and II, similar pattern of inter-individual variability is observed; also, equivalent motifs of increase (hyaline cells), regularity (basophils), and decline (eosinophils) are observed.

### Short comparative conclusion from cannulation and normal sampling

Table 5.1 presents the data from the sections 0 It suggests that hyaline cells, basophils and eosinophils ratio fluctuations are following the same patterns. The impact of the sampling will be discussed further on in the discussion.

Table 5.1: Variation encountered in haemocyte populations during the 5-day experiment. Cell type variations observed between the control and the treatment are similar for tested groups with the exception of the treated horse mussel.

	variation of hyaline cells	variation of basophils	variation of eosinophils
Cramond mussels control	31%	0%	-30%
Cramond mussels treated	27%	-3%	-24%
farmed mussels control	26%	-1%	-25%
farmed mussels treated	21%	3%	-25%
horse mussels control	31%	-2%	-29%
horse mussels treated	40%	-13%	-27%
highest and lowest observed standard variation (+/-)	3 to 6%	2 to 5%	2 to 5%

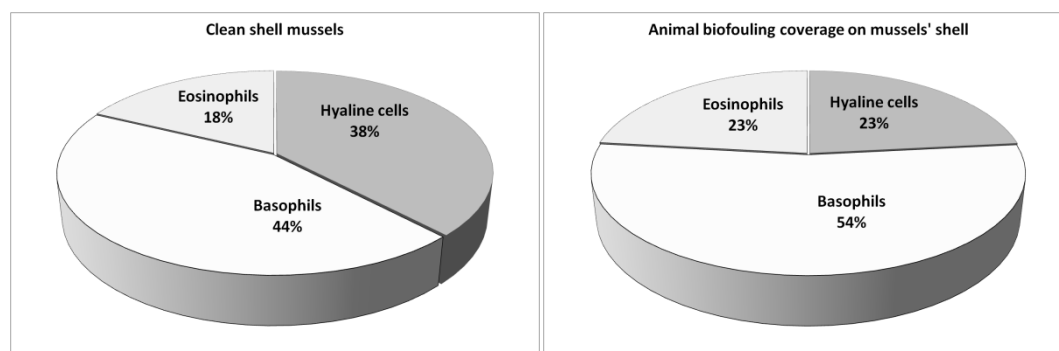
### 5.3 Impact of biological stress:

To evaluate the impact of biological stress on two levels, externally and internally, the immune system of *Mytilus edulis* was investigated from populations with heavy biofouling (covered with epizoic macro-organisms), as well as bacterially challenged individuals.

#### 5.3.1 Biofouling of the shell

Mussels were collected in Cramond from the same mussel bed, clean shell mussels and biofouled shell mussels were brought back to the aquarium. After an acclimatisation time of two days, the mussels were bled using the conventional method from the adductor muscle. The haemolymph was analysed by flow cytometry.

Figure 5.16 presents the percentages of haemocytes population. Underneath the figure, the standard deviations of the experiment are given. The immune cell ratios observed in biofouled individuals are comparable with those of clean shell individuals.



#### Standard variation

	Hyaline cells	Basophils	Eosinophils
Clean shell (N=7)	11%	7%	8%
Biofouling (N=7)	12%	6%	9%

Figure 5.16: Haemocytes percentage of clean and biofouling mussels.

### 5.3.2 Bacterial exposure

#### 5.3.2.1 Description of bacterial communities

#### Bacterial isolated from mussels and grown on marine agar

Two adjacent tanks with mussels acclimated for three weeks were investigated. Mussels in tank B developed spontaneously a none-induced bacterial outbreak, mussels from adjacent tank S was then used as a reference for healthy individuals. The investigation of the bacterial communities was focused on the water column, on the tank wall, on the mussel shell, on the internal cavity water, on the gills and on the guts. The ten bacterial strains isolated are listed in Tables 5.2 and 5.3.

Table 5.2: Characteristics of isolated strains of bacteria collected from the aquarium environment






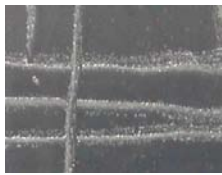



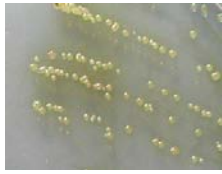
Strain name	Colony size	Colour	Light characteristic	Edges of colonies	Odour strength	Picture
A	large 3 to 5mm	creamy	opaque	white	+	
B	large 2 to 3 mm	creamy white	translucide		+	
C	large	white	Translucid heterogeneous (white dots)		+	
D	medium	creamy	opaque		+	
E	medium	creamy	diffuse		+	



Table 5.3: Characteristics of isolated strains of bacteria collected from the aquarium environment.

In strain H and I, the isolate show no colouration although strong colour was observed on the mother colony (overlapping photos).

Strain name	Colony size	Colour	Light characteristic	Edges of colonie	Odour strength	Picture
F	small/ medium	creamy white	opaque		+	
G	large	pale cream to orange	opaque		++	
H	large	red in community creamy in isolation	opaque		++	
I	medium	very yellow in community creamy in isolation	opaque	diffuse	++	
J	large	brown	opaque	colour diffusion	++	

### Bacterial strain communities observed on the mussel environment and tissues

The surfaces samples were collected with a sterile cotton bud and plated on marine agar Petri dishes. Liquid samples (tank water and internal cavity water) were plated pure, 100x, and 200x diluted in sterile seawater. One hundred microlitres of the bacterial suspension were plated and incubated for two days at 25°C.

Strains A, B, and F were common to both tank mussels. The strain C, D, and E were not found in diseased mussels, but strains G, H, I and J were. H was found in the internal cavity and digestive tissues of ill mussels, J was detected in the water column and the gills.

Table 5.4: Compilation of the bacterial strains found in the control and outbreak tanks. The data regarding the tank walls and mussel shell could not be analysed as they were too densely grown, see Appendix IV.

Strain name	Control				Bacterial outbreak			
	Water column	Internal cavity	Gills	Guts	Water column	Internal cavity	Gills	Guts
A	+	+	+	+	+	+	+	+
B	+	+	+	+	+	+	+	+
C	+	+	+	+				
D	+	+	+	+				
E	+	+	+	+				
F	+	+	+	+	+	+	+	+
G					+	+	+	+
H						+		+
I						+		
J					+		+	

## 5.3.2.2 Impact on the visceral mass, histological level

**Eosinophil population patterns in the visceral mass**

Ten organisms were prepared as presented in Chapter 2.3. Figure 5.17 shows the upper part, and Figure 5.18 the lower part of the visceral mass of a bacterially challenged mussel. A depletion of the eosinophil population is observed compared to of a non-infected organism (Figure 4.20).

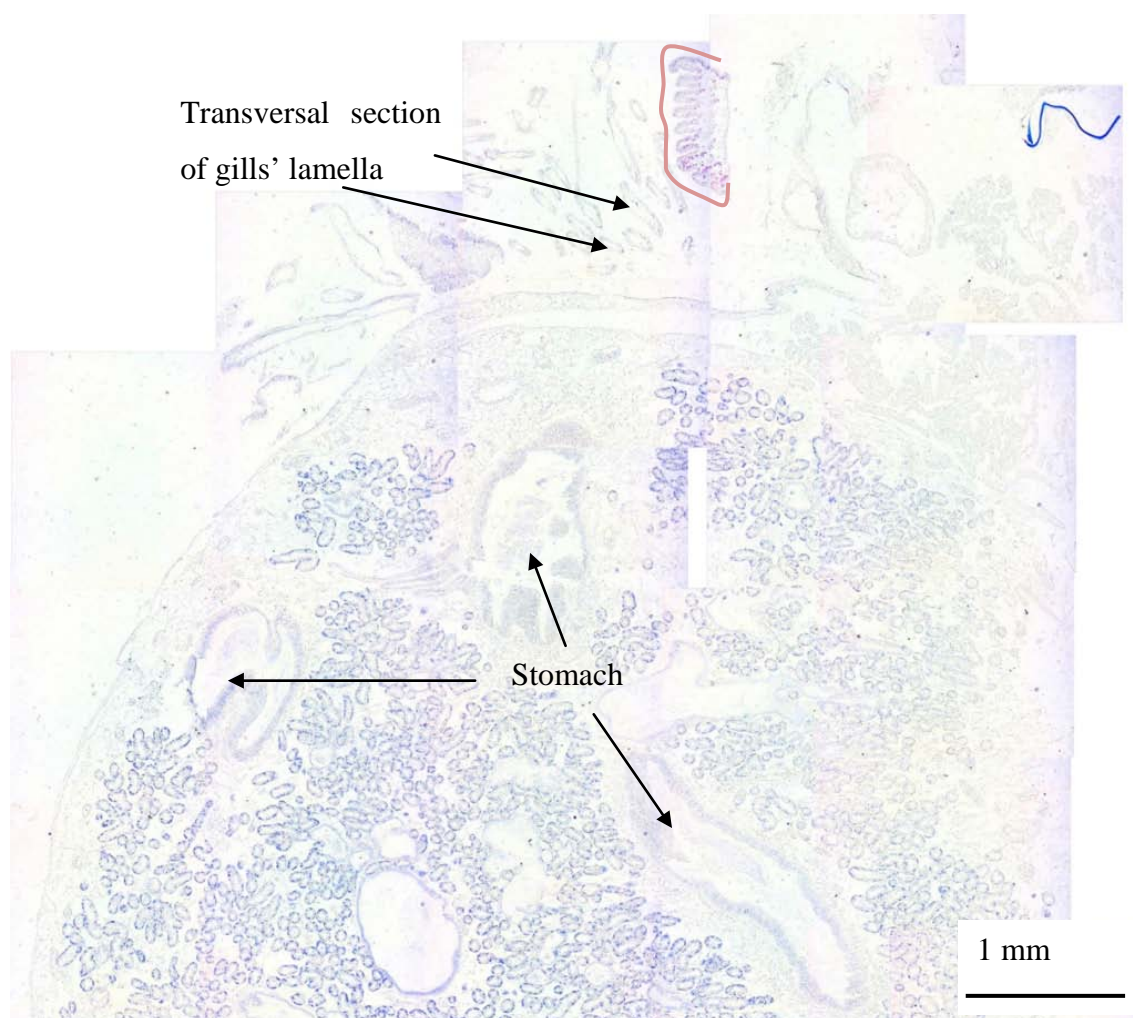


Figure 5.17: Upper part of visceral mass of a bacterially challenged *Mytilus edulis*. Image from 25 fields of view under bright field microscopy. Eosinophils (—) are only found outside of the visceral mass in association with the gills epithelium.

Figure 5.18 shows a complete depletion of eosinophil population compared with that from non-infected organisms (Figure 4.20, Figure 4.21). The labial palp has also lost its associated eosinophil population

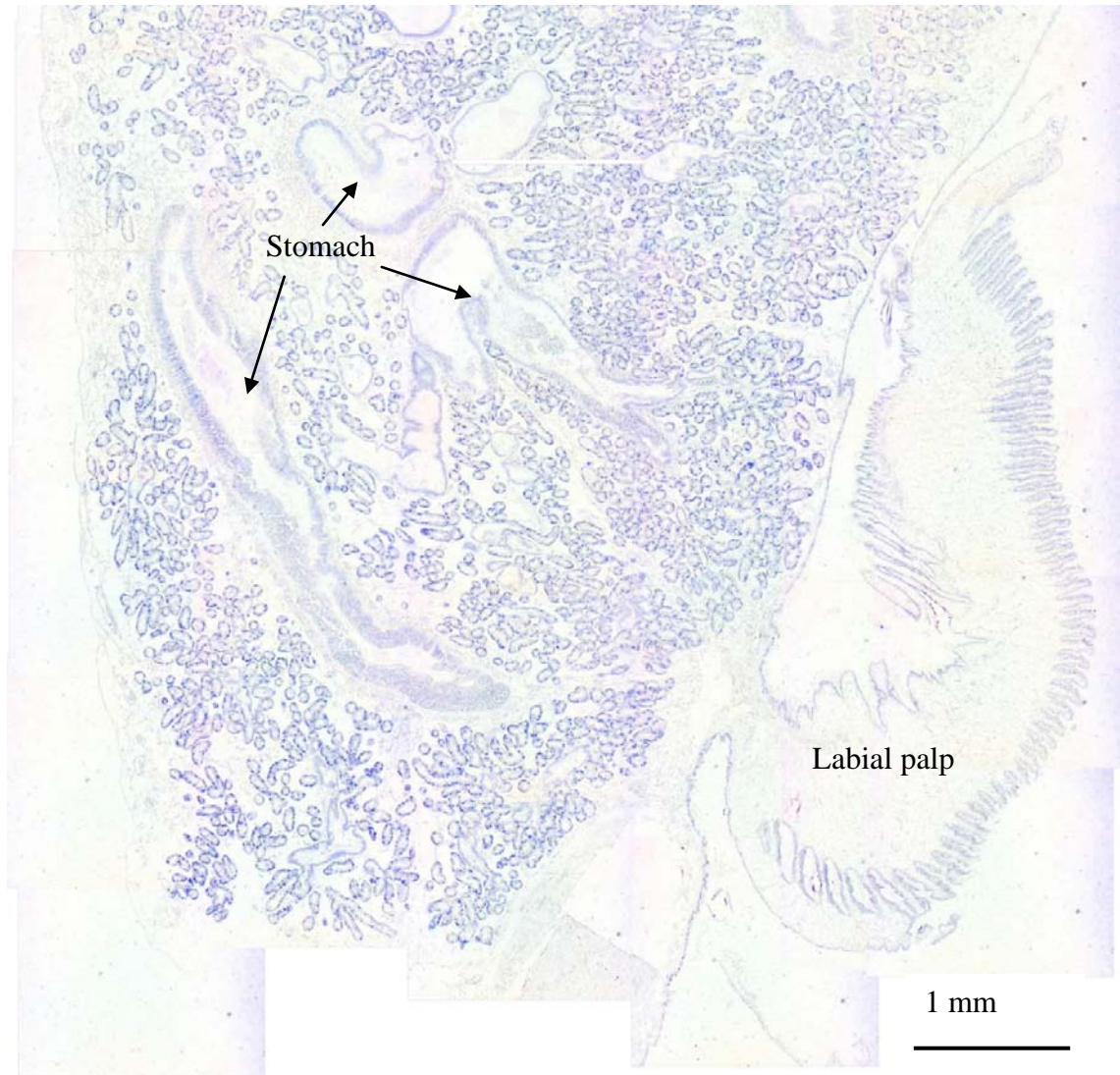


Figure 5.18: Lower part of visceral mass of a bacterially challenged *Mytilus edulis*. Image from 27 fields of view under bright field microscopy. No eosinophils are found in the visceral mass compared with control organisms (Figure 4.21).

### Basophil and hyaline cell population patterns in the vicinity of the stomach

Data from Figure 5.19 present a longitudinal section of the stomach. In association with the muscular stomach wall, basophilic cells in the interface of the caecum can be observed.

In addition, individual cells are observed at the basal end of the stomach wall. These cells are strongly stained and smaller than the basophils. They are similar in size and in cytoplasm/nucleus ratio to hyaline cells.

Longitudinal histological preparation of the stomach of *Mytilus edulis* stained with Wright's stain

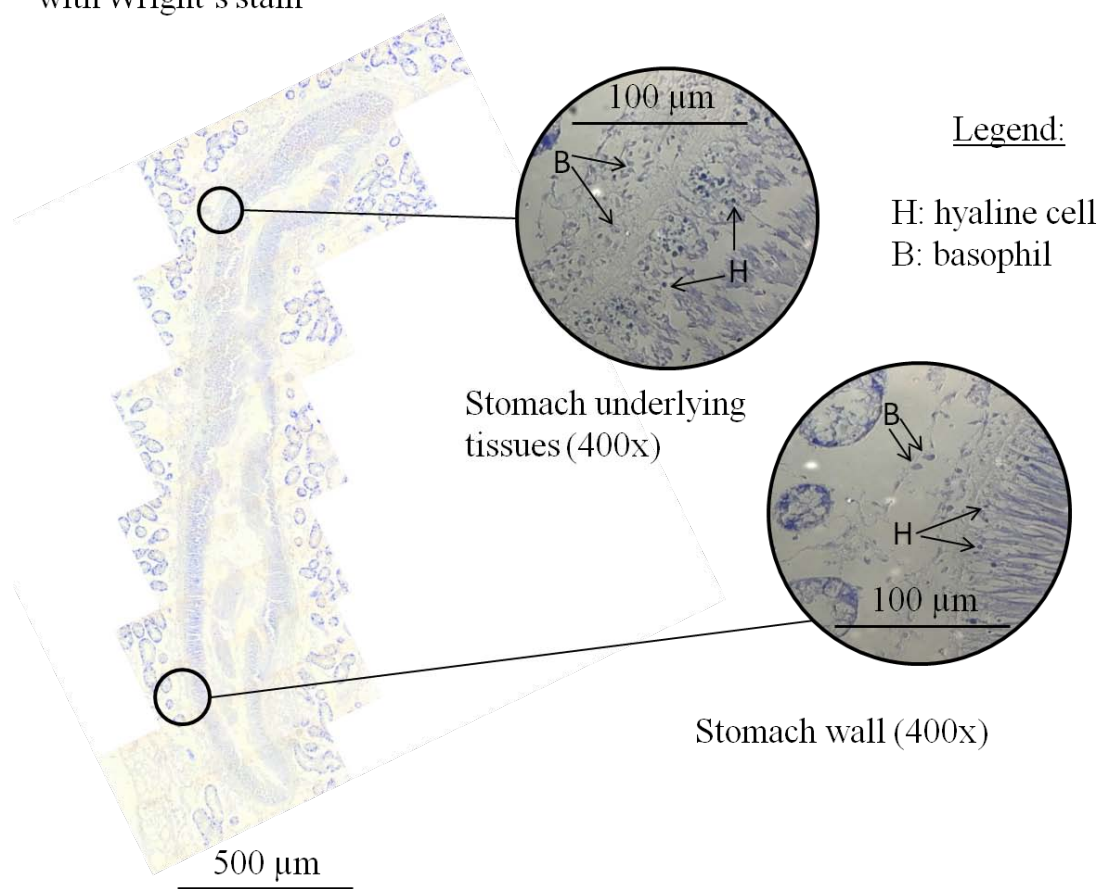


Figure 5.19: *Mytilus edulis* stomach from 29 fields of view under bright field microscopy. No eosinophils are found, basophils and hyaline cells are observed at the vicinity and in the stomach wall. The magnified areas present the structures and cell types observed in periphery of the stomach wall.

### 5.3.2.3 *Impact of bacterial challenge on the circulating immune system*

Cramond mussels acclimatised for at least three days in the aquarium were sampled by conventional procedure in the adductor muscle. Seven hundred and fifty microlitre of haemolymph were withdrawn and analysed by flow cytometry.

Data are presented in Figure 5.20, where shore sampled, aquarium non-infected and infected mussels are compared.

Figure 5.20 I shows environmental samples and Figure 5.20 II aquarium control samples. The inter-individual variation measured is similar to circulating haemocyte concentration observed in the higher range of Figure 3.5 and to circulating haemocyte populations observed in Figures 3.1 (Chapter 3.2.2), and Figure 4.6, 4.7, 4.8 (Chapter 4.3.1).

Figure 5.20 III presents results from bacterially challenged mussels. The inter-individual variation measured is similar to circulating haemocyte concentrations observed in the lower range of Figure 3.1 (Chapter 3.2.2) and to circulating haemocytes populations observed in Figure 4.6, site C. The observed depletion of eosinophils in the haemolymph circulation is similar to the exhaustion observed in the digestive tissues (Figure 5.17 and Figure 5.18); the high percentage of hyaline cells and basophils can be related to the data of Figure 5.19.

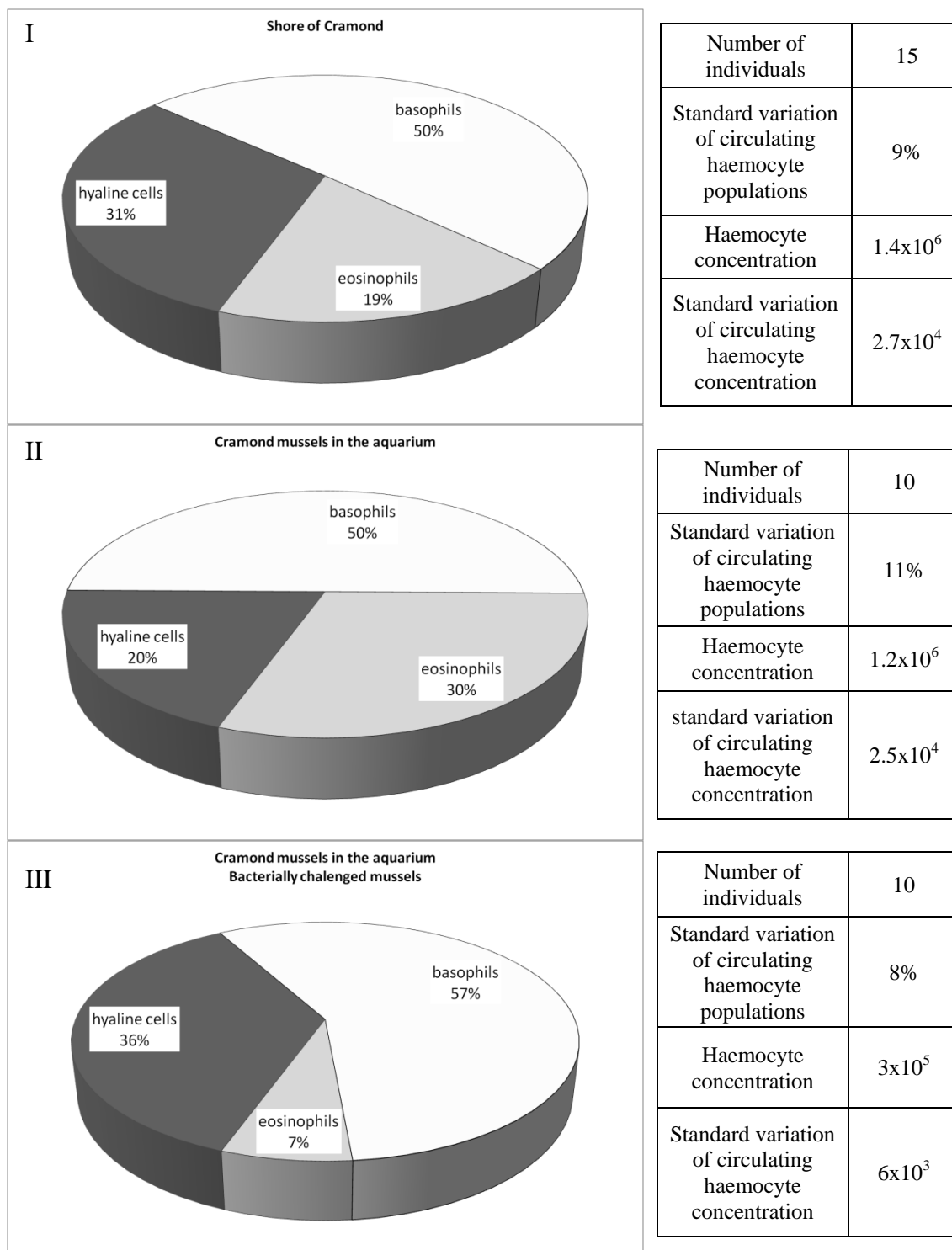


Figure 5.20: Circulating haemocytes in shore, control and bacterially challenged *Mytilus edulis*.  
 I: environmental sample, inter-individual variability is high, haemocyte concentration is similar to other environmental samples (Figures 3.1, 4.6, 4.7 and 4.8)  
 II: control organisms, inter-individual variability is high, but on average, the haemocyte populations are comparable to the environmental samples.  
 III: bacterially challenged organisms, inter-individual variability is high, but on average, the haemocyte population is low in eosinophils, and high in hyaline cells and basophils.

## 5.4 Discussion

### 5.4.1 Impact of physical stress

Environmental factors, such as wave exposure, air-exposed, or exposure to iron precipitate, show little sign of impact on the circulating immune system. This characteristic may possibly be linked to the extremely variable environment of *M. edulis*. In these conditions, it is very difficult to define what constitutes “stress” for the intertidal organism because it is for them what normality is. Similar studies have been driven on mechanical stress, air-exposed and temperature stress showing increases in phagocytic activity and circulating haemocytes (Bussell et al., 2008; Malagoli et al., 2007). In these studies, however, the cell type composition was not investigated, thus making the phagocytosis assays results difficult to interpret, and the large variability was probably triggered by the sampling method and the migration of the eosinophils in the haemolymph. In the perspective of the present study, the variations observed in the literature could simply be linked to the natural variation of circulating haemocytes.

The tolerance of the surgical window allowed a good experimental set-up to investigate *in vivo* gill damage. The re-growth of the excised shell and mantle of a closely related species, *Bathymodiolus azoricus* (Bivalvia: Mytilidae), is described in the literature using the same technique and materials showing the involvement of eosinophilic cells in the wound repair and shell regeneration processes (Kádár, 2008; Kadar et al., 2008).

Most research linked to barium investigation is found in the field of oil production (Barlow and Kingston, 2001). Barium sulphate is a weighting agent used in drilling mud on offshore production platforms. The toxicity of these muds has been studied extensively regarding the light oils and anti-scaling compounds contained in their composition (Daan et al., 1994; Jorissen et al., 2009; Pivel et al., 2009; Pozebon et al., 2009; Vega et al., 2009). Investigation of the impact of oil on the physiology and immune system of *Mytilus edulis* has shown little impact on circulating haemocytes' concentration and cell type ratio (Dyrynda et al., 1997; Hannam et al., 2008; Lowe et al., 1981; Marigómez and Baybay-Villacorta, 2003). To over-come early formulation toxicity of these drilling muds, the light oils have been exchanged for aromatic free oils in low toxicity mud (LTM). However, to overcome any further controversies, the oil industry has funded further research on the other components of these LTM to mitigate



their impact on the sea floor. This barium sulphate investigation in collaboration with Maia Strachan is included in these studies of mitigation processes.

Tissue erosion was observed in all the species investigated (*Mytilus edulis*, *Modiolus modiolus*, *Dosinia lupines* (Strachan et al, personal communication) and *Venerupis senegalensis* (Strachan et al, personal communication)). The gill and digestive tissues show signs of tegument thickening, also shown in *Corophium volutator* (Appendix V), or a high level of infiltration by eosinophils. The circulating immune system appeared to present a decline in eosinophils and a rise in agranular cells in cannulated mussels.

To assess the influence of the mussel adaptation to its environment during its development, farmed mussels (grown on ropes, thereby greatly reducing potential exposure to wave action and sand erosion) and Cramond mussels (grown on an exposed shore near a sandy bank) were both exposed to barium sulphate. However, no difference was observed in the haemocyte ratios between the two groups. In *Mytilus edulis* and *Modiolus modiolus*, the trends in cell type proportions were extremely similar in the controls and the challenged organisms. These trends were directly induced by the sampling technique where the experimental organisms were over-bled. This impact has already been suggested for *Salmo gairdneri* Richardson regarding the cannulation versus conventional sampling (Railo et al., 1985), in *Crassostrea gigas* haemolymph for sampling of over 50µl (Jones et al., 1993), for daily sampling in *Eledone cirrhosa* (Malham et al., 1998), and in repeated sampling in *Ruditapes philippinarum* (Ford and Paillard, 2007).

#### 5.4.2 Impact of biological stress

The bacterial communities described were low in number. The marine agar is a non-selective medium, but only ten strains were isolated. It should be noted that two strains (H, I, table 5.3) lost their pigmentation in pure culture. This observation could also either be due to a manipulation error or a mixed population in the original colonies.

The visceral mass shows signs of basophil and possibly hyaline cell infiltration in the tissues surrounding the stomach. Eosinophils appear depleted from the epithelium of the digestive tissues and from the haemolymph. Circulating haemocytes are in lower concentration compared to healthy individuals.

The micro flora of *Mytilus edulis* has been studied (Montilla et al., 1994; Svärth, 1999; Töbe et al., 2004) showing variability but a dominance of *Vibrio spp.* In addition to the normal microflora, the deleterious impact of bacteria were studied to show impact on gene expression (Costa et al., March 2009 ; Li et al., 2008b) or guts levels (Galimany et al., 2008; Töbe et al., 2004). The pathological effects observed in this project are therefore consistent with the literature.

# Chapter 6

## Conclusions



Title: Handy concept.

This photo was taken in Kirkcaldy, on the coast of eastern Scotland. The background shows the interface of sea and shore. Centred in the frame is a hand holding a colourful stone on which run patterns of white waves on brown ground. This stone mirrors the background of waves running onto the gravelled shore, as if the shore and the sea were combined in the palm of the hand.

Here, the symbolic role of the hand as agent of the self (in the existentialists' sense of 'you are what you do') is, to highlight the comprehension (etymologically derived from the Latin word *prehendere*: catch up with; reach shore; catch; capture; take hold of) of these two dramatically different environments, home of the blue mussel. The image was chosen to illustrate this project's conclusion that the impact of the environment (here a blurred background) is masked by the intrinsic variability of agents acting on the self.

## 6 Conclusion

A vertical investigation has led this project: from the ecosystem to the individual. The relevance of this approach will be discussed in the following section to assess the complexity of *Mytilus edulis* haemocytes.

### Impact of sampling procedure and analytical methods

This project showed the bias induced by the conventional haemolymph sampling procedure in THC measurements due to the equipment and sampling procedure potentially generating levels of variation of more than 25% in the THC results. This bias can be mitigated by the use of precision syringes and precise volume measurements.

The staining procedure with Wright's stain requires relatively light laboratory equipment and little cost. Nevertheless, the cell identification is very dependent on the observer's judgment and the results will be difficult to compare with flow cytometry data, as the direct link of the cell types is ambiguous. The image analysis technique has the same cost as the visual investigation. The price of an eyepiece video camera is negligible next to the cost of a microscope and the image analysis can be done by freely downloaded software (ImageJ). A more objective and constant cell type determination is obtained. The method increases the number of samples and counted cells compared with analysis by eye, and allows the evaluation of the data analysis quality via its quality index. Yet, one set of information (i.e. the discrimination of hyaline cells versus basophils) is lost.

The use of flow cytometry was validated by indirect and direct methods. It allows working with small samples reducing sampling stress on the organism, has a good discrimination of the cell types, is time effective, easy to use, and does not depend on the observer's judgement. Nevertheless, the cell sorting process showed a mixed cell population of hyaline cells, and basophils in the groups regarded as agranular and semi-granular cells. The cell nomenclature should then be dictated by the identification technique: the differential staining technique should refer to hyaline cells, basophils and eosinophils and flow cytometry analysis to agranular, semi-granular and granular cells. It is also a costly technique and the generated data are difficult to relate to previous research.

The results also show a degree of impact of the sampling procedure upon the organism immune system. An intensive haemolymph withdraw triggers a decrease in circulating eosinophils and an increase in hyaline cells and basophils. Mitigations of the stress can be done at two levels. The individual should be equipped with a cannulation to avoid handling and sampling related stresses and the sampling volume should not exceed 50  $\mu$ l in case of repeated sampling of single individual. However, this technique is costly in time and labour, and requires flow cytometry or micro-fluidic technologies for the data analysis.

### System variability

The main conclusion of the project concerns the underestimated levels of variability of *Mytilus edulis* circulating haemocytes. This misjudgement may challenge or invalidate a number of past studies, such as those that either based their results on sampling without evaluating cell concentration or cell type ratio, or/and those who accounted for these variables, yet based their observations on single data points (e.g., x individuals sampled on the shore on day y and day y+n). Eosinophil ratio fluctuations up to 46% were measured at population level (Outer Hebrides, west coast of Scotland, Cramond Island; n=10). The variations can be explained by the reproduction mode of the organism allowing for a high mixing pattern of adjacent populations, as well as by the travelling ability of larval stages before settling. These two factors will lead to a high degree of genetic variability. This interpretation is supported by the observation of high levels of hybridisation in the *Mytilus* genus from the Mediterranean Sea to the Arctic Sea through the east Atlantic, leading some experts to identify three different members of this genus (*M. edulis*, *M. trossulus*, and *M. galloprovincialis*) as a single species (Seed, 1992). The eosinophils fluctuation up to 40% was also observed within a mussel population such as individuals living at the same location and in the same environmental condition (n=50). These changes can also be attributed to their potentially heterogeneous origin triggered by their larval stage pelagic life and their settlement.

The most striking results certainly are the hourly measured haemocyte ratio variations on single individuals. Results indicate fluctuation of over 20% in eosinophils over the period of one hour. Such short temporal variation cannot be explained by cell replication. The observations of mussel tissues give a clue to interpret the observed fluctuations. The investigation of gills, mantle, and visceral mass tissues revealed large

populations of infiltrated eosinophils (up to  $3 \times 10^7$  cells in mantle teguments) and to a lesser degree infiltration of basophil populations.

The physical and biological challenges showed a measurable impact only in the most extreme cases. Bacterial challenge triggered a strong reduction of infiltrated and circulating haemocytes, eventually leading to the liquefaction of the tissues and to the organism's death. Contrastingly, the acute physical challenge induced by the barium sulphate smothering stimulated eosinophil and basophil infiltration in the gills and visceral mass. The decline of eosinophilic populations observed in the haemolymph is attributed to the sampling method as the control organism showed the same patterns of haemocyte ratios. Intermediate challenges such as wave exposure, and iron precipitate smothering presented no measurable impact on the circulating haemocytes. The stress induced by air-exposed could be measured after a three-day period by a slight decrease of the ratio of eosinophilic cells. Further study at the histological level could reveal if the eosinophils have been infiltrating the tissues or if a prolonged anoxia would have been deleterious to them. To conclude, the use of *M. edulis* haemocyte concentration and -cell type ratio as biomarkers is highly compromised. This system has an important scientific interest but its variability will mask the causality stress/reaction necessary for an efficient biomarker.

#### Further studies

In the field of eco-immunology, the implication suggested in this work stresses the necessity to better understand the fundamental mechanisms driving the immune system of the blue mussel. The tools developed for this project deliver handy and accurate tools such as cell count by image analysis, cannulation and flow cytometry. The image analysis can be further automatised and its field of use widened. The cannulation system reduces the animal stress allowing a more accurate measurement of the immune reaction, and permits a better temporal resolution. These two factors will allow mitigating the impact of the intra- and inter-individual variability of the concentration and cell type ratio of circulating haemocytes.

In addition to the immune system study, the use of modular lab-on-a-chip systems may become a cheap and reliable tool when the field of micro-fluidics will have developed modelisation tools. In this study, the centrifugation-like effect obtained could be improved with mixing modules, chemical reservoirs and a low footprint reading

apparatus. This technology will allow field studies the potential of the flow cytometric procedure obtained today in conventional laboratories, and to work with small haemolymph samples.

## References

- Abramoff, M.D., Magelhaes, P.J., and Ram, S.J. (2004). Image processing with ImageJ. *Biophotonics Int 11*, 36-42.
- Akaishi, F.M., St-Jean, S.D., Bishay, F., Clarke, J., Rabitto, I.d.S., and Ribeiro, C.A.d.O. (2007). Immunological responses, histopathological finding and disease resistance of blue mussel (*Mytilus edulis*) exposed to treated and untreated municipal wastewater. *Aquatic Toxicology 82*, 1-14.
- Asensio Gil, L. (2007). PCR-based methods for fish and fishery products authentication. *Trends in Food Science & Technology 18*, 558-566.
- Ashton-Alcox, K.A., and Ford, S.E. (1998). Variability in molluscan hemocytes: a flow cytometric study. *Tissue and Cell 30*, 195-204.
- Auffret, M., Mujdzic, N., Corporeau, C., and Moraga, D. (2002). Xenobiotic-induced immunomodulation in the European flat oyster, *Ostrea edulis*. *Marine Environmental Research 54*, 585-589.
- Auffret, M. and Oubella, R. (1997). Hemocyte aggregation in the oyster *Crassostrea gigas*: In vitro measurement and experimental modulation by xenobiotics. *Comparative Biochemistry and Physiology Part A: Physiology 118*, 705-712.
- Barlow, M.J. and Kingston, P.F. (2001). Observations on the Effects of Barite on the Gill Tissues of the Suspension Feeder *Cerastoderma edule* (Linné) and the Deposit Feeder *Macoma balthica* (Linné). *Marine Pollution Bulletin 42*, 71-76.
- Bayne, B.L. (1976). *Marine mussels, their ecology and physiology, illustrated edn* (Cambridge University Press) 15-17, 20-45.
- Bayne, C.J., Moore, M.N., Carefoot, T.H., and Thompson, R.J. (1979). Hemolymph functions in *Mytilus californianus*: The cytochemistry of hemocytes and their responses to foreign implants and hemolymph factors in phagocytosis. *Journal of Invertebrate Pathology 34*, 1-20.
- Benazzi, G., Holmes, D., Sun, T., Mowlem, M.C., and Morgan, H. (2007). Discrimination and analysis of phytoplankton using a microfluidic cytometer. *Nanobiotechnology 1*, 94-101.
- Bihari, N., Micic, M., Batel, R., and Zahn, R.K. (2003). Flow cytometric detection of DNA cell cycle alterations in hemocytes of mussels (*Mytilus galloprovincialis*) off the Adriatic coast, Croatia. *Aquatic Toxicology 64*, 121-129.



Bussell, J.A., Gidman, E.A., Causton, D.R., Gwynn-Jones, D., Malham, S.K., Jones, M.L.M., Reynolds, B., and Seed, R. (2008). Changes in the immune response and metabolic fingerprint of the mussel, *Mytilus edulis* (Linnaeus) in response to lowered salinity and physical stress. *Journal of Experimental Marine Biology and Ecology* 358, 78-85.

Canesi, L., Betti, M., Ciacci, C., Lorusso, L.C., Pruzzo, C., and Gallo, G. (2006). Cell signalling in the immune response of mussel hemocytes. *Invertebrate Survival Journal* 3, 40-49.

Canesi, L., Ciacci, C., Betti, M., Fabbri, R., Canonico, B., Fantinati, A., Marcomini, A., and Pojana, G. (2008). Immunotoxicity of carbon black nanoparticles to blue mussel hemocytes. *Environment International* 34, 1114-1119.

Canesi, L., Lorusso, L.C., Ciacci, C., Betti, M., Regoli, F., Poiana, G., Gallo, G., and Marcomini, A. (2007). Effects of blood lipid lowering pharmaceuticals (bezafibrate and gemfibrozil) on immune and digestive gland functions of the bivalve mollusc, *Mytilus galloprovincialis*. *Chemosphere* 69, 994-1002.

Cao, A., Mercado, L., Ramos-Martinez, J.I., and Barcia, R. (2003). Primary cultures of hemocytes from *Mytilus galloprovincialis* Lmk.: expression of IL-2R[alpha] subunit. *Aquaculture* 216, 1-8.

Caselgrandi, E., Kletsas, D., and Ottaviani, E. (2000). Neutral endopeptidase-24.11 (nep) deactivates PDGF- and TGF-[beta]-induced cell shape changes in invertebrates immunocytes. *Cell Biology International* 24, 85-90.

Cerón-Carrasco, R. (2005). Marine shells, the excavation of four caves in the Geodha Smoo near Durness. In *Scottish Archaeological Internet Report* (e Society of Antiquaries of Scotland). < <http://www.sair.org.uk/sair18/sair18.pdf> > [Accessed 11 Mars 2006]

Chen, X., Cui, D., Liu, C., Li, H., and Chen, J. (2007). Continuous flow microfluidic device for cell separation, cell lysis and DNA purification. *Analytica Chimica Acta* 584, 237-243.

Ciacci, C., Citterio, B., Betti, M., Canonico, B., Roch, P., and Canesi, L. (2009). Functional differential immune responses of *Mytilus galloprovincialis* to bacterial challenge. *Comparative Biochemistry and Physiology Part B: Biochemistry and Molecular Biology* 153, 365-371.

Coles, J.A. and Pipe, R.K. (1994). Phenoloxidase activity in the haemolymph and haemocytes of the marine mussel *Mytilus edulis*. *Fish & Shellfish Immunology* 4, 337-352.

Collis, J. (2001). Coral, Amber and cockle shells: Trade in the middle la Tène period. The newsletter of the prehistoric society 38.

Costa, M.M., Dios, S., Alonso-Gutierrez, J., Romero, A., Novoa, B., and Figueras, A. (2009). Evidence of high individual diversity on myticin C in mussel (*Mytilus galloprovincialis*). Developmental & Comparative Immunology 33, 162-170.

Costa, M.M., Prado-Alvarez, M., Gestal, C., Li, H., Roch, P., Novoa, B., and Figueras, A. (2009). Functional and molecular immune response of Mediterranean mussel (*Mytilus galloprovincialis*) haemocytes against pathogen-associated molecular patterns and bacteria. Fish & Shellfish Immunology 26(3), 515-523.

Daan, R., Mulder, M., and Van Leeuwen, A. (1994). Differential sensitivity of macrozoobenthic species to discharges of oil-contaminated drill cuttings in the North Sea. Netherlands Journal of Sea Research 33, 113-127.

Dawkins, R. (1999). The Extended Phenotype : The long reach of the gene, Vol 1 (New York: Oxford University Press) 1-8.

Domouhtsidou, G.P., and Dimitriadis, V.K. (2001). Lysosomal and lipid alterations in the digestive gland of mussels, *Mytilus galloprovincialis* (L.) as biomarkers of environmental stress. Environmental Pollution 115, 123-137.

Dyrynda, E.A., Law, R.J., Pipe, R.K., and Ratcliffe, N.A. (1997). F8 4:00 Modulations in cell-mediated immunity of mussels (*Mytilus edulis*) following the 'Sea Empress' oil spill. Developmental & Comparative Immunology 21, 124-124.

Dyrynda, E.A., Pipe, R.K., Burt, G.R., and Ratcliffe, N.A. (1998). Modulations in the immune defences of mussels (*Mytilus edulis*) from contaminated sites in the UK. Aquatic Toxicology 42, 169-185.

Fagotti, A., Di Rosa, I., Simoncelli, F., Pipe, R.K., Panara, F., and Pascolini, R. (1996). The effects of copper on actin and fibronectin Organization in *Mytilus galloprovincialis* haemocytes. Developmental & Comparative Immunology 20, 383-391.

FAO.© (2003-2009). Cultured Aquatic Species Information Programme, *Mytilus edulis* (Linnaeus, 1758) In FI Programme Websites, F.a.A. Department, ed. (Rome, Fisheries Global Information System). < [http://www.fao.org/fishery/culturedspecies/Mytilus\\_edulis/en](http://www.fao.org/fishery/culturedspecies/Mytilus_edulis/en) > [Accessed 14 February 2006]

Findlay, C. and Smith, V.J. (1995). Antimicrobial factors in solitary ascidians. Fish & Shellfish Immunology 5, 645-658.

Foighil, D.O. and Thiriot-Quievreux, C. (1991). Ploidy and Pronuclear Interaction in Northeastern Pacific *Lasaea* Clones (Mollusca: Bivalvia). *Biological Bulletin* 181, 222-231.

Ford, S.E. and Paillard, C. (2007). Repeated sampling of individual bivalve mollusks I: Intraindividual variability and consequences for haemolymph constituents of the Manila clam, *Ruditapes philippinarum*. *Fish & Shellfish Immunology* 23, 280-291.

Foster-Smith, R.L. (1975). The role of mucus in the mechanism of feeding in three filter feeding bivalves. *Proceedings of the Malacological Society of London* 41, 571-588.

Friebel, B. and Renwranz, L. (1995). Application of density gradient centrifugation for separation of eosinophilic and basophilic hemocytes from *Mytilus edulis* and characterization of both cell groups. *Comparative Biochemistry and Physiology Part A: Physiology* 112, 81-90.

Galimany, E., Sunila, I., Hégaret, H., Ramón, M., and Wikfors, G.H. (2008). Pathology and immune response of the blue mussel (*Mytilus edulis* L.) after an exposure to the harmful dinoflagellate *Prorocentrum minimum*. *Harmful Algae* 7, 630-638.

García-García, E., Prado-Álvarez, M., Novoa, B., Figueras, A., and Rosales, C. (2008). Immune responses of mussel hemocyte subpopulations are differentially regulated by enzymes of the PI 3-K, PKC, and ERK kinase families. *Developmental & Comparative Immunology* 32, 637-653.

Gardner, J.P.A. (1995). Developmental stability is not disrupted by extensive hybridization and introgression among populations of the marine bivalve molluscs *Mytilus edulis* (L.) and *M. galloprovincialis* (Lmk.) from south-west England. *Biological Journal of the Linnean Society* 54, 71-86.

Gilbride, K.A., Lee, D.Y., and Beaudette, L.A. (2006). Molecular techniques in wastewater: Understanding microbial communities, detecting pathogens, and real-time process control. *Journal of Microbiological Methods* 66, 1-20.

Goldzahl, L. (1995). *Erreurs: contes et récits scientifiques* (Éd. Frison-Roche) 1-20.

Gracey, A.Y., Chaney, M.L., Boomhower, J.P., Tyburczy, W.R., Connor, K., and Somero, G.N. (2008). Rhythms of Gene Expression in a Fluctuating Intertidal Environment. *Current Biology* 18, 1501-1507.

Grundy, M.M., Moore, M.N., Howell, S.M., and Ratcliffe, N.A. (1996). Phagocytic reduction and effects on lysosomal membranes by polycyclic aromatic hydrocarbons, in haemocytes of *Mytilus edulis*. *Aquatic Toxicology* 34, 273-290.

Hagger, J.A., Depledge, M.H., and Galloway, T.S. (2005). Toxicity of tributyltin in the marine mollusc *Mytilus edulis*. *Marine Pollution Bulletin* 51, 811-816.

Hannam, M.L., Bamber, S.D., Sundt, R.C., and Galloway, T.S. (2008). Immune modulation in the blue mussel *Mytilus edulis* exposed to North Sea produced water. *Environmental Pollution* 157(6), 1939-1944.

Hendriks, I.E., van Duren, L.A., and Herman, P.M.J. (2005). Image analysis techniques: A tool for the identification of bivalve larvae? *Journal of Sea Research* 54, 151-162.

Jones, T.O., Bourne, N.F., Bower, S.M., and Iwama, G.K. (1993). Effect of repeated sampling on haemolymph pH, PO<sub>2</sub> and haemocyte activity in the Pacific oyster, *Crassostrea gigas* (Thunberg). *Journal of Experimental Marine Biology and Ecology* 167, 1-10.

Jorissen, F.J., Bicchi, E., Duchemin, G., Durrieu, J., Galgani, F., Cazes, L., Gaultier, M., and Camps, R. (2009). Impact of oil-based drill mud disposal on benthic foraminiferal assemblages on the continental margin off Angola. *Deep Sea Research Part II: Topical Studies in Oceanography* 56 (23), 2270-2291.

Kádár, E. (2008). Haemocyte response associated with induction of shell regeneration in the deep-sea vent mussel *Bathymodiulus azoricus* (Bivalvia: *Mytilidae*). *Journal of Experimental Marine Biology and Ecology* 362, 71-78.

Kadar, E., Tschuschke, I.G., and Checa, A. (2008). Post-capture hyperbaric simulations to study the mechanism of shell regeneration of the deep-sea hydrothermal vent mussel *Bathymodiulus azoricus* (Bivalvia: *Mytilidae*). *Journal of Experimental Marine Biology and Ecology* 364, 80-90.

Kaplan, J.E., Chrenek, R.D., Morash, J.G., Ruksznis, C.M., and Hannum, L.G. (2008). Rhythmic patterns in phagocytosis and the production of reactive oxygen species by zebrafish leukocytes. *Comparative Biochemistry and Physiology - Part A: Molecular & Integrative Physiology* 151, 726-730.

La Peyre, J.F., Chu, F.-L.E., and Meyers, J.M. (1995). Haemocytic and humoral activities of eastern and Pacific oysters following challenge by the protozoan *Perkinsus marinus*. *Fish & Shellfish Immunology* 5, 179-190.

Lane, E., and Birkbeck, T.H. (1999). Toxicity of bacteria towards haemocytes of *Mytilus edulis*. *Aquatic Living Resources* 12, 343-350.

Leonardos, N., and Lucas, I.A.N. (2000). The nutritional value of algae grown under different culture conditions for *Mytilus edulis* L. larvae. *Aquaculture* 182, 301-315.

Letendre, J., Chouquet, B., Manduzio, H., Marin, M., Bultelle, F., Leboulenger, F., and Durand, F. (2009). Tidal height influences the levels of enzymatic antioxidant defences in *Mytilus edulis*. *Marine Environmental Research* 67, 69-74.

Letendre, J., Chouquet, B., Rocher, B., Manduzio, H., Leboulenger, F., and Durand, F. (2008). Differential pattern of Cu/Zn superoxide dismutase isoforms in relation to tidal spatio-temporal changes in the blue mussel *Mytilus edulis*. *Comparative Biochemistry and Physiology Part C: Toxicology & Pharmacology* 148, 211-216.

Li, H., Parisi, M., Toubiana, M., Cammarata, M., and Roch, P. (2008). Lysozyme gene expression and hemocyte behaviour in the Mediterranean mussel, *Mytilus galloprovincialis*, after injection of various bacteria or temperature stresses. *Fish Shellfish Immunol.* 25(1-2), 143-152.

Loomis, S.H., Carpenter, J.F., and Crowe, J.H. (1988). Identification of strombine and taurine as cryoprotectants in the intertidal bivalve *Mytilus edulis*. *Biochimica et Biophysica Acta (BBA) - Biomembranes* 943, 113-118.

Lowe, D.M., Moore, M.N., and Clarke, K.R. (1981). Effects of oil on digestive cells in mussels: Quantitative alterations in cellular and lysosomal structure. *Aquatic Toxicology* 1, 213-226.

Malagoli, D., Casarini, L., Sacchi, S., and Ottaviani, E. (2007). Stress and immune response in the mussel *Mytilus galloprovincialis*. *Fish & Shellfish Immunology* 23, 171-177.

Malagoli, D., Franchini, A., and Ottaviani, E. (2000). Synergistic role of cAMP and IP3 in corticotropin-releasing hormone-induced cell shape changes in invertebrate immunocytes. *Peptides* 21, 175-182.

Malham, S.K., Coulson, C.L., and Runham, N.W. (1998). Effects of repeated sampling on the haemocytes and haemolymph of *Eledone cirrhosa* (Lam.). *Comparative Biochemistry and Physiology - Part A: Molecular & Integrative Physiology* 121, 431-440.

Marigómez, I., and Baybay-Villacorta, L. (2003). Pollutant-specific and general lysosomal responses in digestive cells of mussels exposed to model organic chemicals. *Aquatic Toxicology* 64, 235-257.

Minc, N., and Viovy, J.-L. (2004). Microfluidique et applications biologiques : enjeux et tendances. *Comptes Rendus Physique* 5, 565-575.

Minier, C., Borghi, V., Moore, M.N., and Porte, C. (2000). Seasonal variation of MXR and stress proteins in the common mussel, *Mytilus galloprovincialis*. *Aquatic Toxicology* 50, 167-176.

Mitta, G., Hubert, F., Dyrinda, E.A., Boudry, P., and Roch, P. (2000). Mytilin B and MGD2, two antimicrobial peptides of marine mussels: gene structure and expression analysis. *Developmental & Comparative Immunology* 24, 381-393.

Molenaar, N., and Martinius, A.W. (1996). Fossiliferous intervals and sequence boundaries in shallow marine, fan-deltaic deposits (Early Eocene, southern Pyrenees, Spain). *Palaeogeography, Palaeoclimatology, Palaeoecology* 121, 147-168.

Montilla, R., Palomar, J., Santmarti, M., Fuste, C., and Viñas, M. (1994). Isolation and Characterization of Halophilic *Vibrio* from Bivalves Bred in Nurseries at the Ebre Delta. *Journal of Invertebrate Pathology* 63, 178-181.

Moore, J.D., Elston, R.A., Drum, A.S., and Wilkinson, M.T. (1991). Alternate pathogenesis of systemic neoplasia in the bivalve mollusc *Mytilus*. *Journal of Invertebrate Pathology* 58, 231-243.

Moore, M.N. and Lowe, D.M. (1977). The cytology and cytochemistry of the hemocytes of *Mytilus edulis* and their responses to experimentally injected carbon particles. *Journal of Invertebrate Pathology* 29, 18-30.

Myers, A.M. and Gourlay, R.B. (1991). Muirtown, Inverness: preliminary investigation of a shell midden. *Proceedings of the Society of Antiquaries of Scotland* 121, p 17-25.

Myrand, B., Tremblay, R., and Sévigny, J.-M. (2009). Impact of suspension culture using mesh sleeves on genetic characteristics of *Mytilus edulis* L. in Canada. *Aquaculture* 291, 147-153.

Parisi, M.-G., Li, H., Jouvét, L.B.P., Dyrinda, E.A., Parrinello, N., Cammarata, M., and Roch, P. (2008). Differential involvement of mussel hemocyte sub-populations in the clearance of bacteria. *Fish & Shellfish Immunology* 25, 834-840.

Pauley, G.B. and Heaton, L.H. (1969). Experimental wound repair in the freshwater mussel *Anodonta oregonensis*. *Journal of Invertebrate Pathology* 13, 241-249.

Pipe, R.K. (1990). Differential binding of lectins to haemocytes of the mussel *Mytilus edulis*. *Cell and Tissue Research* 261, 261-268.

Pipe, R.K., Porte, C., and Livingstone, D.R. (1993). Antioxidant enzymes associated with the blood cells and haemolymph of the mussel *Mytilus edulis*. *Fish & Shellfish Immunology* 3, 221-233.

Pivel, M.A.G., Freitas, C.M.D.S., and Comba, J.L.D. (2009). Modeling the discharge of cuttings and drilling fluids in a deep-water environment. *Deep Sea Research Part II: Topical Studies in Oceanography* 56, 12-21.

Pozebon, D., Santos, J.H.Z., Peralba, M.C.R., Maia, S.M., Barrionuevo, S., and Pizzolato, T.M. (2009). Metals, arsenic and hydrocarbons monitoring in marine sediment during drilling activities using NAFs. *Deep Sea Research Part II: Topical Studies in Oceanography* 56, 22-31.

Railo, E., Nikinmaa, M., and Soivio, A. (1985). Effects of sampling on blood parameters in the rainbow trout, *Salmo gairdneri* Richardson. *Journal of Fish Biology* 26, 725-732.

Ramadan, Q., Samper, V., Poenar, D., Liang, Z., Yu, C., and Lim, T.M. (2006). Simultaneous cell lysis and bead trapping in a continuous flow microfluidic device. *Sensors and Actuators B: Chemical* 113, 944-955.

Rasmussen, L.P.D., Hage, E., and Karlog, O. (1985). An electron microscope study of the circulating leucocytes of the marine mussel, *Mytilus edulis*. *Journal of Invertebrate Pathology* 45, 158-167.

Reynolds, O. (1883). An experimental investigation of the circumstances which determine whether the motion of water shall be direct or sinuous, and of the law of resistance in parallel channels. *Philosophical Transactions of the Royal Society of London* 174, 935-982.

Sai, Y., Yamada, M., Yasuda, M., and Seki, M. (2006). Continuous separation of particles using a microfluidic device equipped with flow rate control valves. *Journal of Chromatography A* 1127, 214-220.

Sato, K., Hibara, A., Tokeshi, M., Hisamoto, H., and Kitamori, T. (2003). Microchip-based chemical and biochemical analysis systems. *Advanced Drug Delivery Reviews* 55, 379-391.

Sauvé, S., Brousseau, P., Pellerin, J., Morin, Y., Sénécal, L., Goudreau, P., and Fournier, M. (2002). Phagocytic activity of marine and freshwater bivalves: in vitro exposure of hemocytes to metals (Ag, Cd, Hg and Zn). *Aquatic Toxicology* 58, 189-200.

Seed, R. (1992). Systematics evolution and distribution of mussels belonging to the genus *Mytilus*: an overview. *American Malacological Bulletin*, 123-137.

Smith, V.J., Swindlehurst, R.J., Johnston, P.A., and Vethaak, A.D. (1995). Disturbance of host defence capability in the common shrimp, *Crangon crangon*, by exposure to harbour dredge spoils. *Aquatic Toxicology* 32, 43-58.

Sollier, E., Rostaing, H., Pouteau, P., Fouillet, Y., and Achard, J.-L. (2009). Passive microfluidic devices for plasma extraction from whole human blood. *Sensors and Actuators B: Chemical* 141, 617-624.

Stein, J.R. (1973). Handbook of physiological methods, Vol 1 (Cambridge University Press) 21-51.

Sunila, I. (1988). Acute histological responses of the gill of the mussel, *Mytilus edulis*, to exposure by environmental pollutants. *Journal of Invertebrate Pathology* 52, 137-141.

Svärdh, L. (1999). Bacteria, *Granulocytomas*, and Trematode *Metacercariae* in the Digestive Gland of *Mytilus edulis*: Seasonal and Interpopulation Variation. *Journal of Invertebrate Pathology* 74, 275-280.

Talbot, G., Topp, E., Palin, M.F., and Massé, D.I. (2008). Evaluation of molecular methods used for establishing the interactions and functions of microorganisms in anaerobic bioreactors. *Water Research* 42, 513-537.

Thompson, R.J., Bayne, C.J., Moore, M.N., and Carefoot, T.H. (1978). Haemolymph volume, changes in the biochemical composition of the blood, and cytological responses of the digestive cells in *Mytilus californianus* Conrad, induced by nutritional, thermal and exposure stress. *Journal of Comparative Physiology B: Biochemical, Systemic, and Environmental Physiology* 127, 287-298.

Töbe, K., Smith, E.A., Gallacher, S., and Medlin, L.K. (2004). Detection of bacteria originally isolated from *Alexandrium* spp. in the midgut diverticula of *Mytilus edulis* after water-borne exposure. *Harmful Algae* 3, 61-69.

Tremblay, R., and Pellerin-Massicotte, J. (1997). Effect of the Tidal Cycle on Lysosomal Membrane Stability in the Digestive Gland of *Mya arenaria* and *Mytilus edulis* L. *Comparative Biochemistry and Physiology Part A: Physiology* 117, 99-104.

Vallièrre, D., Guderley, H., and Larochelle, J. (1990). Cryoprotective mechanisms in subtidally cultivated and intertidal blue mussels (*Mytilus edulis*) from the Magdalen Islands, Québec. *Journal of Thermal Biology* 15, 233-238.

Vassar, P.S., Hards, J.M., Brooks, D.E., Hagenberger, B., and Seaman, G.V.F. (1972). Physicochemical effects of aldehydes on the human erythrocyte. *The Journal of Cell Biology* 53, 809-818.

Vega, M.P., Vieira, F.R.B., Mancini, M.C., Jacek, J., and Jan, T. (2009). Optimization Studies of an Oil Well Drilling Process. In *Computer Aided Chemical Engineering* (Elsevier), 629-634.

Viarengo, A., Canesi, L., Pertica, M., Mancinelli, G., Accomando, R., Smaal, A.C., and Orunesu, M. (1995). Stress on stress response: A simple monitoring tool in the assessment of a general stress syndrome in mussels. *Marine Environmental Research* 39, 245-248.



Winston, G.W., Moore, M.N., Kirchin, M.A., and Soverchia, C. (1996). Production of reactive oxygen species by haemocytes from the marine mussel, *Mytilus edulis*: Lysosomal localization and effect of xenobiotics. *Comparative Biochemistry and Physiology Part C: Pharmacology, Toxicology and Endocrinology* 113, 221-229.

Wootton, E.C., Dyrinda, E.A., and Ratcliffe, N.A. (2003). Bivalve immunity: comparisons between the marine mussel (*Mytilus edulis*), the edible cockle (*Cerastoderma edule*) and the razor-shell (*Ensis siliqua*). *Fish & Shellfish Immunology* 15, 195-210.

Zhang, C., Xu, J., Ma, W., and Zheng, W. PCR microfluidic devices for DNA amplification. *Biotechnology Advances* 24, 243-284.